Chapter 3 – SYSTEM MODELS

3.1 GAS TURBINE CYCLE ANALYSIS

This section introduces the various gas turbine cycles as they are used for propulsion (air, land and sea vehicles) as well as for power generation. It begins with an ideal cycle and continues with more realistic cycles in which the losses that are unavoidable in real world applications are introduced step-by-step.

3.1.1 Ideal Joule Process

3.1.1.1 Simple Cycle

The ideal thermodynamic process of the simple cycle gas turbine is composed of three major parts: isentropic compression (stations 2 – 3), heat addition at constant pressure (3 – 4) and isentropic expansion (stations 4 – 45 – 5). Station 45 is an intermediate station which is here defined in such a way that the work done between stations 4 and 45 covers the work required for driving the compressor. Consequently the enthalpy difference between stations 45 and 5 is available as useful power. **Figure 3.1** shows this process in an enthalpy-entropy diagram. Note that the enthalpy rise in the compressor H_C equals the enthalpy drop H_{HPT} in the high pressure turbine.

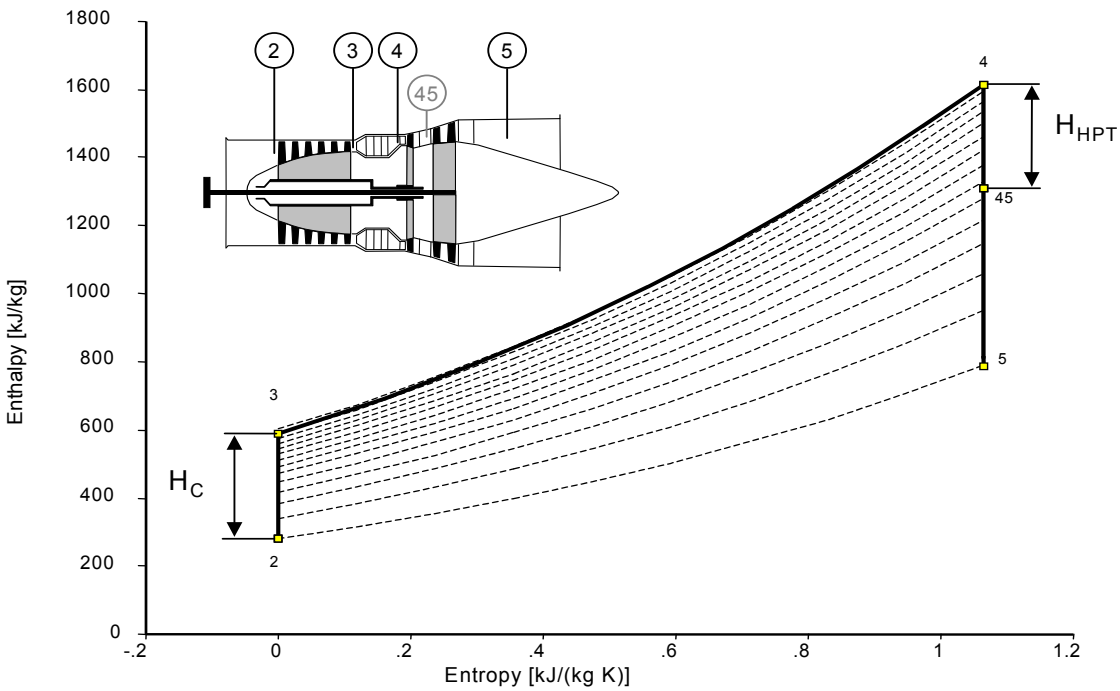

Figure 3.1: Ideal Joule Process in the Enthalpy-Entropy Diagram.

From the enthalpy-entropy diagram shown in **Figure 3.2** one can easily see what the main influence of burner temperature T_4 on the shaft power produced is: Increasing T_4 enlarges the useful work output because the isobars diverge with increasing entropy. However, the distance between stations 3 and 4 increases also and therefore more heat has to be added and thus more fuel is needed.

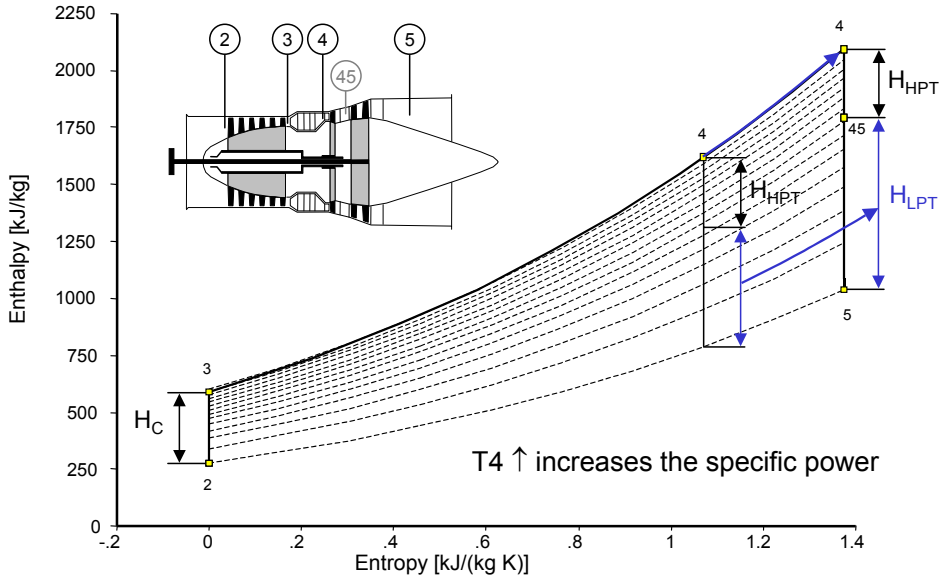

Figure 3.2: Influence of Burner Exit Temperature T_4 on Specific Power.

With the ideal Joule process, and assuming constant isentropic exponent, γ, the thermal efficiency of the cycle is only dependant on cycle pressure ratio P_3/P_2 and does not change with T_4. Highest pressure ratio yields the best thermal efficiency.

In reality the isentropic exponent is not constant but decreasing when temperature increases and therefore the thermal efficiency of the ideal Joule process decreases slightly with increasing burner exit temperature, see **Figure 3.3**.

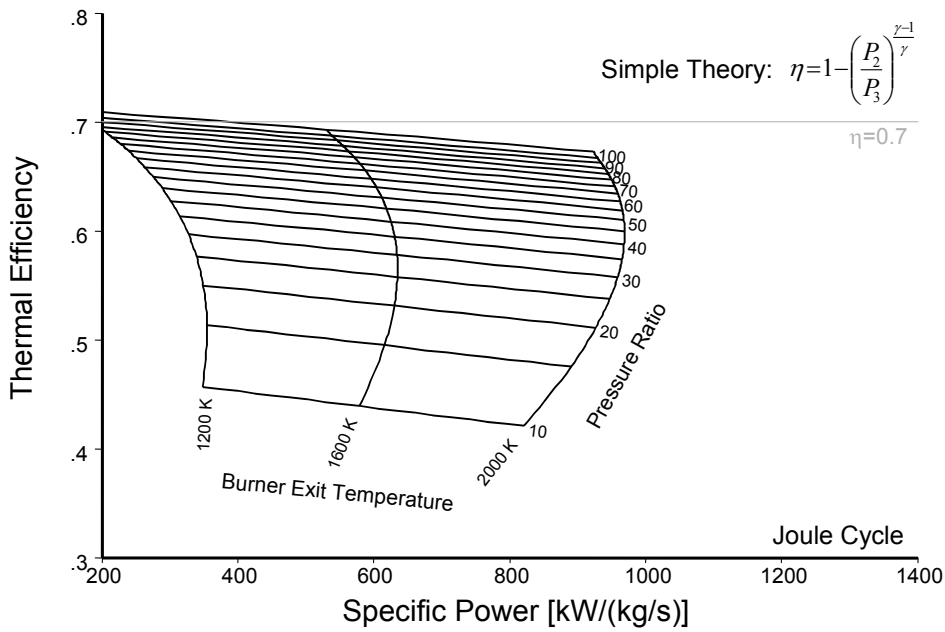

Figure 3.3: Thermal Efficiency and Specific Power of the Ideal Joule Cycle.

3.1.1.2 Recuperated Cycle

The thermal efficiency of the Joule process can be improved by adding a recuperator (heat exchanger) which recovers some of the heat in the exhaust gas and uses it to heat the compressed air before it enters the combustor at station 35 (see **Figure 3.4**).

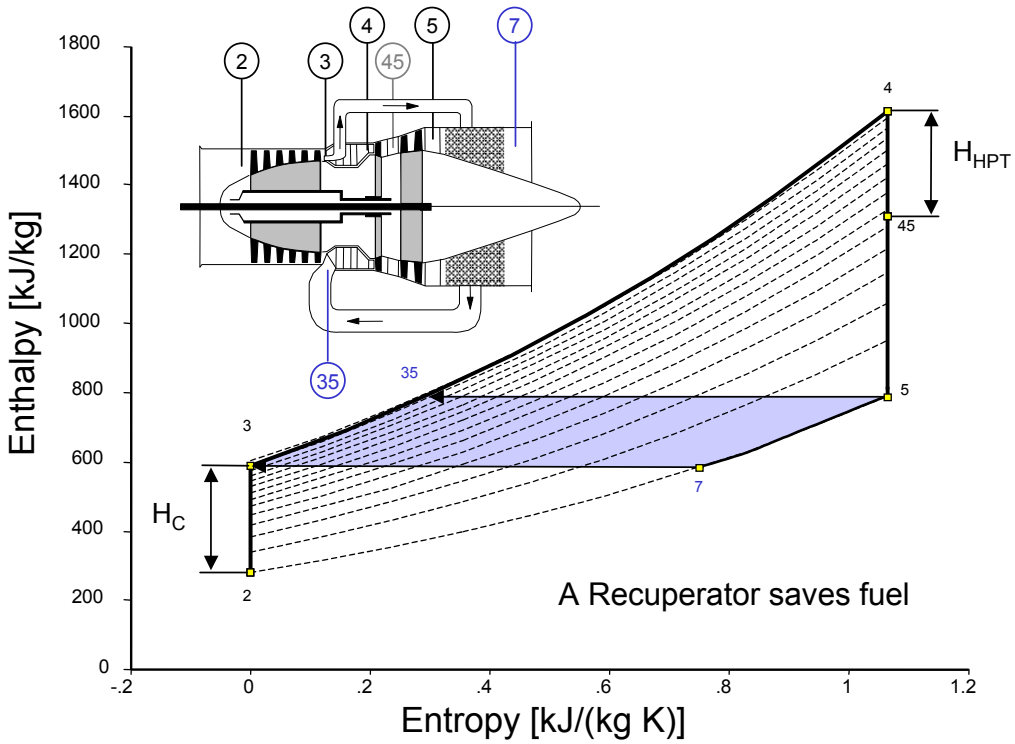

Figure 3.4: Joule Cycle with Recuperator.

Obviously the recuperator has no influence on the specific power produced; it reduces only the fuel consumption because the temperature difference in the burner is smaller than without a recuperator. While for the ideal Joule cycle the thermal efficiency was primarily a function of pressure ratio, with the recuperated cycle also the burner exit temperature has an influence, see **Figure 3.5**. The pressure ratio for best efficiency is fairly low, because with low pressure ratio the temperature difference $T_5 - T_3$ gets big and thus allows significant energy transfer from the exhaust to the burner inlet. The best achievable cycle efficiency is slightly above 70% and is connected with relatively low pressure ratios in the range of 3 to 8. The specific power at a given burner exit temperature is significantly lower than with the simple cycle, compare **Figure 3.3** and **Figure 3.5**.

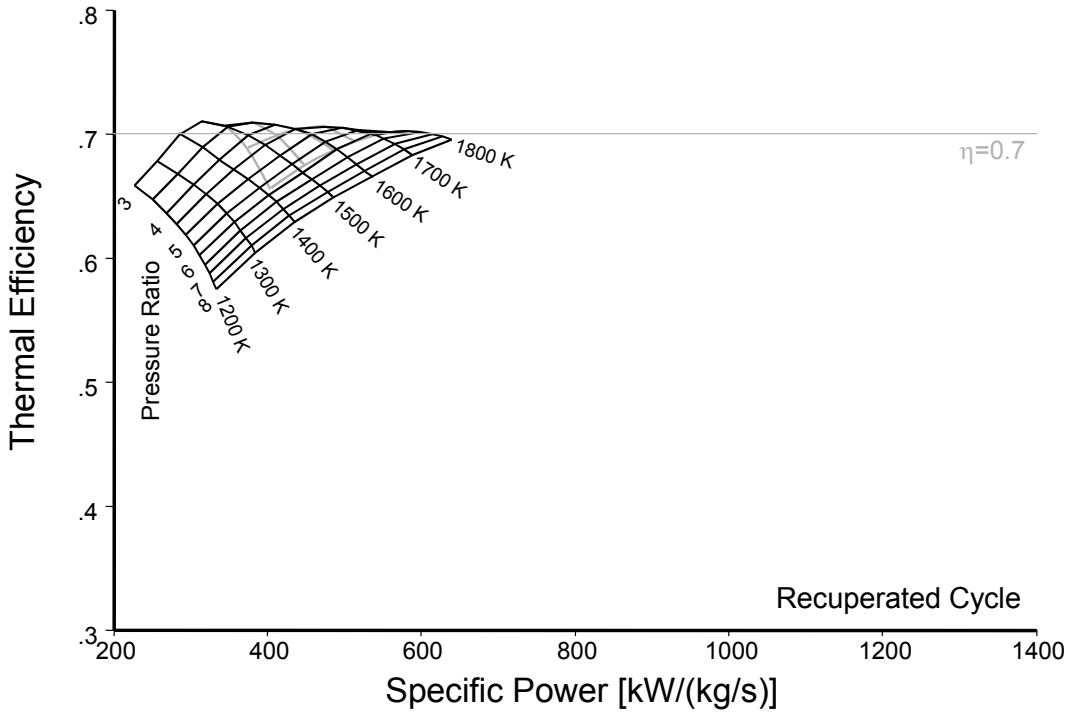

Figure 3.5: Thermal Efficiency and Specific Power of the Ideal Cycle with Recuperator.

3.1.1.3 Intercooled Cycle

By intercooling the gas during the compression process the total work required for compression is reduced. The first part of the compression from station 2 to station 24 requires the specific work H_{C1} (see **Figure 3.6**). Then the gas is cooled down again to the compressor inlet temperature (i.e. $T_{25} = T_2$). The second compression process from station 25 to compressor exit station 3 requires the specific work H_{C2} which is less than the work required for a compression to the same exit pressure when commencing at the temperature T_{24}. Thus the total work required for the compression is reduced and consequently the usable net power is increased.

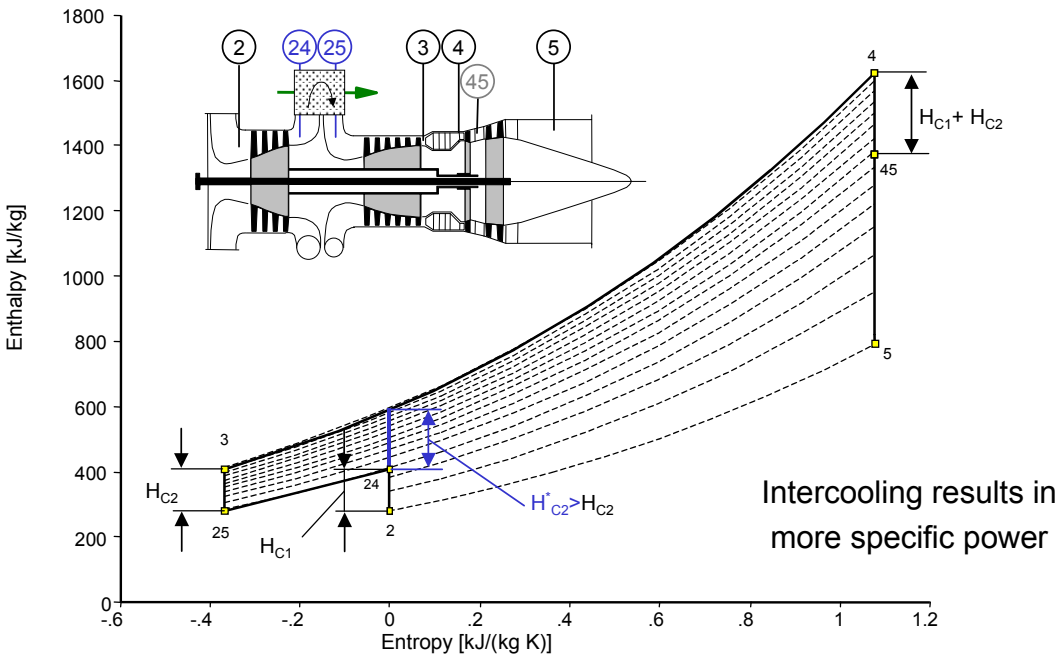

Figure 3.6: Ideal Joule Cycle with Intercooler.

However, the combustor inlet temperature T_3 is lower with an intercooler and more fuel is needed to because the temperature difference in the burner is increased. In an efficiency analysis this effect more than compensates the net power increase and therefore the thermal efficiency of the cycle with intercooling is worse than that of the simple cycle (compare **Figure 3.7** with **Figure 3.3**).

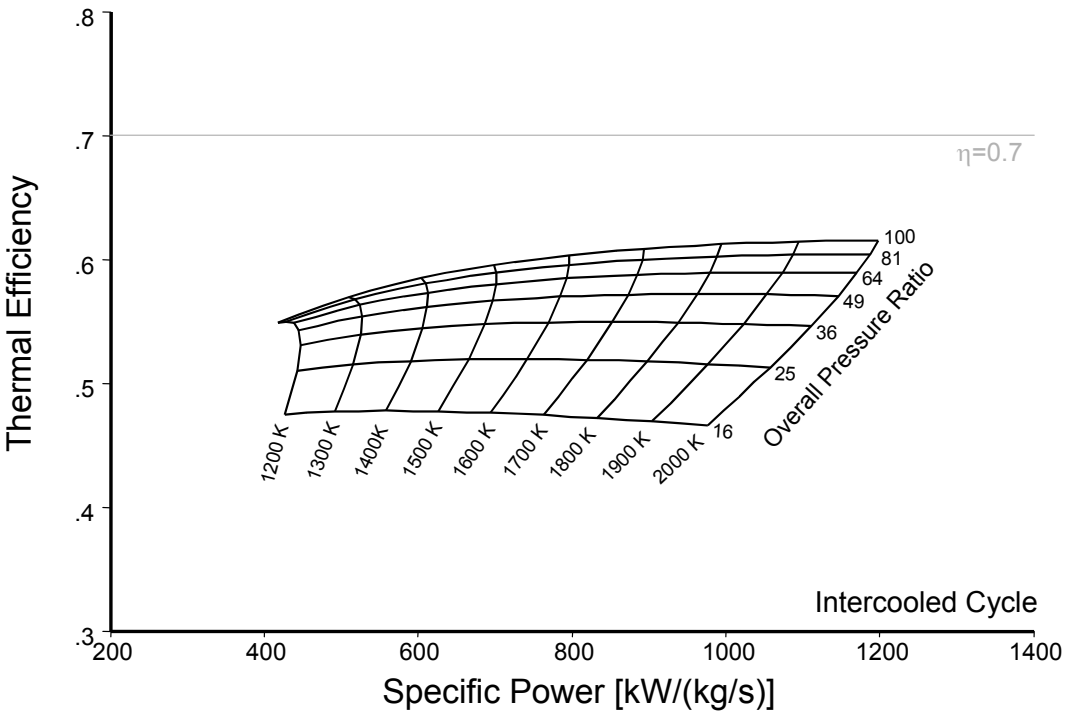

Figure 3.7: Efficiency of the Ideal Cycle with Intercooler.

3.1.1.4 Combined Intercooling and Recuperating

The lower compressor exit temperature T_3 combined with the unchanged turbine exit temperature T_5 increases the temperature difference which is available for heat exchange. The efficiency of the intercooled recuperated ideal cycle is very attractive, see **Figure 3.8**.

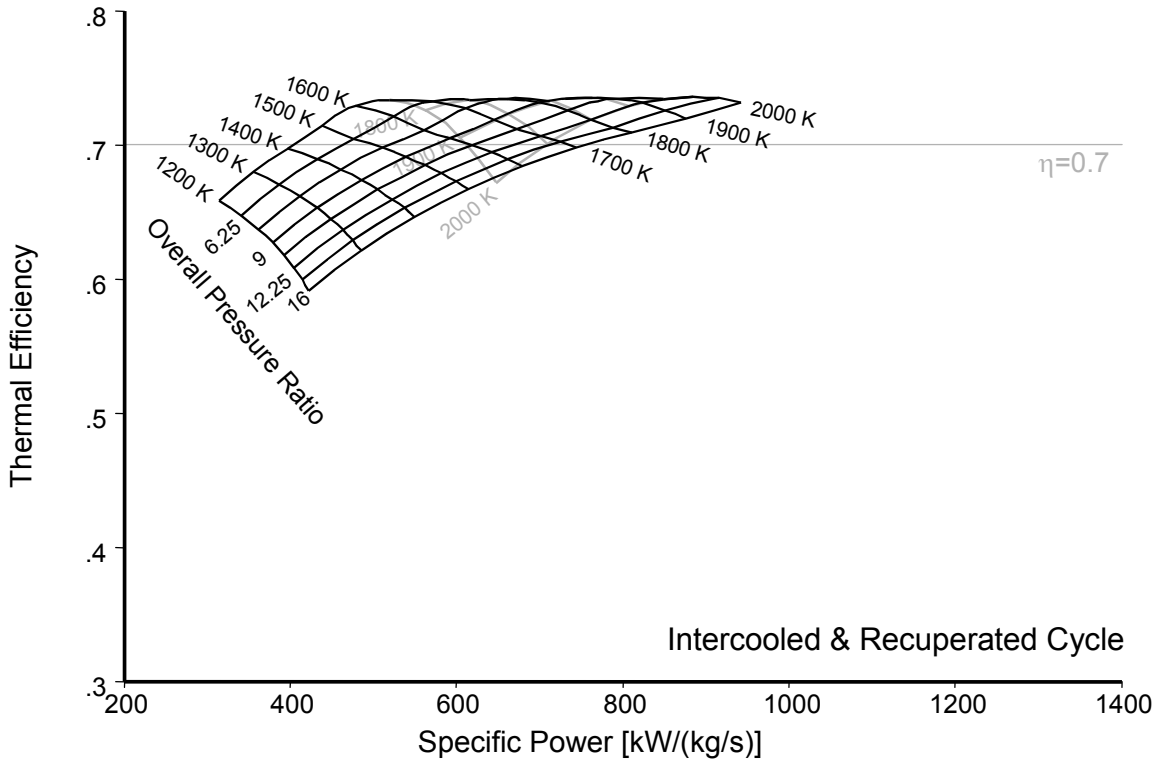

Figure 3.8: Efficiency of the Ideal Cycle with Intercooler and Recuperator.

Adding the intercooler and the recuperator makes the engine a rather bulky device, and the high power concentration in the turbo machines is only a minor advantage. Removing the heat from the intercooler requires a significant heat sink. In case of ship propulsion this is not a real problem since sea water can be used in the intercooler.

3.1.1.5 Reheated Cycle

Reheating the gas downstream of the high pressure turbine to the burner exit temperature again is equivalent to intercooling on the compressor side. The net work is increased with reheat because of the divergence of the isobar lines. The additional fuel required to get the increased power output decreases the thermal efficiency and makes it even worse than that of a cycle with intercooling. Specific power, however, is a bit higher than with the intercooled cycle, compare **Figure 3.7** and **Figure 3.9**.

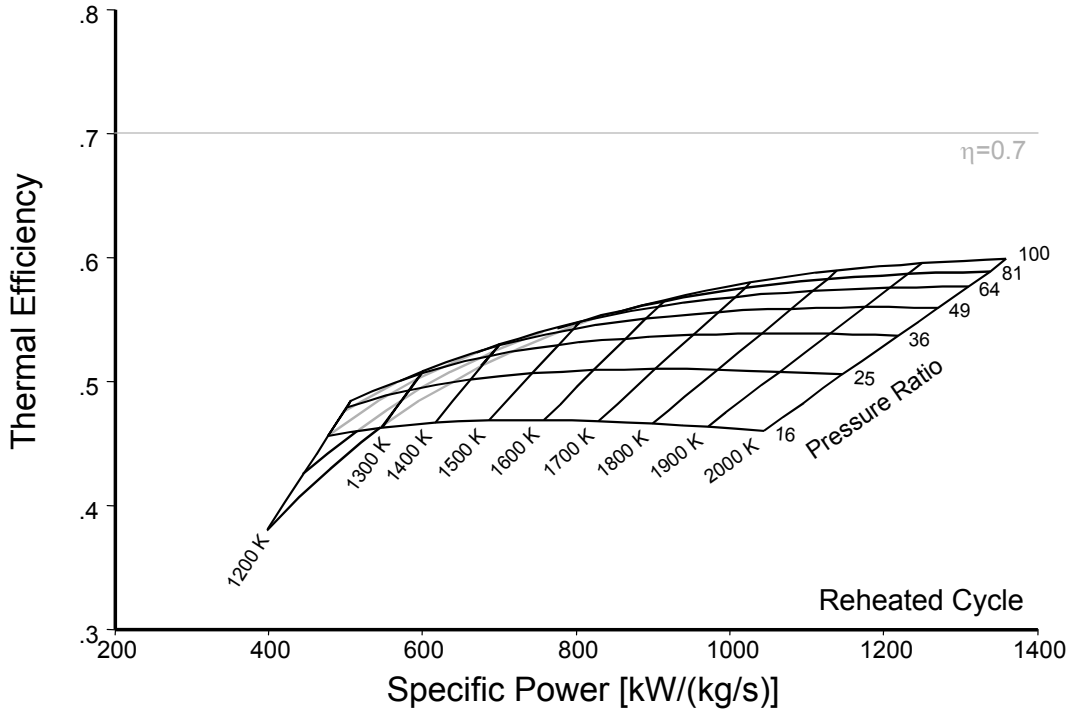

Figure 3.9: Efficiency of the Ideal Cycle with Reheat.

3.1.1.6 Combined Intercooling and Reheat

Both intercooling and reheating increase the temperature difference between turbine exit and compressor exit and thus make the use of a recuperator more attractive, see **Figure 3.10**. Without the recuperator the cycle yields very high specific work, but not a very good efficiency (see **Figure 3.11**).

Because of the high specific work for given absolute power, the compressors and turbines of this cycle would be rather small. However, especially the intercooler is a bulky device and the additional burner adds also to the volume of the machine. Overall the intercooled and reheated cycle without recuperator is not an attractive cycle.

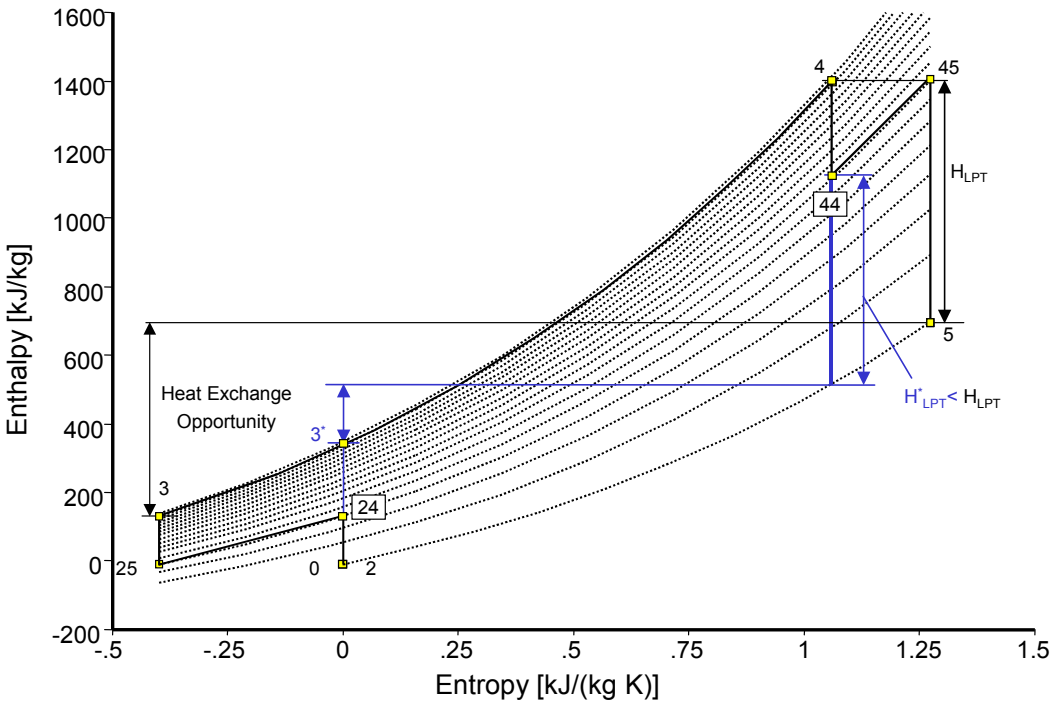

Figure 3.10: Ideal Cycle with Intercooling and Reheat.

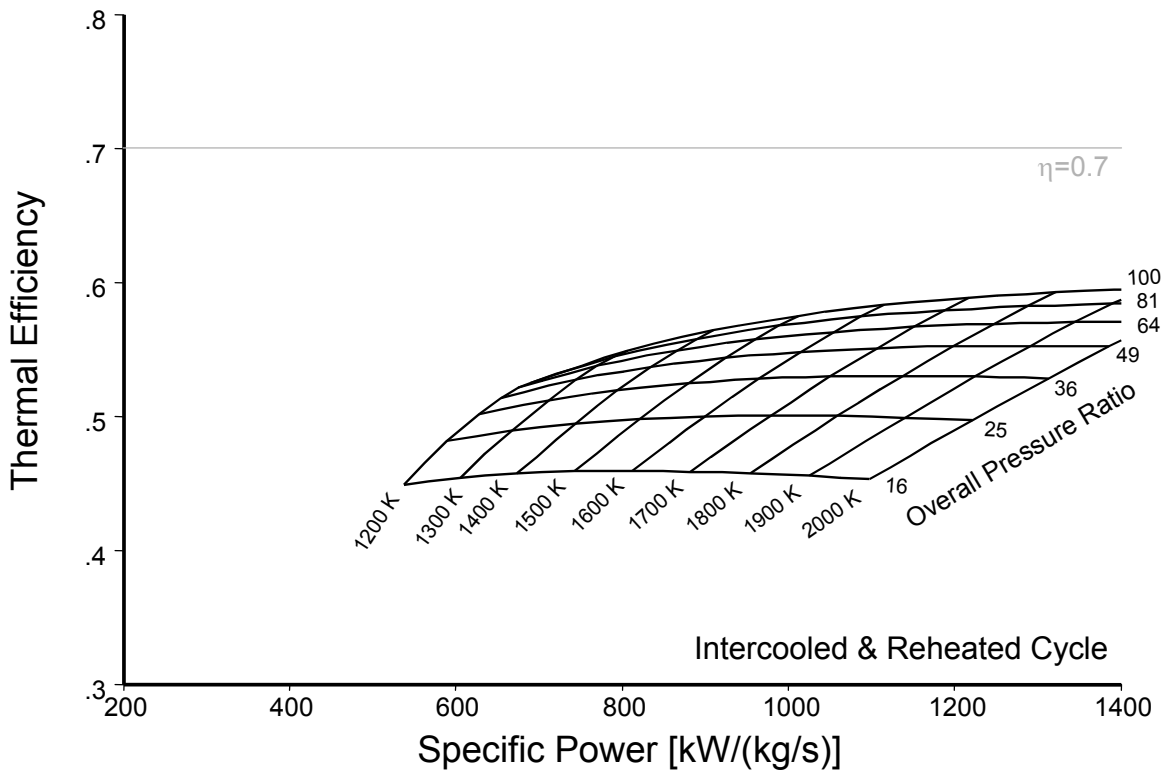

Figure 3.11: Efficiency of the Ideal Cycle with Intercooling and Reheat.

3.1.1.7 Combined Intercooling, Reheat and Recuperator

A machine with intercooler, reheat and recuperator yields, with a very moderate overall pressure ratio, the best efficiency (see **Figure 3.12**) of all the cycles discussed above. Certainly this machine has a significantly bigger volume than a simple Joule cycle gas turbine because of the additional components. Compared to the Joule cycle with recuperator the efficiency advantage is not very big so in summary the intercooled reheated ideal cycle with recuperator is not attractive.

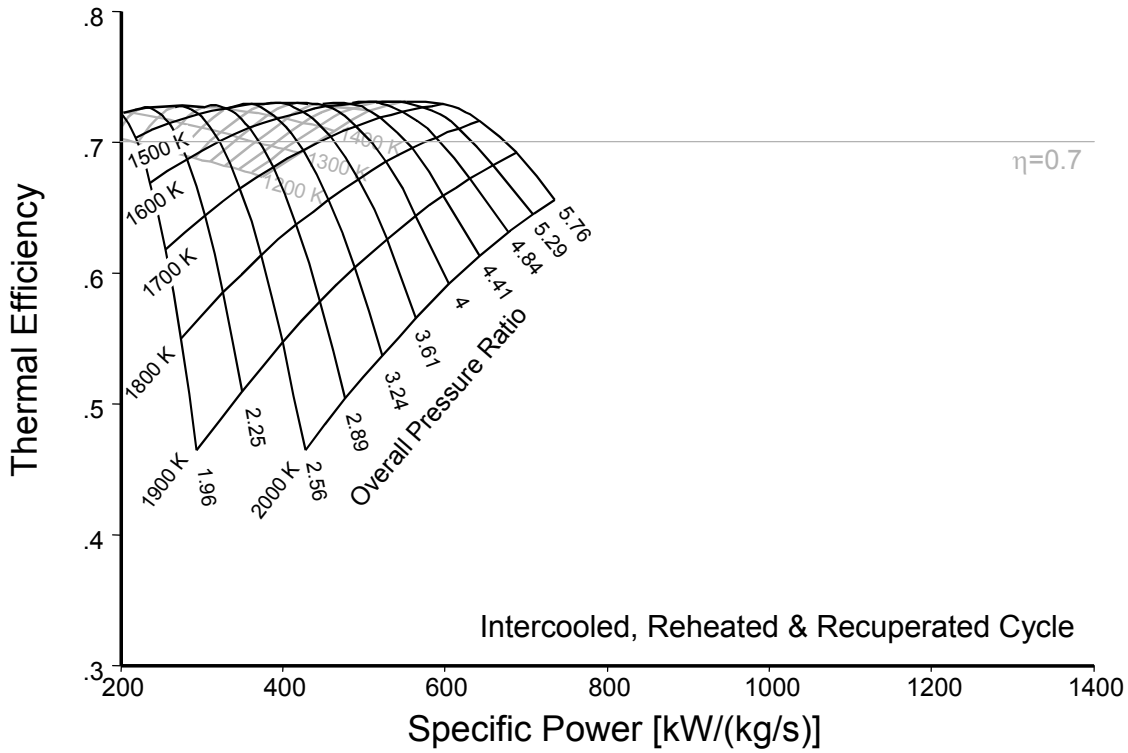

Figure 3.12: Efficiency of the Ideal Cycle with Intercooling, Reheat and Recuperator.

3.1.2 Real Joule Process

In a real cycle all turbo machines have an efficiency of less than 1.0 and the other components like ducts, the burner, and the inlet and exhaust system have pressure losses. Furthermore cooling air may be required for disks and blades, sealing of the bearings consumes also some air and some leakage is unavoidable. In the following we will not go into the details of a full engine cycle simulation but concentrate on the effect of the efficiencies of the major components on the thermal efficiency.

3.1.2.1 Nearly Real Joule Process

In a first step for both compressors and turbines the polytrophic efficiency is set to 0.9. No further losses are assumed, neither pressure losses nor leakages and cooling air. **Figure 3.13** shows in an enthalpy-entropy diagram the comparison of the ideal cycle with the "nearly real" cycle for the same specific power. To produce the same power, a higher turbine inlet temperature T_4 is required if there are losses. To achieve the higher turbine inlet temperature more fuel is needed and the consequence is decreased thermal cycle efficiency.

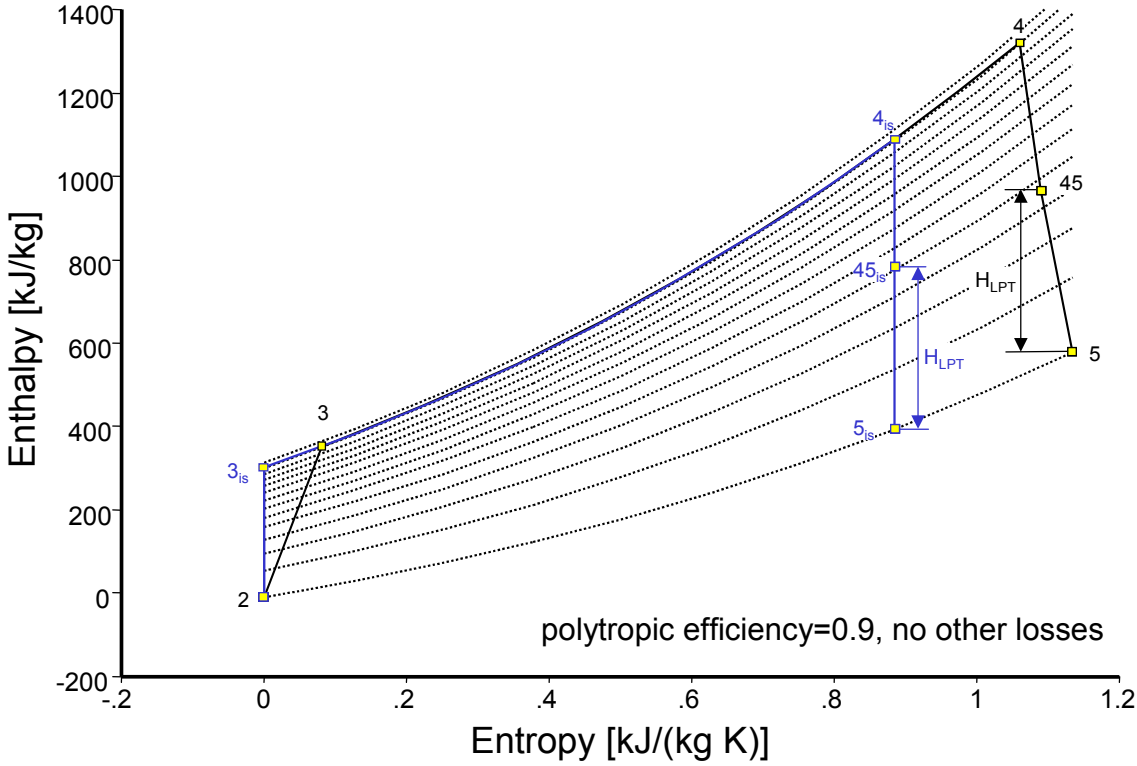

Figure 3.13: Ideal and Real Cycle for the Same Specific Work H_{LPT}.

While for the ideal cycle the thermal efficiency was nearly independent from turbine inlet temperature this is not the case for the real cycle. Both the thermal efficiency and the specific power are dependant on turbine inlet temperature. The maximum of the specific power is always at a lower pressure ratio than the maximum of the thermal efficiency.

For pressure ratio 50 and burner inlet temperature $T_4 = 2000$ K the thermal efficiency of the ideal process is above 0.6 (see **Figure 3.3**) while with the "nearly real" cycle (see **Figure 3.14**) only about 0.5 is achievable. Note that both figures employ the same scale to make comparisons simple.

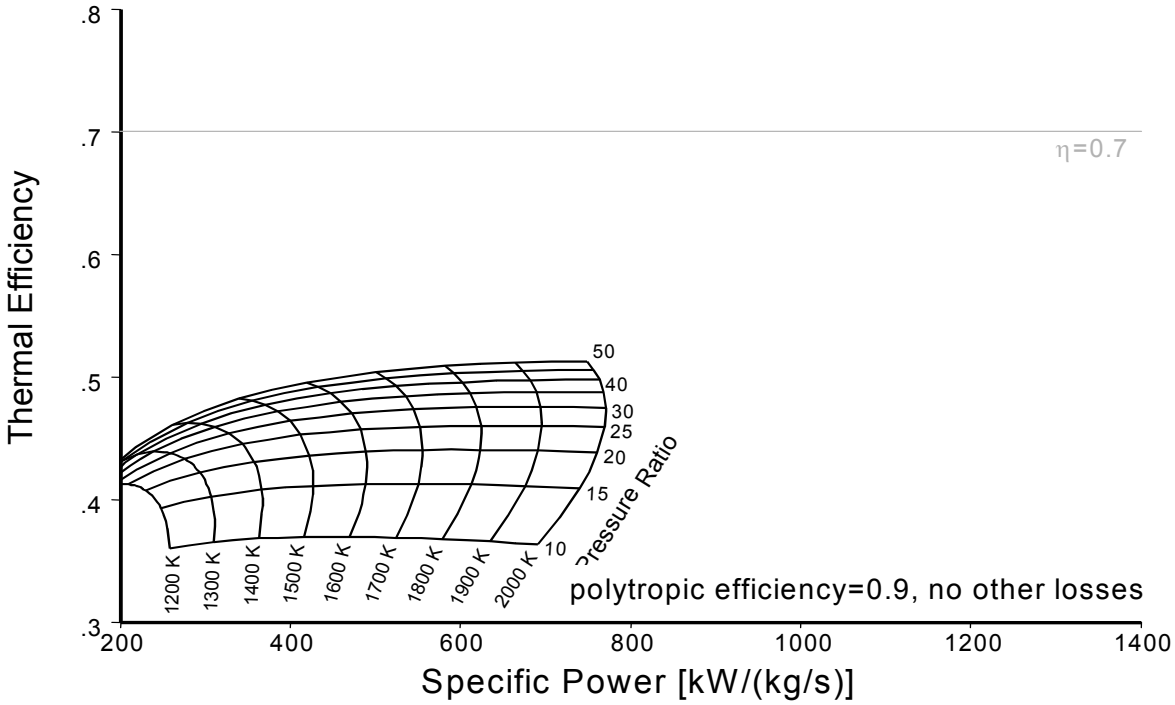

Figure 3.14: Thermal Efficiency of the "Nearly Real" Simple Cycle.

3.1.2.2 Turbine Cooling

Modern gas turbines operate at high burner exit temperatures and use significant amounts of cooling air for the high pressure turbine. This must be taken into account in more realistic cycle simulations. One often used modeling method separates the cooling and the expansion process in such a way that first the cooling of the turbine inlet guide vane is modeled, next follows the expansion and last the rotor cooling is considered, see **Figure 3.15**.

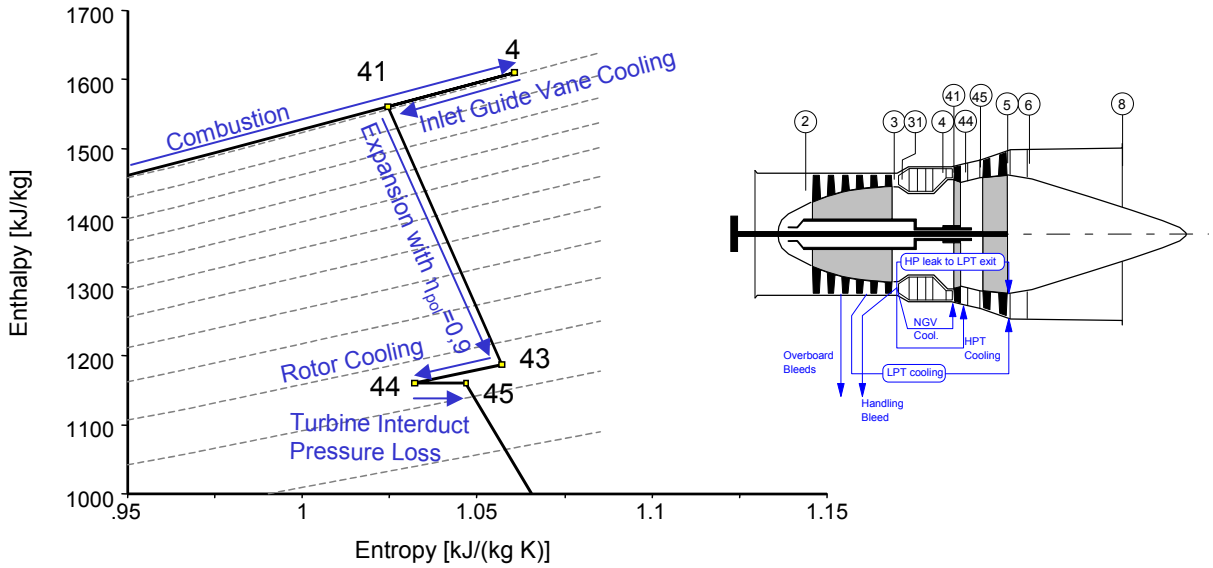

Figure 3.15: Simulation of a Cooled Turbine.

This modeling method works fine for single stage turbines, but requires some abstraction when applied to two stage turbines. For given compressor power and turbine pressure ratio the numbers employed for the amount of cooling air mixed upstream and downstream of the turbine rotor and the aerodynamic efficiency of the expansion process are interrelated.

The amount of cooling air must be adapted in parametric cycle design studies while high turbine inlet temperatures are considered. When constant metal temperature for the turbine inlet guide vane and the rotor blade are limitations then the relative cooling air mass flow W_{cl}/W_2 must be a function of both the hot gas temperature T_4 and the cooling air temperature T_3 which is dependant on cycle pressure ratio. Cooling effectiveness of a row of blades or vanes can be empirically described by the following formula:

$$\eta_{cl} = \frac{W_{cl} / W_{ref}}{W_{cl} / W_{ref} + C_1} \qquad \textbf{Eq. 3-1}$$

Using for the constant C_1 a value in the range of 0.03…0.07 yields a reasonable correlation which is valid for all sorts of cooling designs beginning with simple radial holes and ending with sophisticated multi-pass configurations combined with film cooling. For the following cycle studies the mean value of C_1 = 0.05 is used for finding the required amount of cooling air. This yields for 8% cooling air for the cooling effectiveness the value 0.615 and this is reasonably well in line with **Figure 3.16**.

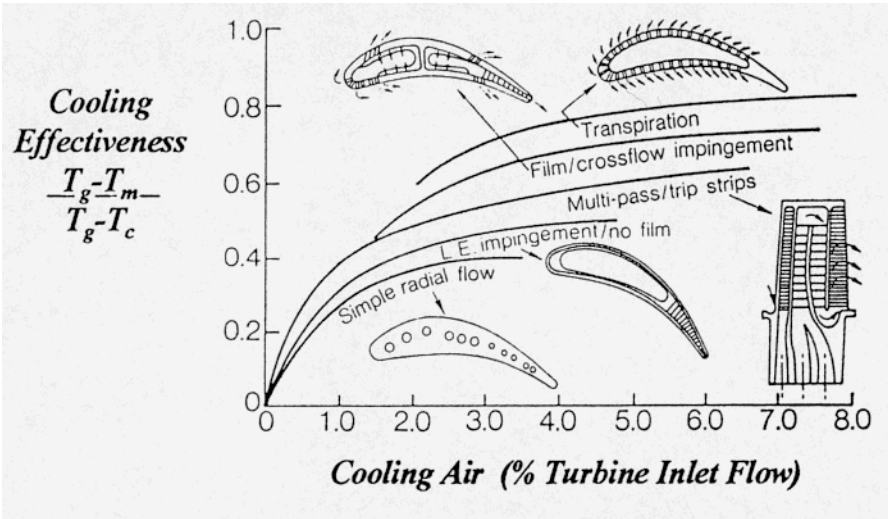

Figure 3.16: Cooling Effectiveness for Different Cooling Configurations [3.1].

The cooling effectiveness for the turbine inlet vane is

$$\eta_V = \frac{T_4 - T_{Metal}}{T_4 - T_3} \qquad \textbf{Eq. 3-2}$$

and for the rotor holds

$$\eta_R = \frac{0.9 * T_{41} - T_{Metal}}{0.9 * T_{41} - T_3} \qquad \textbf{Eq. 3-3}$$

In this correlation it is assumed that the total temperature of the hot gases relative to the rotor can be approximated by the term $0.9*T_{41}$.

Figure 3.17 shows the amounts of cooling air that are calculated from the formulae above for a metal temperature of 1200 K. The rotor cooling air is less than the stator vane cooling air because of the lower main gas temperature.

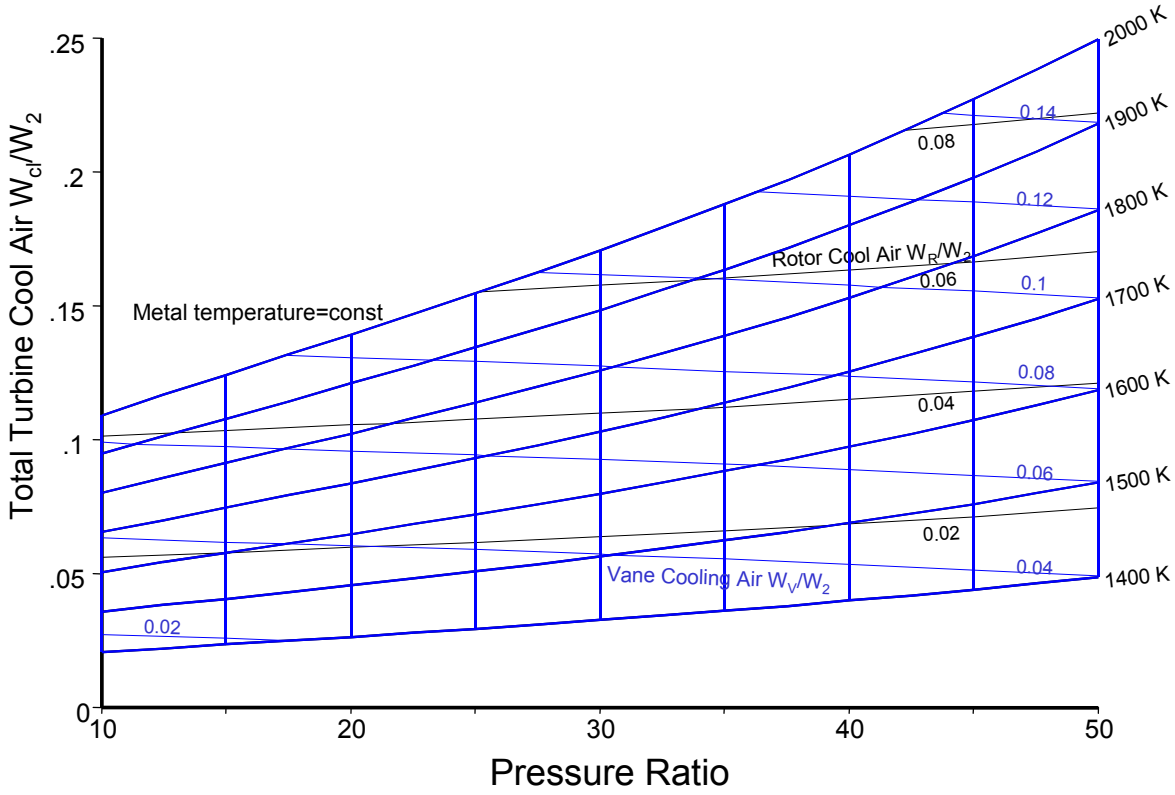

Figure 3.17: Cooling Air Amount for Constant Metal Temperature of 1200 K.

3.1.2.3 Real Joule Process

Up to now we have spoken about the losses in compressors and turbines as well as the cooling air. For a fully realistic cycle simulation also the pressure losses in the non-rotating components, some secondary air leakages and the kinetic energy of the exhaust gas stream have to be simulated. As typical numbers for the total pressure loss we introduce now 5% as the burner pressure loss and 1.02 as total/static pressure ratio at the exhaust of the turboshaft engine. Losses in the secondary air system are represented by 0.5% overboard leakage of high pressure air and the parasitic power required for driving the accessories are covered by a reduction of 0.2% of the high pressure turbine power.

Figure 3.18 shows the resulting cycle performance which should be compared with **Figure 3.3**. Note that in spite of the progressively increasing amount of cooling air the cycle with the highest burner exit temperature and pressure ratio yields the best thermal efficiency.

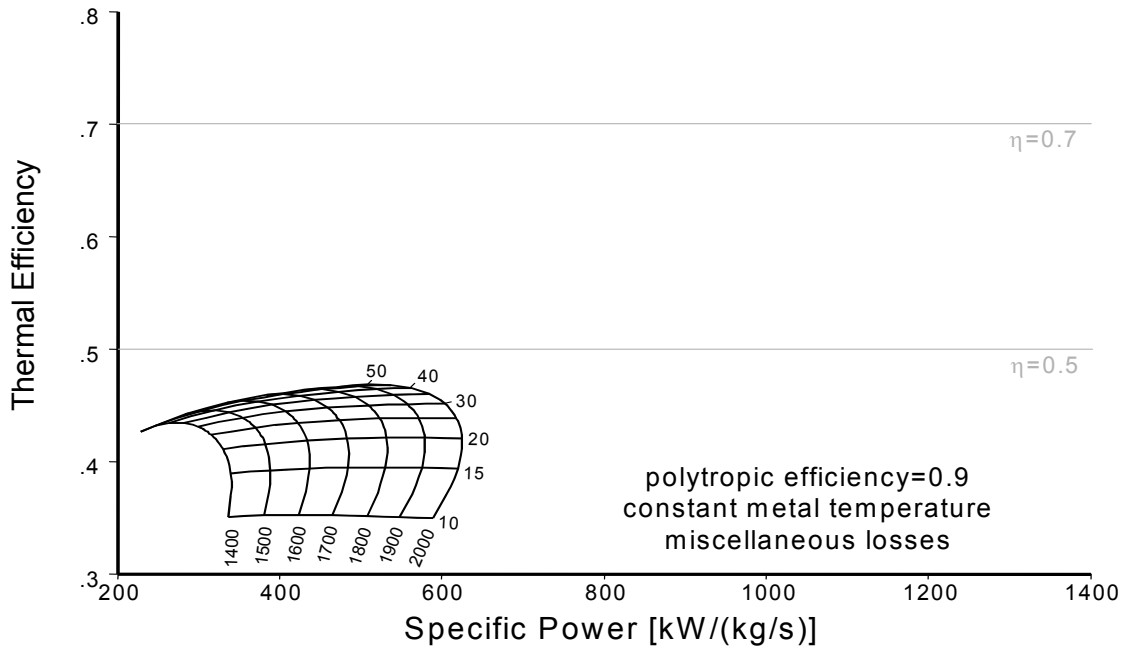

Figure 3.18: Performance of the Real Cycle with Constant Turbine Metal Temperature.

In **Figure 3.19** the results for the recuperated engine are shown. As can be seen the thermal efficiency is much better than that of the simple cycle, and the pressure ratio for the optimum efficiency is rather low.

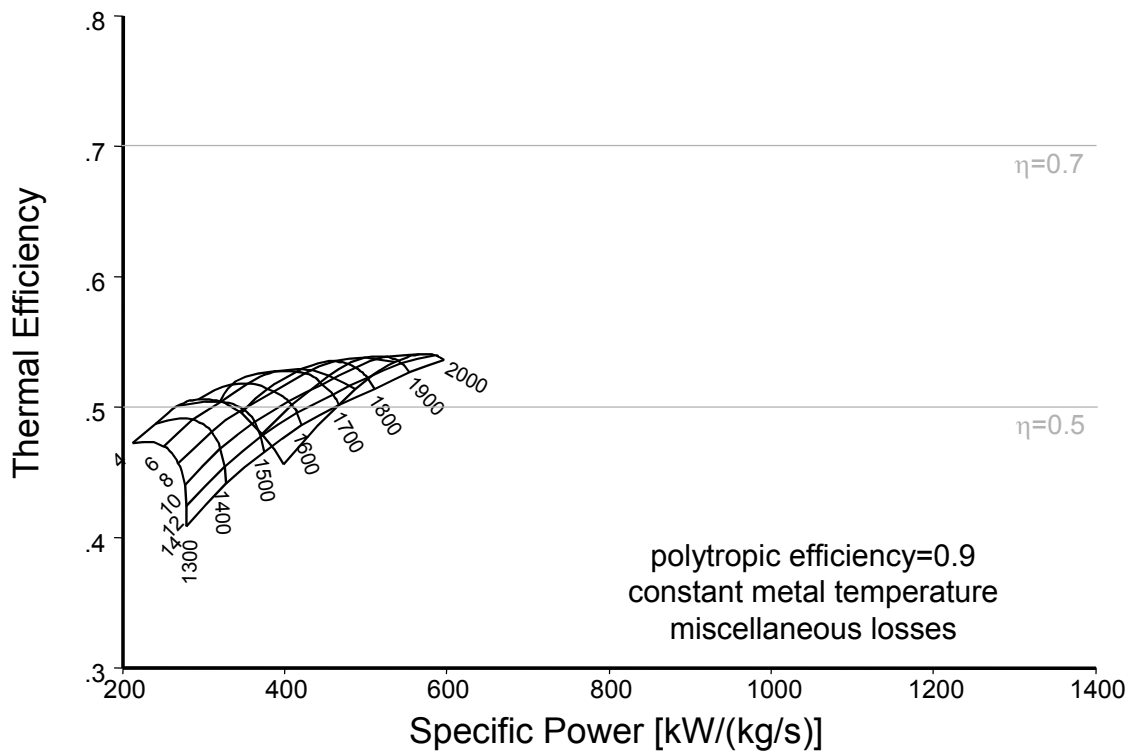

Figure 3.19: Thermal Efficiency of the Recuperated Cycle with Constant Turbine Metal Temperature.

Adding an intercooler increases specific work and also the thermal efficiency as can be seen from **Figure 3.20**. The pressure ratio for optimum efficiency is between the values found optimum for the simple cycle and the recuperated cycle.

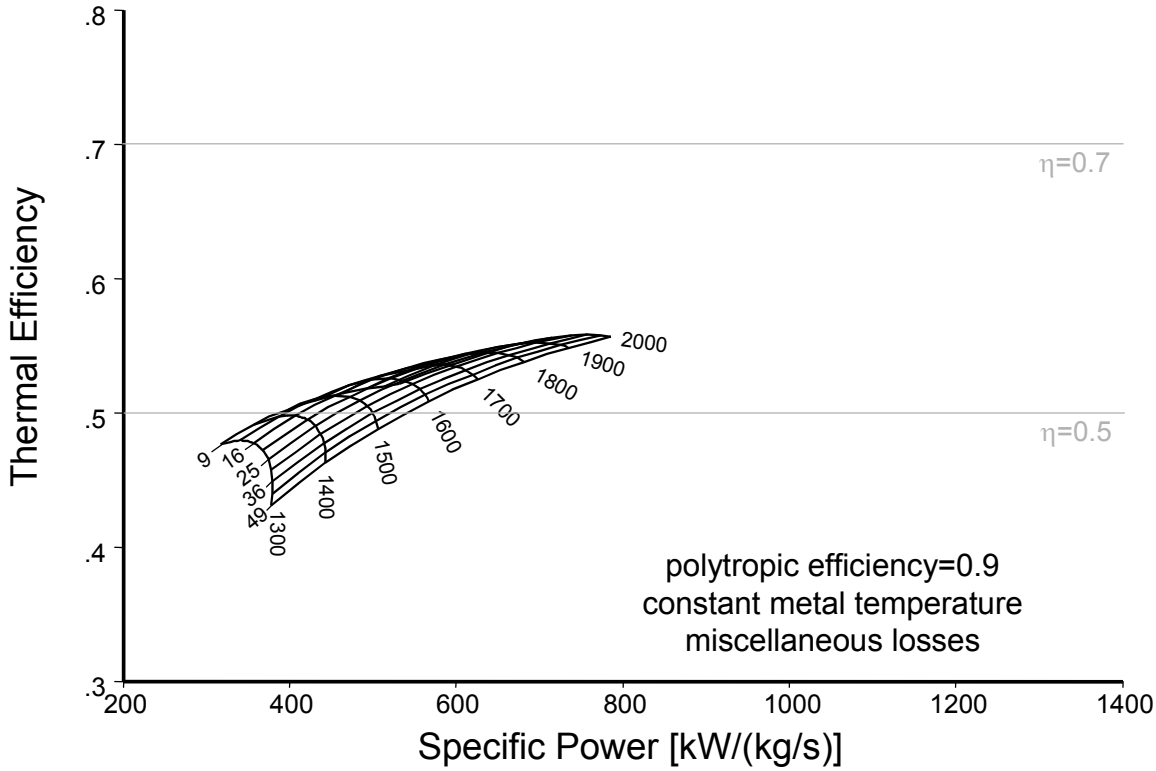

Figure 3.20: Thermal Efficiency of the Intercooled and Recuperated Cycle with Constant Turbine Metal Temperature.

The last three figures give an idea about which performance can be achieved with gas turbines. This however, is not the end of the story: the heat in the exhaust gas can be used for generating steam which is used to drive a steam turbine, for example. The steam can also be used for various other purposes and can even be injected into the burner of the gas turbine. The thermal efficiency of such an enhanced cycle will be better than shown above.

3.1.3 Efficiency Potential of the Simple Gas Turbine Cycle

The simple gas turbine cycle is of relevance for power generation, for ship, helicopter and turboprop aircraft propulsion. Moreover, considerations about this cycle give also an insight into the future of the aero engine gas turbine – which is typically a turbofan. This is because the turbofan engine cycle can be easily split into two parts: There is a core stream process (see **Figure 3.21**) which comprises of the primary flow commencing with ambient conditions up to a location within the low pressure turbine which is defined in such a way that all the compressor power needed for the core stream is covered. The second and third process parts deal with the bypass stream compression and expansion as well as with generating the core stream thrust.

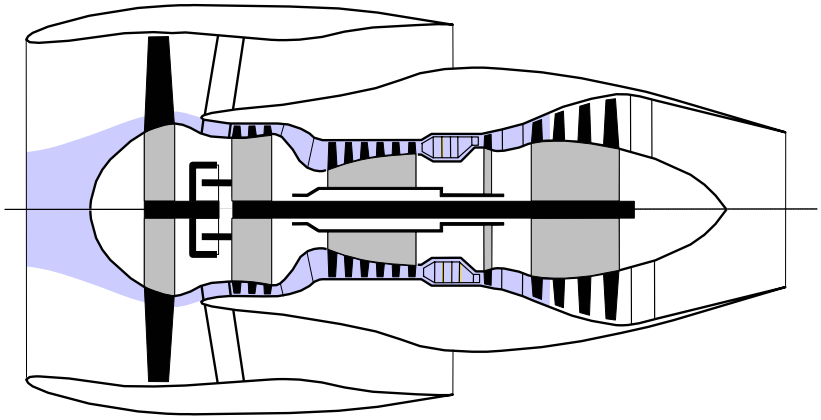

Figure 3.21: Core Stream Process of a Turbofan.

Apart from the compression of the incoming air from ambient conditions to inlet total pressure and temperature the core stream process is exactly the same as that of the simple cycle gas turbine.

The following discussions are restricted to the thermal efficiency of the gas turbine cycle and they do only touch shortly the specific power, i.e. the power per unit mass flow. Keep in mind that for aero propulsion applications the power developed per frontal area, per volume and per weight is an equally important attribute of any gas turbine core as its thermal efficiency.

The abstract of reference [3.2] begins with the statements: "Thermal efficiency of gas turbines is critically dependent on temperature at the turbine inlet; the higher this temperature, the higher the efficiency. Stoichiometric combustion would provide maximum efficiency". This view about gas turbine efficiency is widely spread, however, it is incorrect. In reference [3.3] it is shown that when gas properties are modeled accurately the variation of cycle efficiency with turbine inlet temperature at constant pressure ratio exhibits a maximum at temperatures well below the stoichiometric limit.

The authors of reference [3.3] come to the conclusion that the dominant influence for this unexpected phenomenon comes from the change of composition of the combustion products with varying fuel-air-ratio, particularly the contribution from the water vapor.

Let's begin with the findings from reference [3.3] and extend the study to effects that were not included in the referenced paper. At first the un-cooled cycle performance is discussed; the accuracy of the gas property modeling is improved in several steps with the aim of isolating the source of the efficiency maximum at temperatures well below the stoichiometric limit.

3.1.3.1 Schoolbook Wisdom

We consider the cycle of a simple gas turbine with 90% polytropic efficiency for both the compressor and the turbine and no pressure losses in other parts of the cycle. To simplify the considerations further the mass flow through compressor and turbine are assumed to be equal. With other words, the amount of high pressure air leakage is equal to the amount of fuel added.

3.1.3.1.1 Definition of Thermal Efficiency

The thermal efficiency of this cycle is equal to the specific turbine shaft power minus specific compressor shaft power divided by the amount of heat added in the burner. For constant specific heat one can write

$$\eta_{th} = \frac{H_T - H_C}{H_B} = \frac{T_4 - T_5 - T_3 + T_2}{T_4 - T_3} = 1 - \frac{T_5 - T_2}{T_4 - T_3} \qquad \textbf{Eq. 3-4}$$

If component efficiencies are 100% then holds

$$\frac{T_3}{T_2} = \frac{T_4}{T_5} \quad \textit{respectively} \quad \frac{T_5}{T_2} = \frac{T_4}{T_3} \qquad \textbf{Eq. 3-5}$$

This yields for the ideal Joule cycle that its thermal efficiency is only a function of pressure ratio:

$$\eta_{th} = 1 - \frac{T_2}{T_3} = 1 - \left(\frac{P_3}{P_2}\right)^{\frac{1-\gamma}{\gamma}} \qquad \textbf{Eq. 3-6}$$

If the component efficiencies are not 100% and the gas properties (isentropic exponent γ and gas constant R) are not constant then the formula becomes

$$\eta_{th} = \frac{\frac{\gamma_T}{\gamma_T - 1} * R_T * \frac{T_4}{T_2} * \left[1 - \left(\frac{P_2}{P_3}\right)^{\frac{\gamma_T - 1}{\gamma_T}}\right] * \eta_T - \frac{\gamma_C}{\gamma_C - 1} * R_C * \left[\left(\frac{P_3}{P_2}\right)^{\frac{\gamma_c - 1}{\gamma_c}} - 1\right] \Big/ \eta_C}{\left(\frac{T_4}{T_2} - \frac{T_3}{T_2}\right) * \left(\frac{\gamma_C}{\gamma_C - 1} * R_C + \frac{\gamma_T}{\gamma_T - 1} * R_T\right) \Big/ 2} \qquad \textbf{Eq. 3-7}$$

Since the temperature ratio T_3/T_2 is directly coupled with P_3/P_2 and compressor efficiency it is obvious that the thermal efficiency of the simply cycle gas turbine is a function of pressure ratio P_3/P_2, temperature ratio T_4/T_2, component efficiencies and the properties of the gas.

3.1.3.1.2 Constant Gas Properties

The most simple model of the cycle employs constant gas properties which means in the example shown below $\gamma_C = \gamma_T = 1.35$ and $R_C = R_T = 287$ J/kg/K. Evaluating thermal efficiency over a wide range of pressure ratios and temperatures with this simple gas property model yields the results shown in **Figure 3.22**. For a better view on the optimum thermal efficiency islands the parametric study is extended to pressure ratios well beyond any realistic case. The tendency in this figure is clear: increasing burner exit temperature at constant pressure ratio yields improved thermal efficiency.

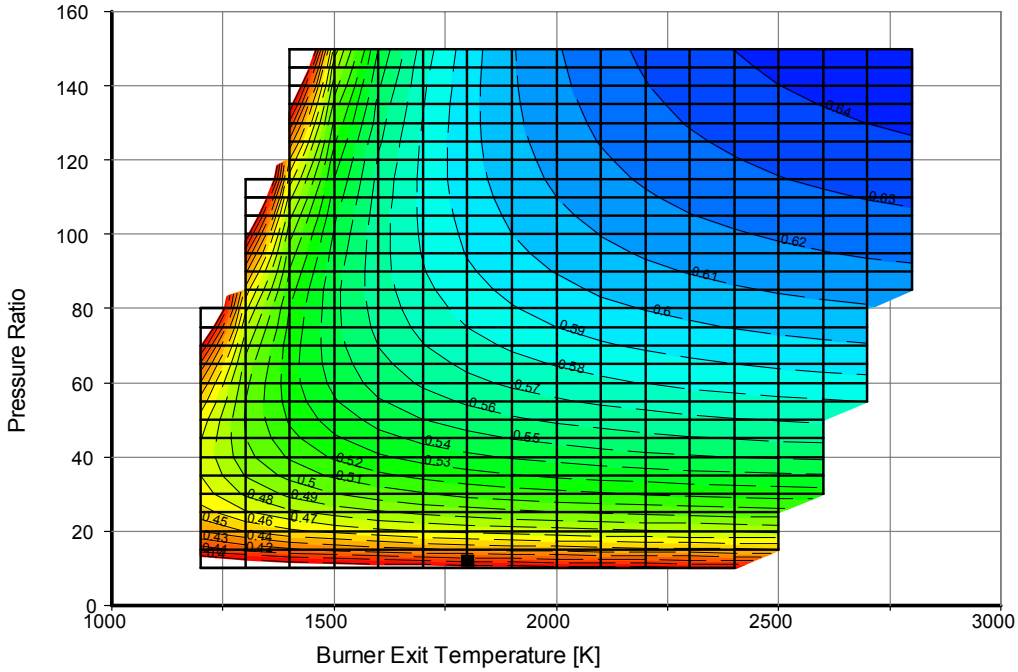

Figure 3.22: Thermal Efficiency Evaluated with Constant Gas Properties.

The top left corner is cut off because there the compressor exit temperature exceeds the burner exit temperature. The right border of the parametric study represents the maximum temperature achievable if Kerosene is used as fuel.

3.1.3.1.3 Temperature Dependent Gas Properties

Burning hydrocarbons (Kerosene, JP4 or Diesel, for example) with air leads to combustion gases that have practically the same gas constant as dry air. Thus the assumption $R_C = R_T = 287$ J/kg/K is valid, but the isentropic exponents γ_C and γ_T are in reality not constant but change significantly with temperature. Moreover, the magnitude of γ_T depends also from the composition of the combustion gases, i.e. the fuel-air-ratio.

The gas properties of combustion gases as well as the temperature rise due to combustion used in this paper have been calculated with the NASA CEA program, [3.4 and 3.5]. The effect of pressure on the heat release is taken into account; the pressure effect on the other gas properties (isentropic exponent, gas constant, enthalpy and entropy) is neglected.

Rerunning the parametric study with variable isentropic exponents – i.e. $\gamma_C = f(T)$ and $\gamma_T = f(T,far)$ – yields the results presented in **Figure 3.23**.

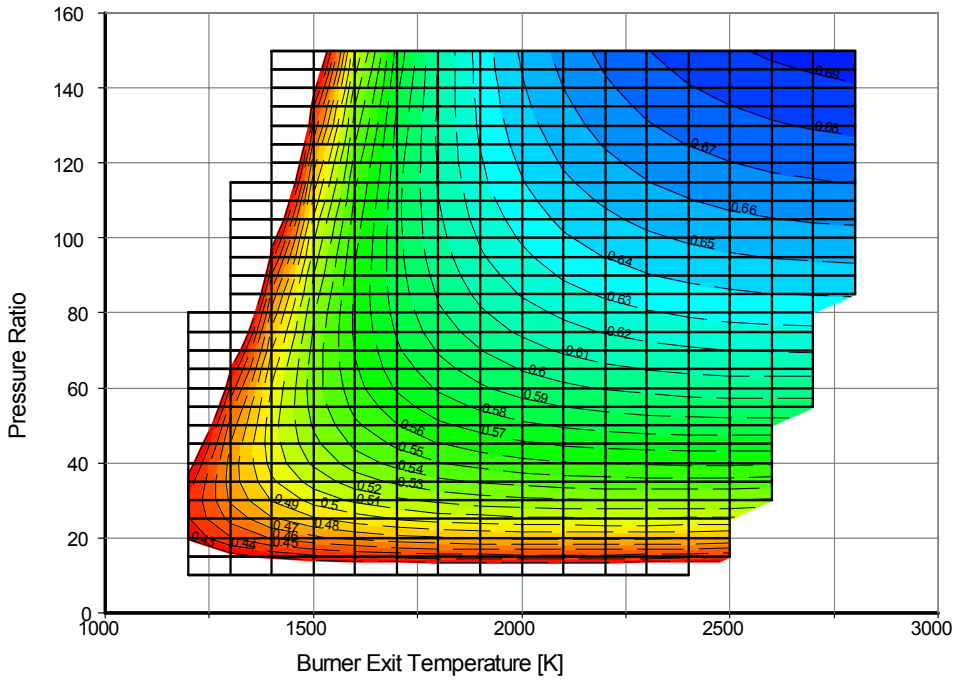

Figure 3.23: Thermal Efficiency Evaluated with Temperature Dependent Gas Properties.

There is not much difference between **Figure 3.22** and **Figure 3.23** and especially the tendency that the highest burner temperature yields the best thermal efficiency is the same in both models.

The question remains if a difference in the gas constant between compressor and turbine can change the basic shape of the efficiency contour lines. In the conclusions of **[3.3]** it is speculated that steam injection could have a mayor impact on the location of the maximum efficiency. The reasoning behind this is that the increased amount of water vapor in the combustion exhaust changes the specific heat in the expansion process significantly.

To study this effect the exercise has been repeated with steam injection (steam-fuel-ratio 1) into the burner. As can be seen from **Figure 3.24** again no significant change in the shape of the contour lines can be observed except that the maximum temperature achievable is reduced. This comes from two effects: first the percentage of oxygen in the gas consisting of a mixture of air and steam is lower than in dry air. Second some of the heat released by the chemical reaction is needed to heat the steam to burner exit temperature.

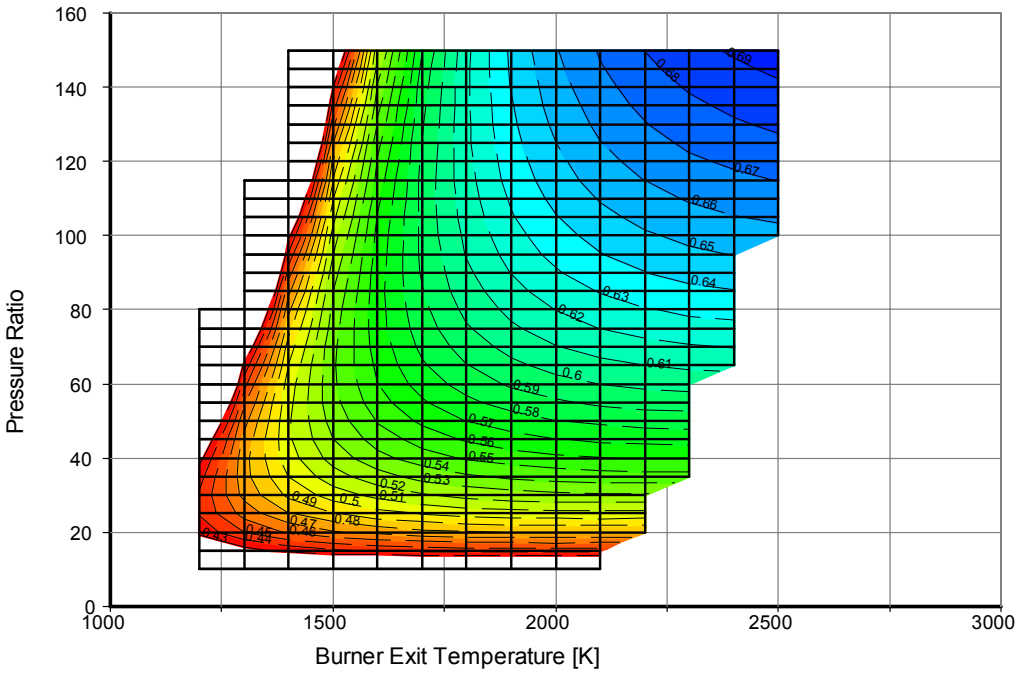

Figure 3.24: Thermal Efficiency with Steam Injection (Steam-Fuel-Ratio = 1), Evaluated with Temperature Dependent Gas Properties.

The authors of [3.3] come to the conclusion that the dominant influence for the thermal efficiency maximum which they have found originates from the change of composition of the combustion products with varying fuel-air-ratio, particularly the contribution from the water vapor. They make the specific heat of water vapor – which is significantly different to that of air and other combustion products – responsible for the maximum efficiency being at temperatures lower than stoichiometric.

The results shown above seem to be a contradiction to the findings from ref. 1 because no efficiency maximum below the stoichiometric temperature could be found even when the gas properties are modeled with the same accuracy as in ref. 1. Especially it has been demonstrated by the steam injection example that the gas properties of water vapor do not create an efficiency maximum at temperatures well below the stoichiometric limit.

In the calculations presented up to now only simple formulae as found in schoolbooks have been employed. Next the full blown cycle code from GasTurb [3.6] will be used for evaluating thermal efficiency.

3.1.3.2 Full Cycle Calculation

There is no difference between the gas property model in GasTurb [3.6] and that employed for getting the results reported above. Actually the calculations for ***Section 3.1.3.1.1*** of this chapter have been done with the same code which allows the user to add his own formulae as needed.

3.1.3.2.1 Definition of Thermal Efficiency

In the cycle code the thermal efficiency is defined as

$$\eta_{th} = \frac{H_T - H_C}{W_F * FHV} \qquad \textbf{Eq. 3-8}$$

The difference between this definition and the one used in ***Section 3.1.3.1.1*** is in the denominator: instead of the burner temperature difference T_4-T_3, multiplied by the mean specific heat, here the product of fuel flow W_F and fuel heating value FHV is used. This is reasonable because in the real world one has to pay for fuel, not for a temperature difference as implied with the schoolbook definition of thermal efficiency.

The result of using this definition of thermal efficiency one gets what is reported in **[3.3]**, see **Figure 3.25.** There is an optimum of thermal efficiency at temperatures well below the stoichiometric limit! At a given pressure ratio of 40, for example, increasing burner exit temperature beyond 2000 K would decrease thermal efficiency even if no cooling air is employed.

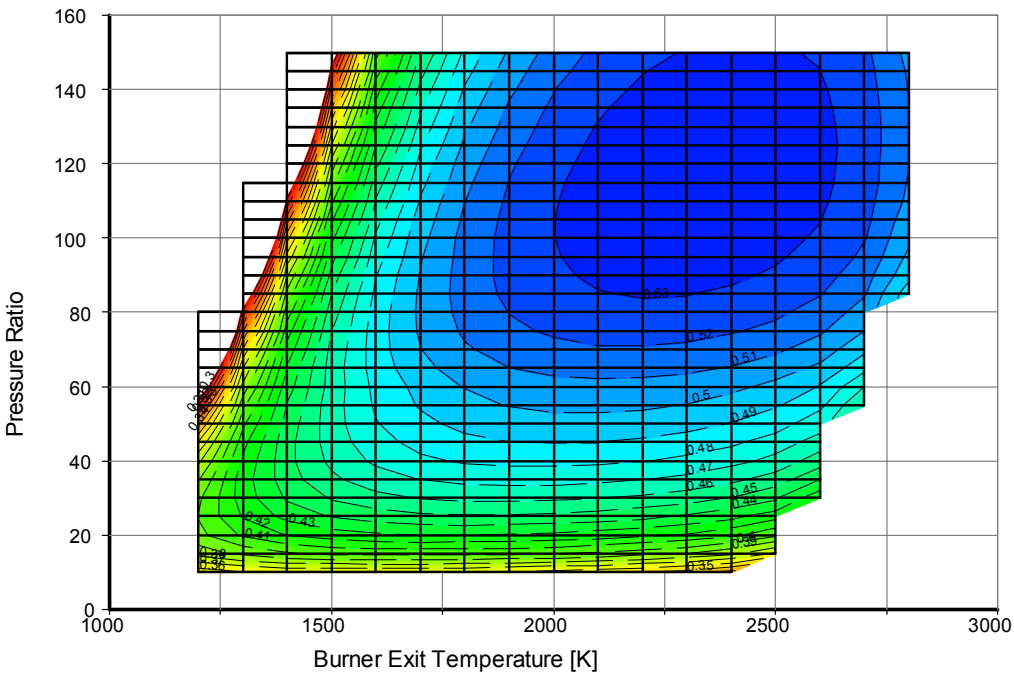

Figure 3.25: Thermal Efficiency Defined with W_F*FHV.

This optimum is obviously caused by using W_F*FHV as denominator and therefore it is adequate to study the heat release process in the burner in some detail.

3.1.3.2.2 Temperature Increase in the Burner

In the schoolbook definition of thermal efficiency the fuel flow is implicitly assumed to be proportional to C_p*(T_4-T_3). In reality fuel flow respectively fuel-air-ratio is not proportional to T_4-T_3 as can be seen from **Figure 3.26**.

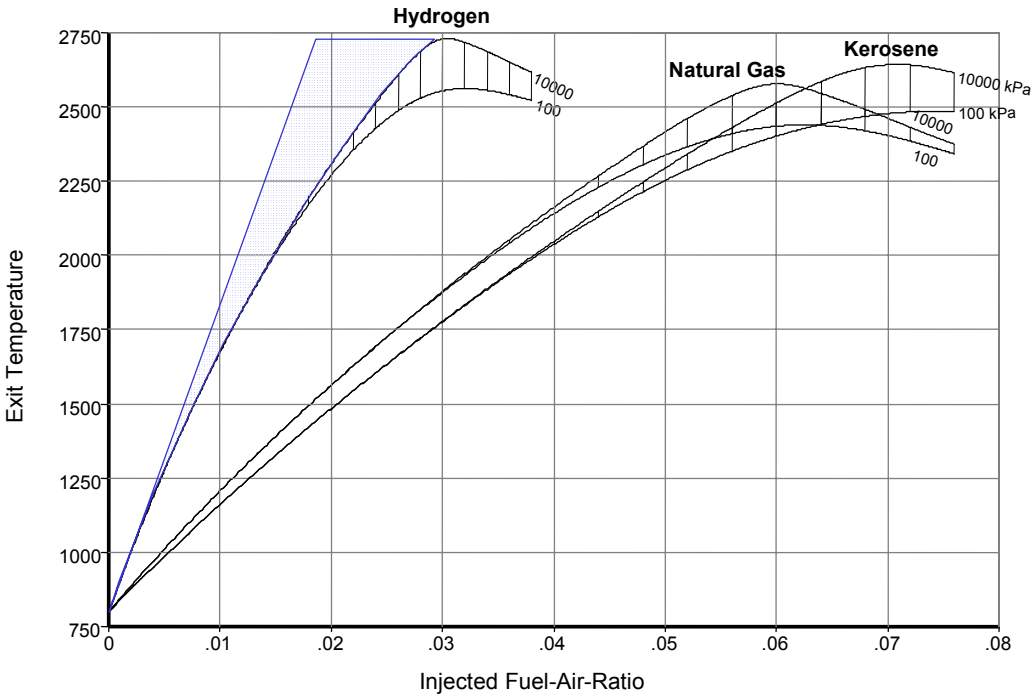

Figure 3.26: Burner Exit Temperature for Different Fuels (T_3 = 800 K).

For example, to get 2000 K exit temperature with hydrogen as fuel would require a fuel-air-ratio of 0.0115 if the amount of fuel would be proportional to the temperature increase as the blue line indicates. However, in reality one needs the fuel-air-ratio of 0.015 – which is 30% more. Note that this effect has nothing to do with dissociation – up to 2000 K the exit temperature is nearly independent from pressure which can also be seen in **Figure 3.26**.

The fact that for achieving high temperatures one needs over-proportional amounts of fuel is the reason for the maximum thermal efficiency being at a temperature much lower than the stoichiometric value. This effect is independent from the fuel type as can be seen from a comparison of **Figure 3.25** (fuel: Kerosene) with **Figure 3.27** which was calculated with hydrogen as fuel.

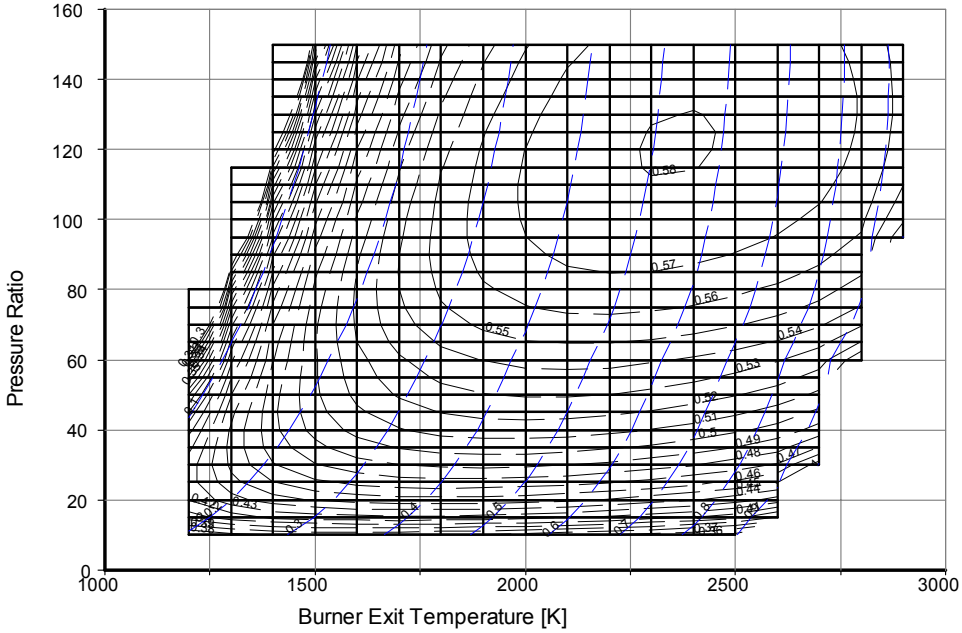

Figure 3.27: Thermal Efficiency with Hydrogen as Fuel with Lines of Constant Equivalence Ratio.

In **Figure 3.27** besides the lines for constant thermal efficiency also lines with constant equivalence ratio are shown. Equivalence ratio is defined as

$$ER = \frac{far}{far_{stoichiometric}} \qquad \textbf{Eq. 3-9}$$

The optimum thermal efficiencies as function of pressure ratio are found along the line ER = 0.5. The same correlation can be observed when lines for constant equivalence ratio are plotted into **Figure 3.25**. Thus the following generally valid statement can be made:

> *The maximum thermal efficiency of the simple gas turbine cycle with polytropic efficiencies equal to 0.9 and no cooling air simulation is found with fuel-air-ratios approximately equal to 50…60% of the stoichiometric value, independently from the type of hydrocarbon fuel burnt.*

3.1.3.2.3 Effect of Component Efficiencies

All the cycle studies discussed above were performed with the same assumption about the quality of the turbo-machinery: polytropic efficiencies were always equal to 0.9 and no further losses were considered except that the amount of air leakage was set to be equal to the amount of fuel used.

What happens if the component efficiencies are different has been already reported in **Ref. [3.3]**. As the efficiencies are increased the point of maximum cycle efficiency shifts at constant pressure ratio to lower values of T_4. **Figure 3.28** shows this for the example of pressure ratio 60.

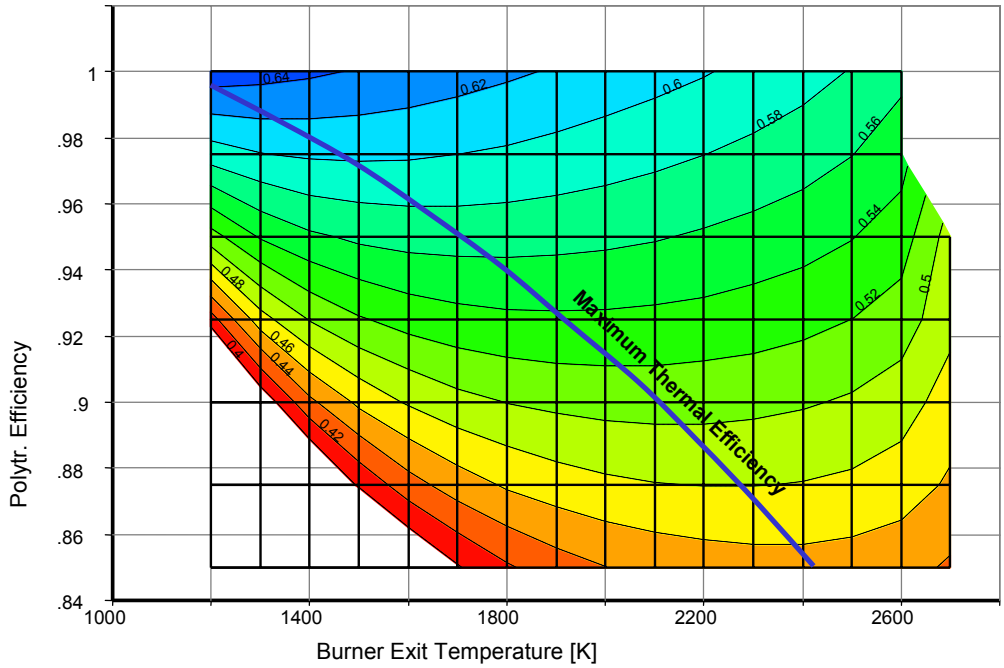

Figure 3.28: Burner Temperature for Maximum Thermal Efficiency, Pressure Ratio = 60.

3.1.3.2.4 Cooling Air Simulation

For more accurate simulations of course the amount of cooling air needed and the associated losses must be modeled adequately. Here we employ a rather simple method for estimating the amount of cooling air which correlates permissible mean metal temperature, cooling air amount, cooling effectiveness, cooling air temperature and T_4.

Only the cooling of the first turbine stage is considered. The vane cooling air is mixed with the main stream before the first rotor and thus the rotor entry temperature T_{41} is lower than the burner exit temperature T_4. With respect to rotor cooling the relative total temperature T_{41R} is the driving parameter. Without going into the details of an aerodynamic turbine design this temperature is approximated as $T_{41R} = 0.9*T_{41}$.

For finding an appropriate amount of cooling air the cooling effectiveness is used:

$$\eta_{cl} = \frac{T_{gas} - T_{metal}}{T_{gas} - T_{coolant}} \quad \eta_{cl} = \frac{T_4 - T_{metal}}{T_4 - T_3} \qquad \textbf{Eq. 3-10}$$

The amount of cooling air needed for achieving a certain cooling effectiveness depends on the design of the vane respectively blade cooling. For low cooling effectiveness it is sufficient to employ a design with convective cooling while for higher η_{cl} values film cooling is required. An approximate value for the amount of cooling air needed can be found from the empirical correlation which is taken from the GasTurb user's manual [3.6]:

$$\frac{W_{cl}}{W_{gas}} = C * \frac{\eta_{cl}}{1 - \eta_{cl}} \qquad \textbf{Eq. 3-11}$$

This expression can also be found in reference [3.7] (which contains also several more similar correlations) together with quite some physical background.

The constant C in the formula is set to 0.05 which yields a reasonable amount of cooling air over the full range in the parametric study. The result for thermal efficiency is shown in **Figure 3.29**.

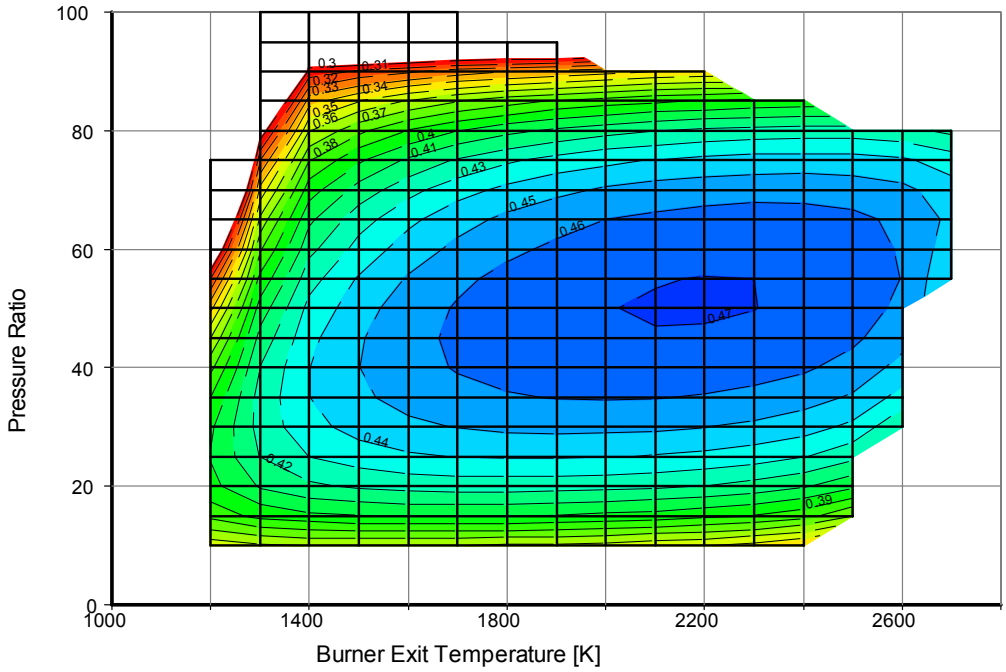

Figure 3.29: Thermal Efficiency with Cooling Air Simulation.

Now we see the optimum at a place which is not far from a realistic cycle. The whole top right part – where high pressure ratios are combined with high temperatures – does no longer exist. The reason is the excessive amount of cooling air which would be needed in this region; **Figure 3.30** shows the amount of NGV cooling air, the numbers for the rotor cooling air are somewhat smaller.

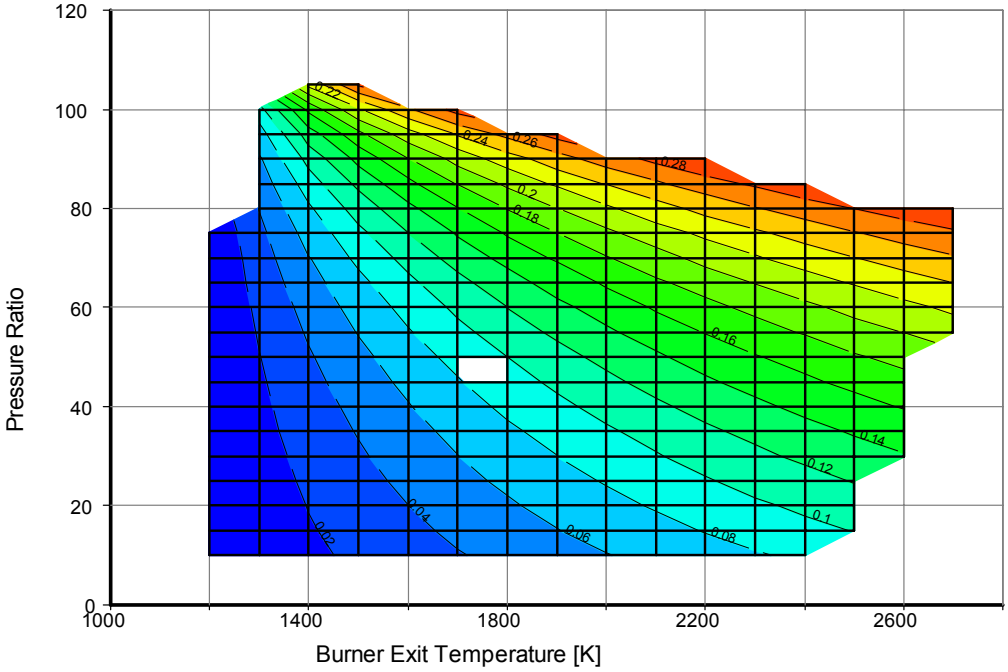

Figure 3.30: NGV Cooling Air W_{CL}/Wgas.

The equivalence ratio at the optimum thermal efficiency is $ER_{max\ eff}$ = 60% and thus about 10% higher than that for the un-cooled cycle, see the elaborations in the section about the temperature increase in the burner.

If **Figure 3.29** would show the design space of a real engine, and the only figure of merit would be the thermal efficiency then one would select from **Figure 3.29** as cycle design point the parameter combination P_3/P_2 = 50 and 2200 K. However, since the combination P_3/P_2 = 40 with 1800 K burner exit temperature yields only 1% less thermal efficiency than at the maximum it would in practice be the better choice because it requires significantly less design effort and cost.

3.1.3.2.5 Discussion

Optimizing an aircraft engine does not only ask for high thermal efficiency but also for low weight and low frontal area, in other words for high specific power per unit of mass flow. Specific power always increases with burner exit temperature and the maximum shows up at significantly lower pressure ratio than that required for optimum thermal efficiency. This is illustrated in **Figure 3.31** in which the dashed arrow indicates maximization of thermal efficiency while the solid arrow connects the maxima of specific power at any given burner exit temperature.

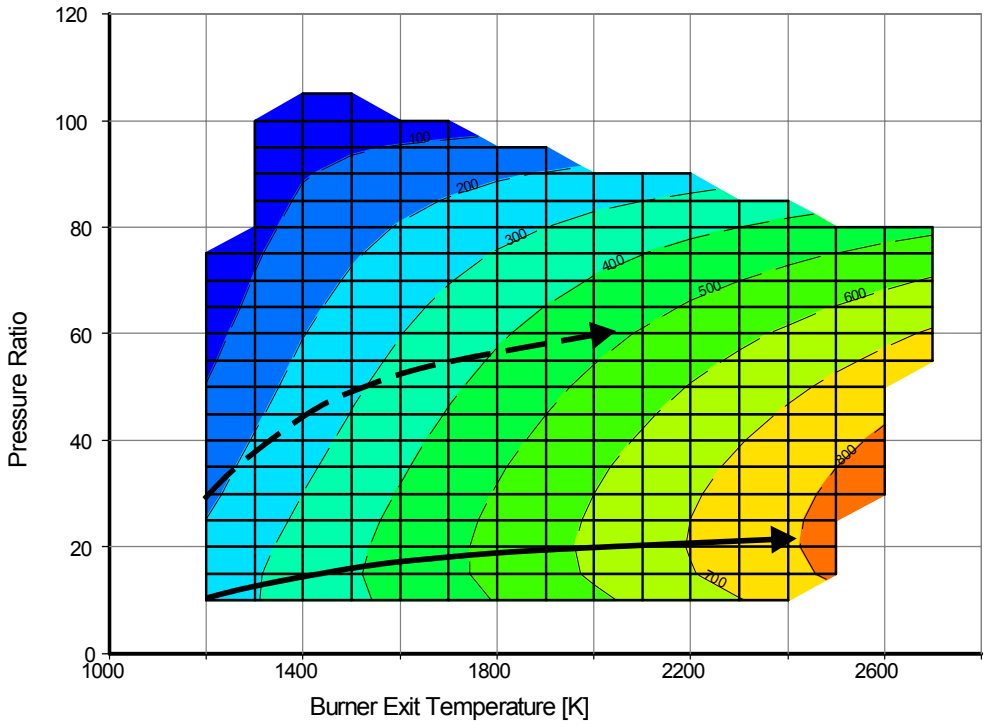

Figure 3.31: Specific Power.

The most economic engine designs of the future will be compromises between optimizing the core thermal efficiency and its power per unit mass flow. Dependent on the flight mission one or the other figure of merit will be more important. Both the pressure ratio and the burner exit temperature of modern engines are already near to their optimum values with respect to thermal efficiency. No significant increase in pressure ratio or burner exit temperature is beneficial for the turbofans of the future. Improvements of specific fuel consumption will be moderate since also the main element of the second process part – the bypass ratio – is already near to its practical limit for a conventional turbofan configuration.

Of course the improvement of component efficiencies and the reduction of the cooling air requirements will remain also in future important goals of any engine maker. However, success in that direction is extremely difficult since at the same time economics require that the number of parts being reduced which has the consequence that the aerodynamic loading increases. Moreover, the technical standard of today is already very high which makes further progress also very difficult.

3.1.3.2.6 Conclusions

- Increasing thermal efficiency is achieved most effectively by increasing pressure ratio, not by increasing burner exit temperature towards the stoichiometric limit.
- At a given pressure ratio limit the thermal efficiency will decrease if the specific power is increased.
- The specific fuel consumption of a conventional turbofan engine can be improved by increasing component efficiencies, overall pressure ratio and bypass ratio, but not by increasing the burner temperature much above the values achieved already today. There is not much room for improvement of the component efficiencies since modern optimized 3-D blade designs are already very good. Raising the efficiency of a low pressure turbine from say 93 to 94% would mean decreasing the losses by 15% and that certainly would be very ambitious.
- There is also not much room for increasing the bypass ratio above 10.

- There is not much to expect from future increases in component efficiencies, pressure ratio and bypass ratio. An increase in burner temperature does not yield improved cycle efficiency. It must be concluded that for commercial turbofan engines significant improvements of the specific fuel consumption can only be expected if a new engine concept invalidates the findings presented in this section.

In the preceding section we considered the generation of shaft power, and its direct relevance for the propulsion system of a helicopter, a ship or a land vehicle. However, instead of creating shaft power we can also create thrust from the energy available at the exit of the high pressure turbine.

3.1.4 From Power Generation to Thrust Generation

3.1.4.1 Turbojet

The easiest way to get thrust from a simple cycle gas turbine is to expand the hot high pressure exhaust gases in a nozzle, see **Figure 3.32**. The performance of any aircraft gas turbine depends not only on compressor pressure ratio and burner exit temperature but also very much on the flight Mach number. The air is pre-compressed by the ram effect and thus the overall pressure ratio $P_3/P_{ambient}$ is much higher than the compressor pressure ratio P_3/P_2. Compressor inlet temperature T_2 is also higher than the ambient temperature and this affects again the thermodynamic cycle.

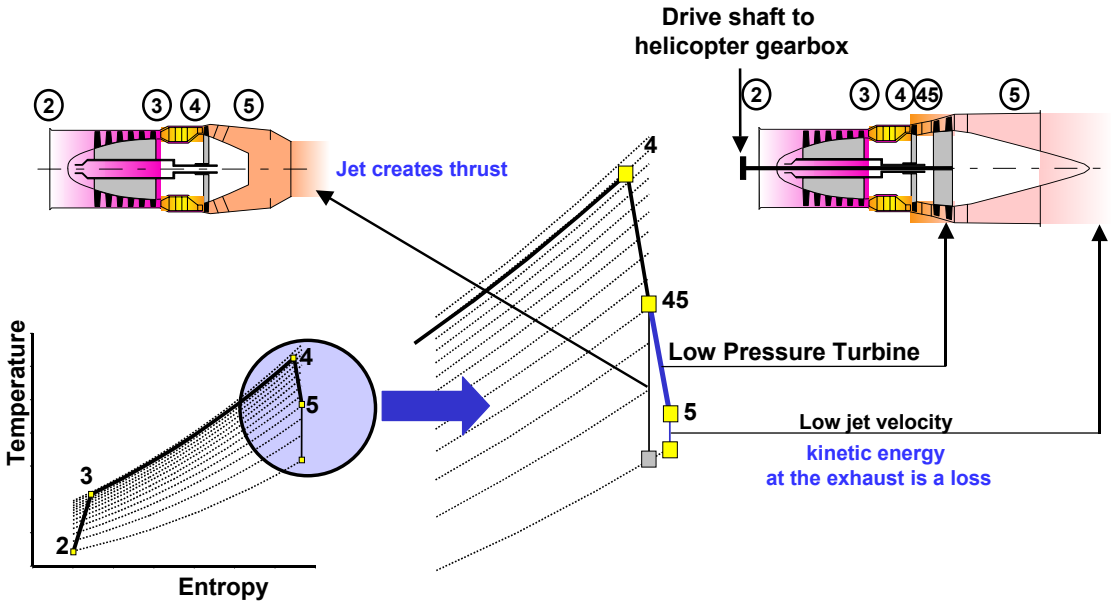

Figure 3.32: Turboshaft and Turbojet.

Figure 3.33 shows performance data for a turbojet flying at an altitude of 11 km. The loss assumptions for the gas turbine are the same as described in the ***Section 3.1.2***. An ideally matched convergent-divergent nozzle expands the exhaust gases to ambient pressure and the intake total pressure recovery is in case of supersonic flight dependent on Mach number Mn as described by **Mil-E-5007** [3.25]:

$$\frac{P_2}{P_1} = 1 - 0.075 * (Mn - 1)^{1.35} \qquad \textbf{Eq. 3-12}$$

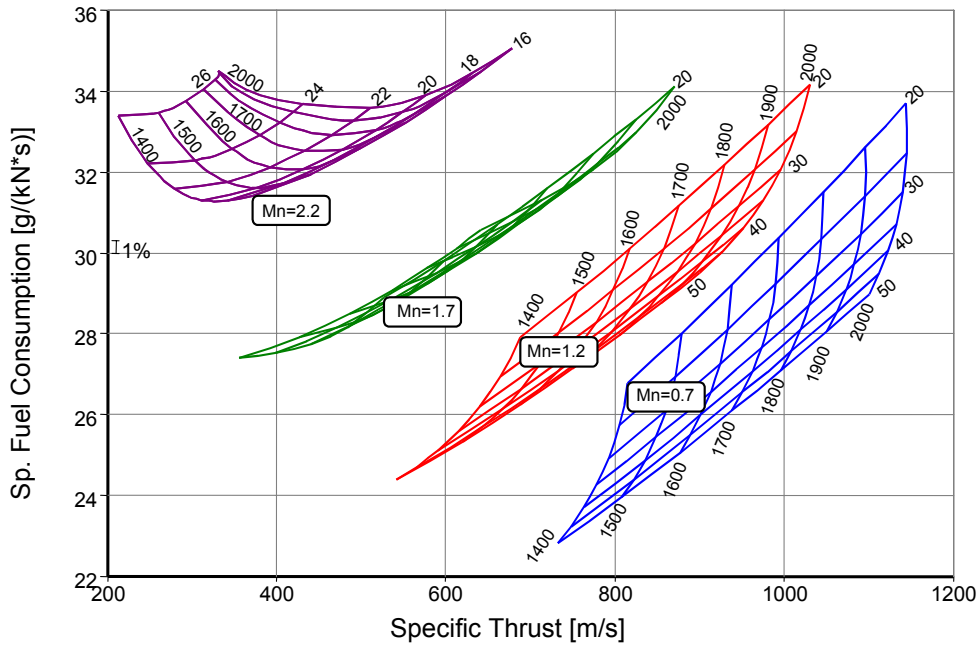

Figure 3.33: Turbojet Performance at 11 km.

All the gas turbines in **Figure 3.32** are of the same quality, if converted to a turboshaft by adding a power turbine with 90% polytropic efficiency they all would have the thermal efficiency shown in **Figure 3.18**. The changing thrust specific fuel consumption SFC with flight Mach number originates from the differences in propulsive efficiency. The definition of propulsive efficiency is given in ***Section 3.1.5.1***.

3.1.4.2 Turbofan

Reducing the jet velocity is the way to increase propulsive efficiency, and this is achieved in a turbofan by extracting energy from the core stream – which decreases core jet velocity – and creating a secondary stream with moderate jet velocity. The engine can be designed such that both streams are expanded separately or they are mixed and then expanded in a common nozzle.

The loss assumptions for the gas generator calculation of the turbofans in **Figure 3.34** are the same as for the turbojet example in the previous section. For both the fan and the low pressure turbine the polytropic efficiency is 0.9; both streams are expanded through convergent nozzles.

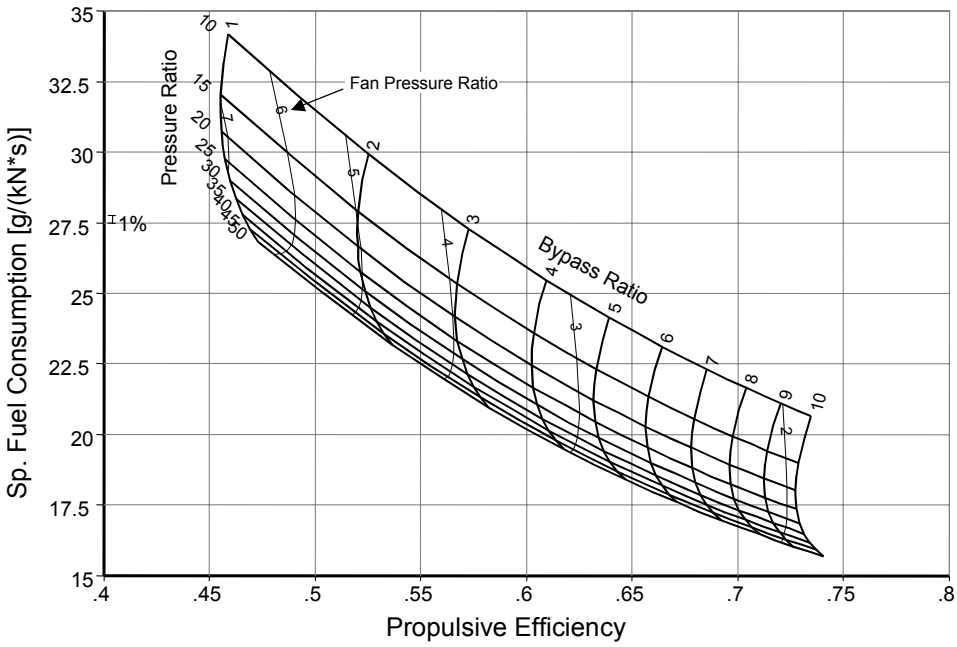

Figure 3.34: Turbofan with T_4 = 2000 K, Alt = 11 km, Mn = 0.85.

Note, however, that the SFC improvement comes at a price: For a given thrust the size of the engine, here expressed as fan tip diameter, increases significantly with bypass ratio because the specific thrust (thrust per unit mass flow) decreases with jet velocity, see **Figure 3.35**. Moreover, the pressure ratio of the low pressure turbine increases also and that means an increase in the turbine stage count.

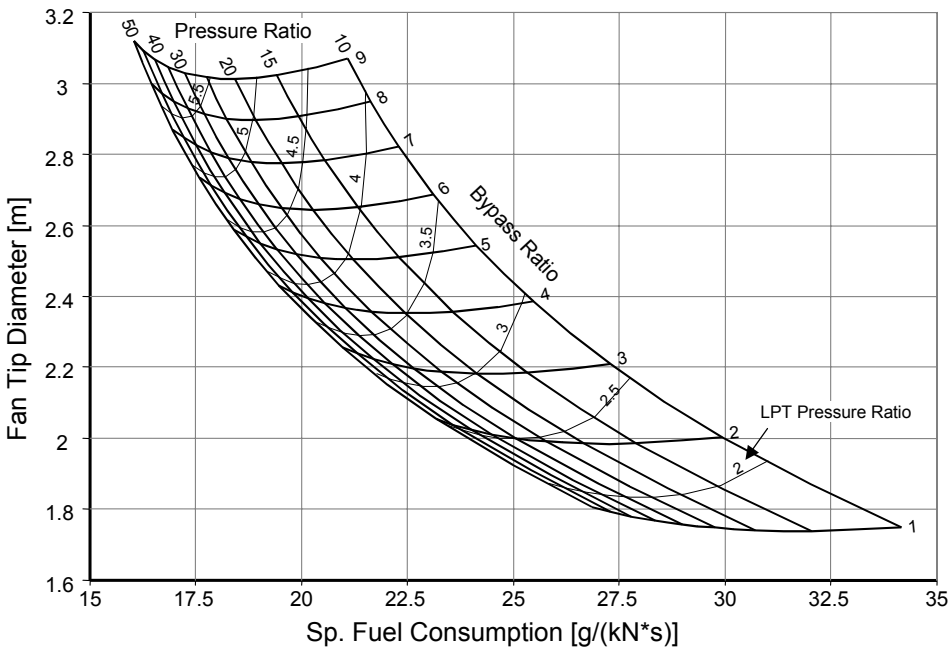

Figure 3.35: Fan Tip Diameter and LPT Pressure Ratio. Constant Thrust @ alt = 11 km, Mn = 0.85.

3.1.5 Quality Criteria

The quality of the thermodynamic cycle and its suitability for a specific task can be expressed in various types of efficiencies.

3.1.5.1 Propulsive Efficiency

Propulsive efficiency is the ratio of useful propulsive energy – the product of thrust and flight velocity – compared to the sum of this energy and the wasted kinetic energy of the jet:

$$\eta_P = \frac{F * V_0}{F * V_0 + W_9 \frac{(V_9 - V_0)^2}{2}} \qquad \textbf{Eq. 3-13}$$

If the nozzle flow is expanded fully to ambient conditions and the inlet mass flow W_0 is equal to the nozzle mass flow W_9 then thrust F equals $W*(V_9-V_0)$ and the above formula can be rewritten as

$$\eta_P = \frac{2 * V_0}{V_0 + V_9} \qquad \textbf{Eq. 3-14}$$

Propulsive efficiency is highest when jet velocity equals flight velocity; however, in this case thrust is zero.

With a turbojet at subsonic flight conditions the exhaust jet velocity is very much higher than the flight velocity of the aircraft. The high kinetic energy which the exhaust jet has relative to the air is a loss and this results in poor propulsive efficiency and finally in high thrust specific fuel consumption even if all the component efficiencies are high.

When propulsive efficiency is evaluated for an unmixed flow turbofan then the core stream and the bypass stream must be considered:

$$\eta_P = \frac{F * V_0}{F * V_0 + W_9 \frac{(V_9 - V_0)^2}{2} + W_{19} \frac{(V_{19} - V_0)^2}{2}} \qquad \textbf{Eq. 3-15}$$

3.1.5.2 Thermal Efficiency

Thermal efficiency is defined as increase of the kinetic energy of the gas stream passing through the engine by the amount of heat employed which is given as product of fuel mass flow W_f and fuel heating value FHV:

$$\eta_{th} = \frac{\frac{1}{2} W_9 * V_9^2 - \frac{1}{2} W_0 * V_0^2}{W_f * FHV} \qquad \textbf{Eq. 3-16}$$

With turbofan engines one can split the thermal efficiency in two terms, the core efficiency and the transfer efficiency.

Core Efficiency is the ratio of energy available after all the power requirements of the core stream compression processes are satisfied – that means at the core exit – and the energy available from the fuel:

$$\eta_{core} = \frac{W_{core} * (dH_{is} - V_0^2 / 2)}{W_f * FHV} \qquad \textbf{Eq. 3-17}$$

The enthalpy difference dH_{is} is evaluated assuming an isentropic expansion from the state at the core exit to ambient pressure.

Transmission Efficiency describes the quality of the energy transfer from the core stream to the bypass stream. It is defined as ratio of the energy at the nozzle(s) to the energy at the core exit and is equal to the thermal efficiency divided by core efficiency:

$$\eta_{trans} = \frac{\eta_{th}}{\eta_{core}} \qquad \textbf{Eq. 3-18}$$

As can be seen from **Figure 3.36** the transmission efficiency is dominated by the efficiencies of the fan and the low pressure turbine, and both efficiencies are equally important.

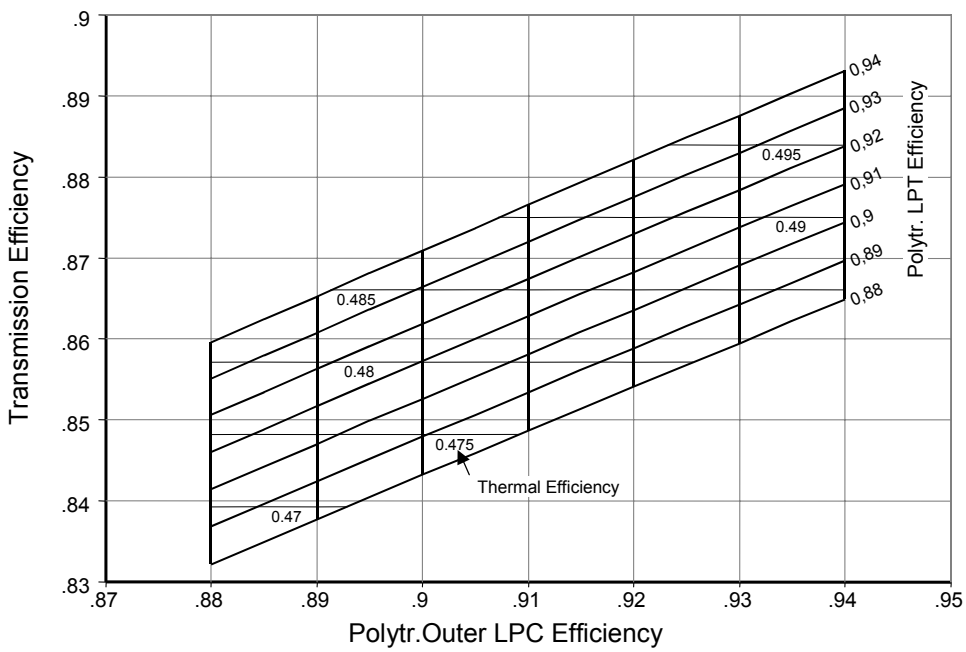

Figure 3.36: Transmission Efficiency for Turbofans with Constant Core Efficiency.

3.1.5.3 Overall Efficiency

The overall efficiency is the ratio of useful work done in overcoming the drag of the airplane to the energy content of the fuel:

$$\eta_o = \frac{F * V_0}{W_f * FHV} \qquad \textbf{Eq. 3-19}$$

With the simplifying assumptions from ***Section 3.1.5.1*** it follows that overall efficiency is equal to the product of thermal efficiency and propulsive efficiency.

The efficiency of an aircraft engine is inseparably linked with the flight velocity as can be seen from the definitions listed in **Figure 3.37**. So the question arises, how to compare the quality of engines being used at different flight speeds.

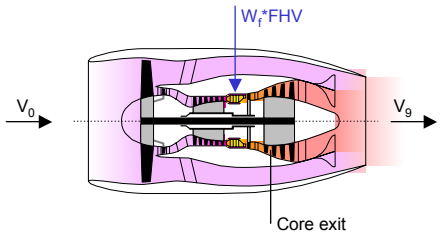

Thermal Efficiency = $\frac{\text{Energy at the Nozzle}}{\text{Energy of the Fuel}}$

Core Efficiency = $\frac{\text{Energy at Core Exit}}{\text{Energy of the Fuel}}$

Transmission Efficiency = $\frac{\text{Energy at the Nozzle}}{\text{Energy at Core Exit}}$

Propulsive Efficiency = $\frac{\text{Useful Work of the Engine}}{\text{Energy at the Nozzle}}$

Overall Efficiency = Thermal Efficiency * Propulsive Efficiency

= Core Eff * Transmission Eff * Propulsive Eff

Figure 3.37: Breakdown of Engine Efficiencies.

We introduce the specific fuel consumption SFC = W_f/F into the formula above and get:

$$\eta_o = \frac{V_0}{SFC * FHV} \qquad \textbf{Eq. 3-20}$$

or

$$SFC = \frac{V_0}{\eta_o * FHV} = \frac{V_0}{\eta_{th} * \eta_P * FHV} = \frac{V_0}{\eta_{core} * \eta_{trans} * \eta_P * FHV} \qquad \textbf{Eq. 3-21}$$

In **Figure 3.38** are SFC data from many different engines shown. The big scatter in the data does not mean necessarily a big difference in thermal efficiency; it results mainly from the differences in propulsive efficiency respectively bypass ratio.

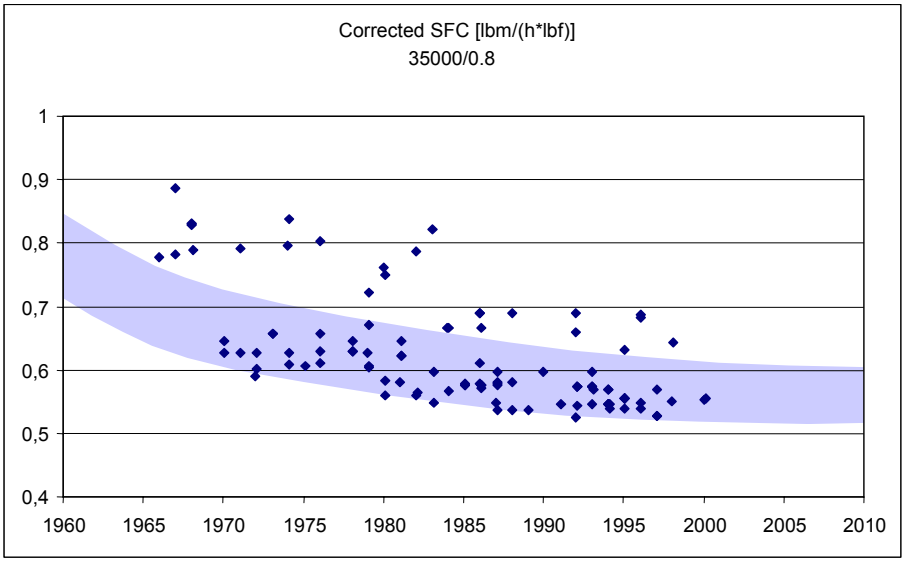

Figure 3.38: Historical Trend in SFC [3.8].

The historical trend of the SFC over time for the best conventional turbofans obviously flattens out and no significant improvement of fuel consumption is to be expected with today's technology.

3.2 GAS TURBINE THERMODYNAMIC ENGINE MODEL

The purpose of this section is to describe the key issues in engine performance simulations. The focus is to make an appropriate selection of model type and component models to meet simulation needs, and to understand the limitations and potential of various types of simulations for potential applications.

The different types of models used in the prediction and simulation of gas turbine engines operations can be classified by application and capability of the model. The range of potential applications and the types of models are shown in **Table 3.1**. Presented in **Table 3.2** are the relative requirements for some of these models in terms of accuracy, fidelity and physics detail. Detail involves how much of the engine is simulated. Fidelity refers to the depth and sophistication of the analytic representations within the model. Accuracy is the ability of the model to match tested or target values for engine and component performance or internal conditions.

Table 3.1: Thermodynamic Property Representation Effect on Model Capability and Execution Speed

	Constant Property	Limited Curve Fit	Full Range Curve Fit	Limited Constituent Equilibrium	Full Equilibrium	Full Kinetics
Speed	Fastest (1x)	Fast (10x)	Fast (20x)	Medium (200x)	Slow (500x)	Slowest (500x – 10000x)
Accuracy / Range	Limited Temperature Range (+/- 500 R)	Limited Temperature Range (< 2500R)	Wide, Limited by Complexity, Range	Wide, Limited by Extreme Disassociation (< 6000 R)	Limited by Physical Model Assumptions	Limited by Physical Model Assumptions
Flexibility	Low	Medium	High	High	Highest	Varies, may be limited by Kinetics Options
Typical Use	Simple 0-D/1-D Models, 2-D/ 3-D Models, Real Time or Condition Monitoring Models	Simple 0-D/1-D Models, 2-D/3-D Models	Most 0-D/1-D Models, Some 2-D/3-D Models	Some 0-D/1-D Cycle Models, Simple Combustion Models	Combustion Models, Special Application Cycle Models	Combustion Models

Table 3.2: Model Fidelity, Accuracy and Detail Needs through the Engine Life Cycle

	Accuracy	Fidelity	Detail
Conceptual	Low	Low	Low
Detail Design	Medium	High	High
Test and Validation	High	Medium	Low
Fleet Support	High	Low	Medium

3.2.1 Selecting the Appropriate Model Type

3.2.1.1 Engine Development Cycle Considerations

The selection of an appropriate engine model depends on the phase of both the engine development cycle and the application (see **Figure 3.39**). Most users of engine simulations are interested in overall engine performance levels, internal conditions that have a direct influence on the aircraft and other internal engine conditions necessary to properly operate and maintain the engine. The most sophisticated models focus on the details of internal components for design purposes or special purpose analysis that is primarily of interest to engine manufacturers or government or academic researchers.

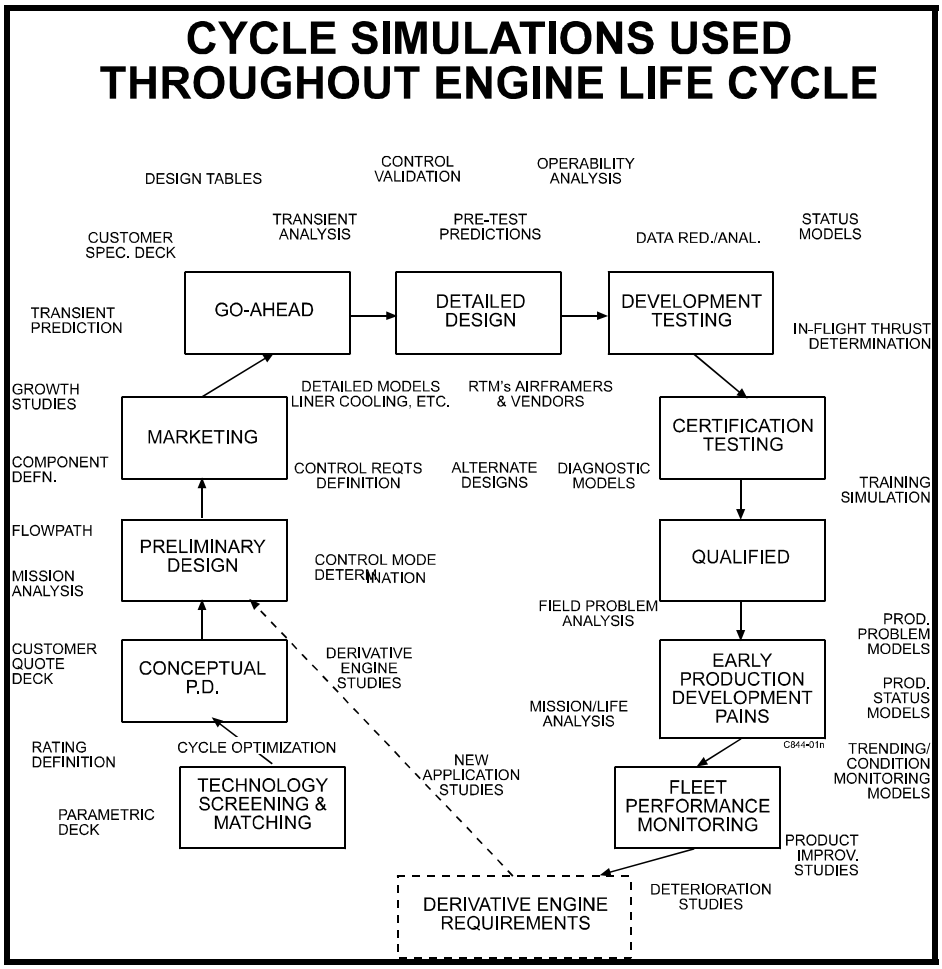

Figure 3.39: Model Types based on Engine Life Cycle.

Models used in the development phase are generally on the low end of the fidelity or depth of analysis spectrum, because of the uncertainty in the engine being modeled. However, for believability, these models may be required to hold very precise performance agreement with existing detailed models from which the component models are derived or will be compared. Similarly, once in production use, the primary modeling is again at the lower fidelity level but at high levels of accuracy due to large amount of data available and the need to maintain close agreement at least the overall engine performance level. The primary use of detailed models is by those involved in design improvements, failure analysis or technology development.

Although model detail tends to follow the model fidelity, the level of detail required may change with the model type shown in **Table 3.2**. A high fidelity 3-D model is often limited to just the primary flow-path while 0-D models may include each cooling flow circuit and the incremental changes in temperature and pressure in the internal cavities of the engine.

3.2.1.2 Minimum, Average, New and Old Engine Models

Due to production scatter and component aging, two engines of the same type, having two different usage histories, will have different performances. However, the engine manufacturer guarantees to his customer a minimum level of performance for a given Time-Between-Overhauls (TBO), or at least defines overhaul criteria that are periodically checked (as part of health monitoring).

To do this, the engine designer has to build minimum, average, new and old engine performance models. This terminology may lead to severe misunderstandings between component designers, performance engineers and customers. The key point for a good understanding of these different models, is that the only representative and accurate model that can be established by the engine manufacturer is the model for a new average engine. This is when all engine components have their average production characteristics, it is sure that the resultant engine has average performances. Conversely, the minimum performances are not necessarily obtained with an engine that has all its components at minimum level. The word *minimum* is in fact relative to an engine-level pass-off criterion (thrust, fuel consumption, TET) for global parameters and not engine components.

There are numerous combinations of component performance reductions that will cause failure of one or more of the pass-off criteria (one with highest TET, one with smallest thrust, one with maximum SFC…). A true minimum engine, at the threshold of failure for each of the criteria, will rarely if ever exist. It is better to talk of minimum *performance* model. Such models give global performance levels that any new engine will achieve. These models are obtained either by applying deltas directly to the performances of the average engine model or applying deltas to each component of the average model. The same issue arises for aged or old engine models. There is infinity of deterioration types that depend on the environment, the mission profile, and other variables that can be envisaged. Thus a general deteriorated engine model may not be possible. It may be better to talk of an *aged* performance model because such models set limits to global parameters throughout the TBO in normal operating conditions.

Although not general, deterioration models can be issued when a database of in-service engines is available. It is then possible to derive statistical deltas on either main engine parameters, or component characteristics, as a function of the number of running hours or cycles. These models are becoming more and more important because they are a basis for any diagnostic models that allow for example:

- Damage detection; and
- Engine fleet management.

A typical question is, 'Is it better to overhaul this engine now or later?' If the answer is now, the engine recovers its initial performance (even when not necessary for its mission, as in cold day conditions) with an economic penalty (overhaul cost). If the answer is later, the engine keeps a higher SFC and lower general performance, which can lead to a reduction in payload, range, or operating conditions, constituting an equally severe economic penalty.

3.2.2 General Nomenclature

The general nomenclature used in engine modeling is covered in **Aerospace Recommended Practices (ARP)** and **Aerospace Standards (AS)** published by the Society of Automotive Engineers (SAE). They have been created in a cooperative effort among the developers and users of engines to simplify the exchange of models and data. **AS755C** [3.9] defines the station definition within an engine, the application to various engine types and the nomenclature for properties and fundamental parameters. **AS681** [3.10] provides definitions, requirements and assumptions for a class of models mostly provided by engine manufacturers to customers, often-called *customer decks*. **ARP1210** [3.11] provides additional guidance on interface requirements for models dealing with test data, **ARP1211** [3.12] for status models that have been matched to specific test data, **ARP1257** [3.13] for transient models and **ARP4148** [3.14] for real-time applications. **ARP4868** [3.15] and **ARP4191** [3.16] are being developed to cover the needs of newer computer systems and to define application program interface (API) standards to facilitate use with object-oriented software or in an event driven environment.

3.2.3 Thermodynamic and Gas Properties

Most physics based engine models make some assumptions for calculating the state properties and energy balance of the various fluid streams. These include converting typical flight conditions into the boundary conditions required by the model, and the capability required to support engine component models.

3.2.3.1 Atmosphere Definitions

Most component-based propulsion system models use a standard atmosphere reference for defining operation conditions. Atmospheric properties for general use are specified in **SAE AS681F** [3.10]. The current standard atmosphere definition is **ISO 2533** [3.17]. This is generally consistent with the **U.S. Standard Atmosphere, 1976** [3.18], which was an extension of the **US Standard Atmosphere, 1966** [3.19] to higher altitudes. For non-standard atmospheric conditions the most common reference is **MIL-STD-210C** [3.20] which defines standards for extreme conditions such as arctic, desert and tropical days. Differences in air composition between these various sources is small but can be noticeable when comparing absolute properties and emissions due to the assumed percentage of CO_2, as shown below:

- ISO 2533 — 0.030%;
- US Standard Atmosphere, 1976 — 0.03140 to 0.0322%;
- NASA TP-1906 — 0.0319%; and
- Keenan and Kayes, 1945 — 0.0000%.

3.2.3.2 Thermo Property Packages

Multiple thermo representations may be used in a single simulation or be an integral part of component models. However, it is common to use a single separable set of routines, often called a thermodynamic property package, for the entire simulation. This is for simplicity and to ensure consistency. The package selection is typically based on the requirements of the simulation, convenience and historical reasons. **AS681** [3.10] requires that the properties be consistent with those provided in **NASA TP-1906** [3.21] and the associated computer code. The level of agreement required will depend on the application. Some considerations when selecting a package are:

- Speed;
- Accuracy over the range of operation;
- Accuracy needs of the engineering application;
- Kinetics;
- Heat transfer requiring transport properties;
- Water vapor, multi-phase water or other constituents such as solid carbon or soot;
- Non-air streams; and
- Alternate or non-hydrocarbon fuels.

The thermo property package should have no impact on the overall simulation accuracy. However, because property calculations are so pervasive in engine simulations, seemingly small speed differences can be significant. When the extra capability or range of accuracy is not required, the speed gain will often justify use of a simpler thermo package. In a typical engine simulation, the thermo property package may account for up to 30% of the execution time. Special application combinations are possible. Kinetics calculation can be based on curve fit properties, but these are normally not seen in general use property packages. **Table 3.1** contains a comparison of the various approaches and basis for selection based on the simulation requirements.

3.2.3.3 Gas Properties Evaluation for Steam/Water Injection

Calculations of thermodynamic processes use properties of a working medium, which is a mixture of gasses. The properties of individual mixture constituents are calculated by means of polynomial functions and the mixture properties are evaluated from its mass composition, through a relation of the form:

$$P = \sum_i X_i \cdot P_i \qquad \textbf{Eq. 3-22}$$

P is a property of the mixture and Xi, Pi is the mass composition and the corresponding property value for the i-element of the mixture respectively. Inlet air is handled as a mixture of gases, including steam due to ambient humidity. The composition of gases at the combustor outlet is computed on the basis of stoichiometric calculations, and depends on the composition of the fuel used. When water is injected, it is also accounted for as an additional element in the gas composition. The variation of cp of the mixture of combustion gases and steam, for the range of temperatures of interest to gas turbine applications, is shown in **Figure 3.40**. The values have been calculated by considering the gases as a mixture of ideal gasses, and the properties of the constituents are derived by polynomial relations. The variation of isentropic exponent γ is also shown.

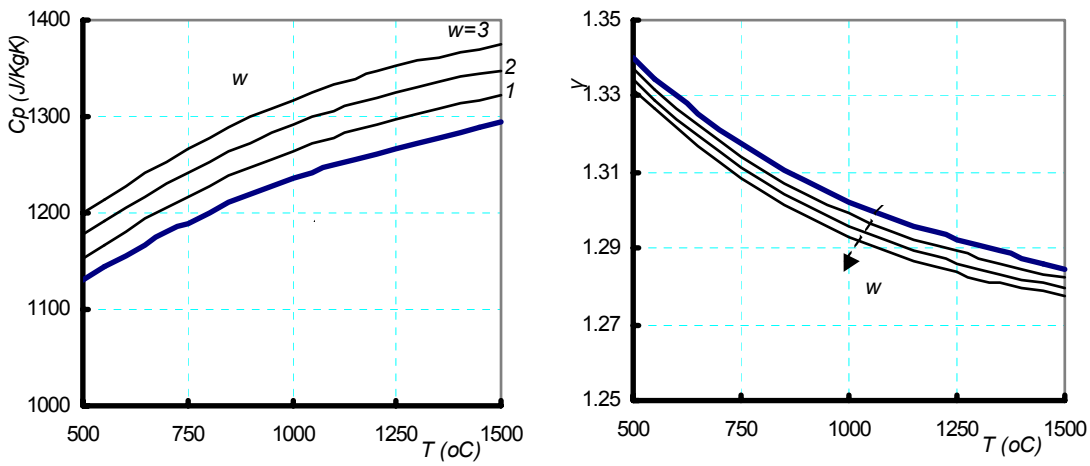

Figure 3.40: Values of Specific Heat C_p and Isentropic Exponent *γ*, for Temperatures Usual in the Hot Section of Gas Turbines.

Variation of gas properties for typical rates of water injection is shown in **Figure 3.41**. The changes of properties of gases after water is injected, with respect to the values with no water injected are shown.

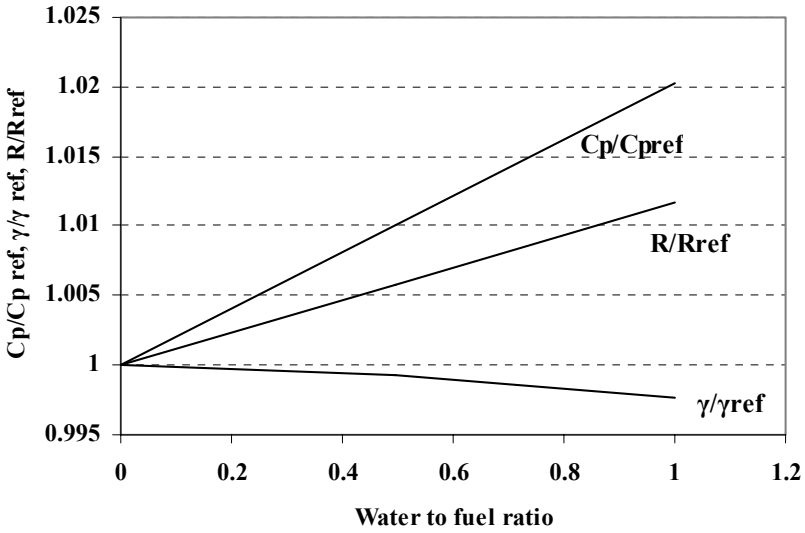

Figure 3.41: Change in Gas Properties for Different Amount of Injected Water (f = 0.02).

Variation of Cp and γ due to the increase of water content in air can be estimated with the use of analytical relations, when the water to air ratio is small, a condition that is fulfilled in the usual gas turbine applications. Such relations have been proposed by Mathioudakis et al. [3.22 and 3.23] and express the deviation of Cp and γ from the dry combustion gas values in function of the water-to-air ratio war.

If property values are known for dry combustion gases, then the change of cp because of the injection of water or steam can be evaluated by the relation:

$$\frac{\delta c_{pg}}{c_{pg}} = war\ (\frac{c_{ps}}{c_{pg}} - 1) \qquad \textbf{Eq. 3-23}$$

Cps: specific heat of steam, Cpg: specific heat of dry gas, δCps: change of gas specific heat, due to addition of water, war is the water to air ratio.

A similar relation can be derived for the change in the value of the gas constant R:

$$\frac{\delta R_g}{R_g} = war\ (\frac{R_s}{R_g} - 1) \qquad \textbf{Eq. 3-24}$$

The change in the isentropic exponent γ results from its definition and the previous expressions:

$$\frac{\delta \gamma_g}{\gamma_g} = (\gamma_g - 1)\left(\frac{\delta R_g}{R_g} - \frac{\delta c_{pg}}{c_{pg}}\right) = (\gamma_g - 1)\left(\frac{R_s}{R_g} - \frac{c_{ps}}{c_{pg}}\right) war \qquad \textbf{Eq. 3-25}$$

Subscripts s and g denote steam and gas respectively, as in **Eq. 3-23**.

The above expressions can be further simplified for gas turbine combustion gases, by taking into account that the specific heat of steam is roughly double the specific heat of the combustion gases, as can be seen

from **Figure 3.42.** For the range of turbine inlet temperatures encountered in today's turbines, and representative values of fuel/air ratio, Cps/Cpg is shown to take values very close to 2.

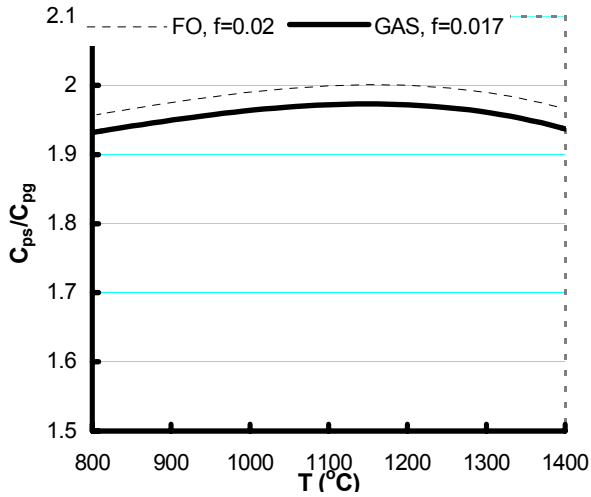

Figure 3.42: Ratio of Specific Heats of Steam and Combustion Gases.

By virtue of this observation, **Eq. 3-23** for Cp becomes:

$$\frac{\delta c_{pg}}{c_{pg}} \approx war \qquad \textbf{Eq. 3-26}$$

For the gas constant R, for Rs = 461.5 and Rg = 287, **Eq. 3-24** gives:

$$\frac{\delta R_g}{R_g} = 0.61 war \qquad \textbf{Eq. 3-27}$$

and for the isentropic exponent, using these relations and **Eq. 3-25**

$$\frac{\delta \gamma}{\gamma} \approx 0.33(1.61-2)war = -0.13\,war \qquad \textbf{Eq. 3-28}$$

3.2.3.4 Impact of Modeling Assumptions

Besides the basic property representation, the assumptions made in applying these properties can affect the accuracy and consistency of model results. Some of the key assumptions that can change the results of simulation models are:

- Whether high temperature mixtures are assumed to be in equilibrium or frozen composition during expansion processes;
- How cooling flow mixing with the main flow is modeled; and
- Behavior with incomplete combustion products or in fuel-rich conditions.

In special circumstances, information on assumptions relative to compressibility effects, combustion product estimates, alternate fuels or operation with other fluids (water, ice, vitiated air, nitrogen diluted test stand air, etc.) may be important. When using the model for data analysis or comparison with on-line performance data generated in test facilities, the model assumptions must match those used in creating the data.

3.2.3.5 Aero-Thermo Process Calculations

Independent of the thermodynamic process package, standard procedures for calculating aero-thermo processes are often used throughout a simulation and can affect the applicability of results. Reverse flow, supersonic conditions, mixer and ejector processes, swirl calculations, expansion and contraction processes are examples that may affect the range of use or accuracy of models. Models that use a thermodynamic process package may make alternate assumptions during some of these local calculations, for speed or simplicity.

3.2.4 Steady State Performance Models

The gas turbine performance simulation can be sharply divided into two categories: design point analysis and off-design modeling.

The first category mainly involves the engine designer because it consists in selecting the best thermodynamic cycle in order to achieve a performance goal: delivered shaft power for helicopter engines, net thrust for airplane engines, bleed air flow at given pressure, temperature conditions for Auxiliary Power Unit (APU) starts.

This analysis is led at a *single* working point, the so called design point, which is supposed to be representative of typical customer use. The design point analysis allows optimization of the cycle and preliminary design of the engine components by:

- Selection of compressor pressure ratios and turbine inlet temperatures;
- Comparison of different engine configurations such as single spool or twin spool; and
- Varying the number and type of stages for compressors and turbines.

It is only after this analysis that a first engine geometry is defined. At this step, the engine performances are known only at design point. In order to estimate the performances under various ambient air conditions and power or thrust settings, it is necessary to create an off-design model which has the ability to describe the behavior of the engine components in conditions other than those at design point. Such modeling involves both designers and engine users (aircraft manufacturers and aircraft operators) because it is common to predict the performances during development and to define them in the whole working domain once the product definition is frozen.

It must be underlined that the importance of such off-design models has increased since the beginning of engine performance simulation. In the late sixties it was found sufficient to optimize the engine at a single working point and extensive testing permitted qualified the technologies and established the performance. But nowadays, mainly for economic reasons, an off-design model is required at a very early stage of engine design:

To match the customer specifications: it is necessary to optimize the engine within the whole working envelope and not just at one design point. For example, a turboshaft engine for a helicopter has to be optimized at both take-off rating and economical cruise power (≈ 50% take-off) to satisfy both the maximum take-off weight, and the range requirements.

The meaning of the word *performance* is becoming wider and wider. It initially dealt with power or thrust and fuel consumption in steady state conditions, but the following topics are now fully part of engine performance:

- Steady state:
    - Exhaust gas emissions; and
    - Noise.
- Transient:
    - Starting time; and
    - Acceleration time.

All these types of performance have their own dimensioning points in the working domain, thus there is an increasing need for global optimization of the engine performances that implies extensive use of off-design modeling.

To reduce testing costs, many tests have been replaced by theoretical analysis in fields such as mechanics, and engine control. These analyses need off-design results as input data.

To reduce development cycles, it is necessary to design all aspects of the engine in parallel. This means that all specialists in aerodynamics, mechanics, control, and external equipment have to be provided with accurate data before the engine has any material existence, and even before the passage of components to partial test bench. The only theoretical source for these data is an off-design model.

For all these reasons, an accurate off-design model is at the heart of the engine design process and becomes increasingly critical.

3.2.4.1 Different Types of Off-Design Steady State Models

All off-design models aim at computing the fluid state in different locations of the mainstream in the engine, from these results, mainly W, T, P, it is possible to derive powers, thrusts, fuel consumption's and all characteristic parameters of the components.

The off-design models can be split into different categories according to the level of discretization of space. Historically, the first models belong to the 0-D category because the *averaged* fluid characteristics are computed at discrete positions inside the engine, generally at the inlet and the outlet of each component such as compressor, combustion chamber, turbine, and exhaust nozzle.

The next generation of model is the 1-D type (see ***Annex A*** for a detailed description of 1-D models) and introduces continuity in the computation: the fluid characteristics are still averaged in each plane, where plane means a fluid section perpendicular to the engine axis. They are computed quasi-continuously, limited by the space discretization step, along a mean line representing the average trajectory of the fluid inside the engine.

2-D and 3-D models extend this description by discretizing the whole flow path inside the engine, and not just the mean line of 1-D models. 2-D models consider there is symmetry of revolution for the stream, while 3-D models make no simplification and use the complete equations of conservation (see ***Annex A*** for detailed descriptions of 2 and 3-D models).

3.2.4.2 0-D Models

The goal of this Section is to describe the 0-D models, which are the simplest and most widely used in the industry, by analyzing the assumptions, the phenomenon modeling, the computation methods and the

limitations of such models. These models are the most widely spread in the world of turbo-machinery for many reasons:

- Historically, they were the first kind of performance model that was used.
- They do not require a detailed description of the engine geometry. Thus they can be used very early in the engine development.
- The engine description is simple and close to reality by considering it as a set of black boxes, one for each major component of the engine.
- The calculation methods are simple because the number of unknowns needed by the modeling is reduced, the goal being to compute the fluid characteristics only at the interfaces of the black boxes. The number of unknowns has the same order of magnitude as the number of individual components considered as black boxes.
- The calculation methods are natural because the fluid characteristics are computed plane by plane, or station by station, in the same order as the one used by the fluid to pass through the engine. The calculation begins at the air inlet, continues with the compressors, the combustion chamber, the turbines, and ends with the exhaust.
- Thanks to the simplicity of 0-D models, they can be run on all computer types, from the small portable PC to the workstation or the main frame. This is a very useful feature of 0-D models, because of the wide range of people who can have to run engine performance models. Such models constitute a common tool for the designer, the integrator, the customer; and the engine designer. As the main model provider, the engine designer finds issuing customer decks, based on the same approach as the one he uses for development, very convenient. This results in time and cost savings and quality gains.

First, we will analyze the steady state models which were the first developed, and which allow simulation of the engine in steady state operation, that is to say, in non time-dependent working conditions.

We will then show how to derive a transient model from the steady state one. Steady state and transient modeling are fully linked but transient modeling raises specific problems, in taking into account the physical transient phenomena. Nevertheless, the performance programs used today by designers generally allow both types of computation. Those issued for external use, engine computer decks for example, are following the same tendency albeit with some delay, as proved in AS 681 revision F aerospace standard which unifies the presentation of computer programs for both steady state and transient operation.

3.2.4.2.1 General Technique

The general technique for obtaining a 0-D solution is illustrated below by way of a simple single-spool turbojet example. The calculations employ iteration; the global iteration approach is described. The calculations can be broken into the modules described earlier in the chapter. Consider an engine represented as follows:

Compressor

Pressure Ratio, Efficiency, Non-dimensional Flow = $f(N\sqrt{T}, \beta)$

Combustion

$T4 = f(T3, FAR, W4)$ pressure loss = $f(W\sqrt{T}/P3)$

Turbine

$W\sqrt{T}/P4$ & Effy = $f(\Delta H/T, N\sqrt{T4})$

Nozzle

Entry W√T/P = f(P7/PAMB)

Boundary Conditions

Required Power Level, Altitude (ALT), Flight Mach No (XM)

(Where Req. Power Level may be expressed in terms of any engine parameter, e.g. thrust.)

A 3x3 multi-variable iterative scheme can be set up to generate steady-state performance given a specified power level. Advanced cycle match models may have very detailed matching schemes for steady-state synthesis – perhaps in excess of 30x30. For steady-state test analysis, the matching scheme can be further extended to vary model assumptions (e.g. efficiencies) to match synthesized data to measured data (see section on Model Calibration, ***Section 3.2.7.3*** or ***Section 3.3.2.6.4.2***).

The cycle-match approach steps through the engine, front-to-back, producing flow conditions at each station. Where a parameter is not known, it is set up as an iteration variable. At the end each pass through the engine calculations, the variables are re-estimated to achieve 'targets' or 'matching quantities'. Once the matching quantities are satisfied within a prescribed tolerance, the process ends.

3.2.4.2.2 Steady-State Solution

The steady state solution using the 0-D simulation technique can be obtained by the following algorithm:

1) Estimate values for iterative variables:
   - N√T (compressor aerodynamic speed);
   - β (a mapping parameter similar to outlet flow-function which allows cartesian look-up of compressor performance. The lines of constant β on a compressor map are arbitrary and have no thermodynamic sense. They can be derived to give optimum iterative reliability; the gradients of dependent parameters should be smooth functions of β); and
   - FAR (fuel-air-ratio).
2) Determine inlet and ambient conditions (e.g. from Altitude and Aircraft Mach number).
3) Perform compressor calcs (use guessed values of N√T and β) … hence compressor outlet conditions.
4) Perform combustor calcs (use guessed values of FAR) … hence combustor outlet conditions.
5) Perform turbine calcs (in steady-state, there is no excess power on the shaft so equate compressor and turbine power):
   - W Cp ΔT compressor = W Cp ΔT turbine;
   - Cp is function of gas properties (known)… hence turbine ΔT; and
   - Read turbine chic for W√T/P4_chic and efficiency = f(N√T, ΔH/T) … hence turbine exit conditions.
6) Perform nozzle calcs.
7) Check matching conditions are within tolerance:
   - Calculated power-level = required power-level;

- W√T/P4 calculated = W√T/P4_turbine (from turbine characteristic);
- W√T/P5 calculated = W√T/P5_nozzle (from nozzle characteristic); and
- … if not, re-run calculations above using re-estimated variables.

The process of re-estimation of variables can be complex. Various techniques can be used; the Newton-Raphson method is common. Rapid convergence can be achieved especially if guess-maps of start values are used (guess maps can generate good initial values as a function of flight case). See the section on Iterative Techniques, ***Section 3.2.6***. Once a matched condition is achieved, other quantities can be derived such as thrust and surge-margin.

3.2.4.2.3 Increasing Cycle Complexity

The principle outlined above can be easily extended to cover any engine architecture to whatever level of complexity is required. The components and thermodynamic processes are represented by characteristics, and where an independent variable is not known at any point through the engine it is set up as an iterative variable. For every extra variable there has to be a corresponding extra matching condition. Two examples of a more complex cycle are given below:

Two Spool Mixed Turbofan

The extra variables are:

- Fan outer β (the fan is split into 2 parts – one serving the bypass duct; one serving the core); and
- Bypass ratio.

The extra matching constraints are:

- W√T/P45 calculated = W√T/P45_turbine (from LP turbine characteristic); and
- PS16 = PS6 (mixer static pressure balance).

More complex representation of the same engine architecture would typically include matching pairs involved with the modeling of re-circulating bleeds, intakes, afterburning, etc.

Addition of Free Power Turbine (Turboshaft Engine)

In this case we are extracting the energy out of the gas stream leaving the (HP) turbine, and replacing the final nozzle constraint with a match to ambient pressure. The extra variables are:

- Delivered power; and
- Power turbine (PT) speed.

The extra matching constraints are:

- W√T/P44 calculated = W√T/P44_turbine (from power turbine characteristic); and
- Specified operating constraint on power turbine, e.g. turbine speed or power.

(Note: both of these are set up as iterative variables so this matching constraint could be fed into the model directly, however in the interests of flexibility the more general approach can be taken.)

The nozzle matching constraint is replaced with:

- Static pressure leaving power turbine = ambient static pressure (given).

The sequence of calculation is the same as in ***Section 3.2.4.2.2*** above, until item 6. This then becomes:

(6) Perform Power Turbine Calcs:

W, P, T at entry (station 44) are known and so calculate power turbine exit (station 5) W, P and T

W5 = W44 (in the absence of any secondary air-system)

T5 = T44 - ΔT

where ΔT is derived from the guessed power (i.e. PW/Cp.W) and efficiency (= f(ΔH/T , N/√T)

P5 follows from the general adiabatic relationship of Pressure ratio and Temperature ratio

(7) Check Matching Conditions are Within Tolerance

There are now 5 matching conditions:

- Calculated core condition = required core condition (e.g. fuel flow from FAR variable = specified value);
- W√T/P4 calculated = W√T/P4_HP turbine (from HP turbine characteristic);
- W√T/P44 calculated = W√T/P4_power turbine (from PT characteristic);
- PS5 = PAMB (environmental condition); and
- Calculated PT condition = required PT condition (e.g. power from variable = specified value).

(See section above for comment on re-estimating variable for convergence.)

The choice of specified parameters will vary depending on how the model is being used:

For example, if a model is being used to generate a series of steady-state cases to form an SFC curve for a technical brochure, then running the model to Power and PT speed is most convenient (fuel flow come out 'in the wash' in this case). If the model is being used to model a transient maneuver (in which case the iterative scheme will need to be further expanded – see ***Section 3.2.5***) then running the model to a specified fuel flow and specified power may be most appropriate. In this case, the PT speed comes out 'in the wash'.

Beware: some combinations of driving constraints can result in a model finding multiple solutions. This is best illustrated in terms of the operating point on the PT map (see **Figure 3.43**): unless speed (y axis) and power (x axis) are specified together, there is some potential to find two feasible operating points at a common power but at a different efficiency (and hence operating speed).

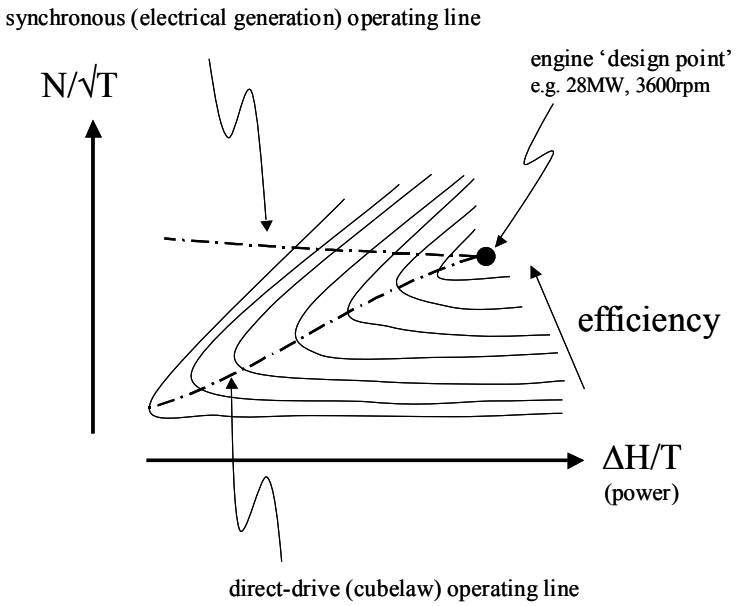

Figure 3.43: Indicative Aeroderivative Power Turbine Characteristic.

Another problem may arise when using power turbine characteristics looked up with ΔH/T and N/√T (as above) in that turbine exit pressure may be calculated during iteration as sub-ambient. Numerically, this is of no consequence, but some thermodynamic routines may need safeguarding against this.

3.2.5 Transient Performance Models

This 3x3 matching scheme is easily extended for a simulation which models the dynamics associated with the shaft. In this case, required power-level must be specified as a function of time. For example WFE might be a ramp function against time.

We now have an extra descriptor of engine behavior, this time a dynamic equation that describes the behavior of a state-variable in the time domain:

$$\frac{dN}{dt} = \frac{\Delta PW}{J.N} \qquad \textbf{Eq. 3-29}$$

where:

- ΔPW is the excess power on the shaft (turbine power – compressor power);
- dN/dt is shaft acceleration (state derivative);
- J is moment of inertia of the shaft (constant); and
- N is shaft speed (state variable).

This is the rotational form of $F = ma$ and concerns the conservation of angular momentum.

The engine calculation process is largely unchanged. The difference lies in the treatment of shaft speed. Numerical integration is required to obtain the speed at each timestep. There are several methods of numerical integration, in the interests of clarity; Euler's explicit method is use in this example.

3.2.5.1 Solution by Explicit Euler Integration

Euler's explicit integration method is:

$$x(t+\Delta t) = x_t + \left.\frac{dx}{dt}\right|_t \cdot \Delta t$$

Eq. 3-30

or for our example:

$$N_{next} = N_{now} + \left.\frac{dN}{dt}\right|_{now} \cdot \Delta t$$

Eq. 3-31

where Δt is the chosen timestep.

Explicit methods are inherently unstable as they involve the prediction of the state variable at the next timestep based on conditions at the current timestep, however judicious selection of timestep can reduce/eliminate problems.

In our example there is now an extra matching pair:

- **Variable**: excess power on shaft; and
- **Matching Condition**: mechanical shaft speed = mechanical speed predicted from last case.

So for *time* = *t*, the calculation process can proceed as for the steady-state case, except that turbine power is now (compressor power + excess power). When the point is matched (matching conditions satisfied), the dynamic equation is used to calculate dN/dT … hence N for next timestep can be calculated using Euler's equation.

Although N is fixed for a particular timestep (having been predicted from previous timestep), the N√T variable can be retained for consistency with the steady-state matching scheme. The iterative solver should not be troubled. Alternatively this variable and the speed matching condition can be extracted from the matching scheme.

The transient solution is started with a steady-state point, the first transient point (time = 0+Δt) solves at the steady-state value of N (as excess power was, by definition, zero at t = 0 hence dN/dt was also zero).

3.2.5.2 Solution by Implicit Euler Integration

A more stable approach can be taken which, instead of predicting forwards, looks back over the previous timestep. The implicit form of Euler's method is:

$$x(t+\Delta t) = x_t + \left.\frac{dx}{dt}\right|_{t+\Delta t} \cdot \Delta t$$

Eq. 3-32

Which can be re-written in the more useful form:

$$x_t = x_{(t-\Delta t)} + \left.\frac{dx}{dt}\right|_t \cdot \Delta t$$

Eq. 3-33

or for our example:

$$N_{now} = N_{last} + \left.\frac{dN}{dt}\right|_{now} \cdot \Delta t$$

Eq. 3-34

At any particular timestep, the speed at time = t-Δt is known and Euler's equation can be solved if the current speed and acceleration (N_dot) can be determined. If the speed is an iteration variable, then state-derivative can be obtained by looking backwards (rearranging implicit Euler equation):

$$\left.\frac{dx}{dt}\right|_t = \cdot \frac{x_t - x_{(t-\Delta t)}}{\Delta t}$$

Eq. 3-35

The iterative/implicit approach requires the matching condition to be:

State-derivative from dynamic equation = state-derivative from Euler's implicit equation:

$$\frac{N_{now} - N_{last}}{\Delta t} = \frac{\Delta PW}{J.N_{now}}$$

Eq. 3-36

In the interests of iterative convergence, this is best rearranged with the excess power expressed in its constituent terms:

$$\frac{J.N_{now}}{\Delta t} + \frac{PW_c}{N_{now}} = \frac{J.N_{last}}{\Delta t} + \frac{PW_t}{N_{now}}$$

Eq. 3-37

Where PWc is the total power requirement (i.e. includes compressor power, losses and off-takes) and PWt is the turbine power.

The bandwidth of a dynamic model, which only contains the shaft dynamic equation, has a bandwidth of around 5 Hz. For wider bandwidth, other dynamic events must be modeled. Better representation in the higher frequency ranges requires the modeling of gas dynamics (the behavior of the air in each area of the engine). For better representation in the lower frequency range, heat soakage (the transfer of heat to and from the blades and carcass) must be modeled. Gas dynamics are fast events and numerical stability of the integration method is a significant issue. The implicit approach described above is perhaps most suitable given that the cycle match process is iterative by nature. Non-iterative 0-D modeling techniques are more constrained to use explicit approaches and in these cases a more sophisticated integration method is required (e.g. Runge-Kutta 4th order).

3.2.5.3 Extension of Simple Example to Include Gas Dynamics

In the example so far, it is assumed that the gas is incompressible, that the flow into any control-volume at any instant is equal to the outlet flow. In reality, there is some storage of gas in a volume. There is

therefore an imbalance of gas properties (inlet to outlet) relative to the quasi-steady values encountered at each timestep in the example above. This imbalance implies a rate of change of properties within each volume.

The dynamic equations that describe these phenomena are listed below. The Δ terms refer to inlet – outlet.

Conservation of Mass

$$\frac{\mathrm{d}\overline{\rho}}{\mathrm{d}t} = \frac{\Delta W}{Volume}$$ **Eq. 3-38**

Momentum

$$\frac{\mathrm{d}\overline{W}}{\mathrm{d}t} = \frac{\Delta(pA + Wv)}{Length}$$ **Eq. 3-39**

Energy: Enthalpy Form

$$\frac{\mathrm{d}}{\mathrm{d}t}(\overline{\rho \mathrm{H} - \mathrm{p}}) = \frac{\Delta(W.H)}{Volume}$$ **Eq. 3-40**

Energy: Entropy Form

$$\frac{\mathrm{d}}{\mathrm{d}t}(\overline{\rho s}) = \frac{\Delta(W.s)}{Volume}$$ **Eq. 3-41**

Some models may use simplified forms of these equations that assume low Mach number flow. A typical equation set is:

Mass

$$\frac{\mathrm{d}P}{\mathrm{d}t} = R.T \times \frac{\Delta W}{Volume}$$ **Eq. 3-42**

Momentum

$$\frac{\mathrm{d}W}{\mathrm{d}t} = \frac{A \times \Delta P}{Length}$$ **Eq. 3-43**

Energy

$$\frac{\mathrm{d}T}{\mathrm{d}t} = \frac{\Delta(W.T).\gamma}{M} - \frac{T.\Delta W}{M}$$

where $M = \frac{P.Volume}{R.T}$ **Eq. 3-44**

The state variables in the equations above refer to the average component properties although in some model implementations, the same equations are used in an 'actuator volume' sense. Rather than being applied to the average component properties, the gas dynamics are applied across a dummy volume at exit to the quasi-steady-state (qss) process.

Returning to the example, the engine can be broken down into several control-volumes, corresponding to each separate component or several components lumped together. For each control-volume there are now 3 more unknown quantities (variables) these are:

- ΔP: 'stored' pressure in volume (cons. of mass);
- ΔW: 'stored' flow in volume (cons. of momentum); and
- ΔT: 'stored' temperature in volume (cons. of energy).

For implicit integration, the matching quantities are set up in the same manner as for the shaft dynamic above. Essentially, the matching condition is the equality of the two expressions of state-derivative. As before, some algebraic re-arrangement helps iterative convergence.

Conservation of Mass

$$Volume.\frac{Pqss_{now}}{\Delta t.R.Tqss_{now}} + Wout_{now} = Volume.\frac{Pqss_{last}}{\Delta t.R.Tqss_{now}} + Wqss_{now} \qquad \textbf{Eq. 3-45}$$

Conservation of Momentum

$$Length.\frac{Wout_{now}}{\Delta t} + A.Pout_{now} = Length.\frac{Wout_{last}}{\Delta t} + A.Pqss_{now} \qquad \textbf{Eq. 3-46}$$

Conservation of Energy

$$\frac{M.Tout_{now}}{\Delta t} + \gamma out_{now}.Wout_{now}.Tout_{now} + Tout_{now}.Wqss_{now} = \frac{M.Tout_{last}}{\Delta t} + \gamma qss_{now}.Wqss_{now}.Tqss_{now} + Tout_{now}.Wout_{now} \qquad \textbf{Eq. 3-47}$$

where $M = \frac{Pqss_{now}.Volume}{R.Tqss_{now}}$

It is not necessary to solve all 3 conservation equations for each volume. For around 10 Hz bandwidth, only the modeling of mass conservation may be necessary.

Note that if the momentum equation is solved, then a length term is introduced into the model, hence the model can be regarded as a 1-D representation.

3.2.5.4 Further Extension of the Example to Include Heat Soakage

The heat transfer between metal and gas can be highly significant. The long-term stabilization of the engine onto a temperature limit at a power level is important from an operational point of view, as is the behavior of the engine on hot re-slams or Bodie maneuvers (i.e. soaked high power → idle → high power). In the latter case, the metal is relatively hot compared to the shaft speeds. The aerodynamic speeds can therefore differ greatly from *normal* idle conditions. Compressor stability can be affected.

A cold slam (soaked idle → max power) modeled without heat-soakage effects can be misleading especially for large engines, as in addition to the aerodynamic speed shifts mentioned above, power lost to the heating up of engine parts results in a slower acceleration.

The temperature of a metal component in a gas stream is described the dynamic equation:

$$\frac{dTm}{dt} = \frac{Tm - Tg}{k} \qquad \textbf{Eq. 3-48}$$

where:

- Tm is temperature of the metal component;
- Tg is the temperature of the surrounding gas; and
- k is a function of metal geometry, properties and gas conditions. These will be specific to the type of component being considered.

Returning to the example, we can model the effects of heat soakage within any control volume. These need not necessarily correspond to the volumes already defined for gas dynamics.

For a turbo-machine, it may be useful to consider the blades and carcass temperatures separately. So the extra iterative variables for each control volume are:

T_{blade}: blade metal temperature

$T_{carcass}$: carcass metal temperature

The associated matching quantities (for implicit Euler integration, rearranged as before) are:

$$Tg - \frac{(k.Tblade_now)}{\Delta t} = Tblade_now - \frac{(k.Tblade_last)}{\Delta t} \qquad \textbf{Eq. 3-49}$$

$$Tg - \frac{(k.Tcarcass_now)}{\Delta t} = Tcarcass_now - \frac{(k.Tcarcass_last)}{\Delta t} \qquad \textbf{Eq. 3-50}$$

3.2.5.5 Non-Iterative Technique

The cycle match approach relies on iteration. A non-iterative technique can be applied to model engine performance, and such techniques are particularly suitable for real-time simulation where a fixed execution time is required.

The non-iterative approach is bound to using explicit integration (unless an outer iteration loop is provided), and also must use gas dynamics to obtain flow compatibility between components (this is achieved by iteration in the cycle-match technique). As a consequence of the gas-dynamics being present, the time step and integration method (the two are linked) must be chosen carefully to ensure numerical stability.

The following example is the simplest non-iterative implementation of a model for the example set out above. There are several variations on this approach. The model is laid out as shown in **Figure 3.44** below:

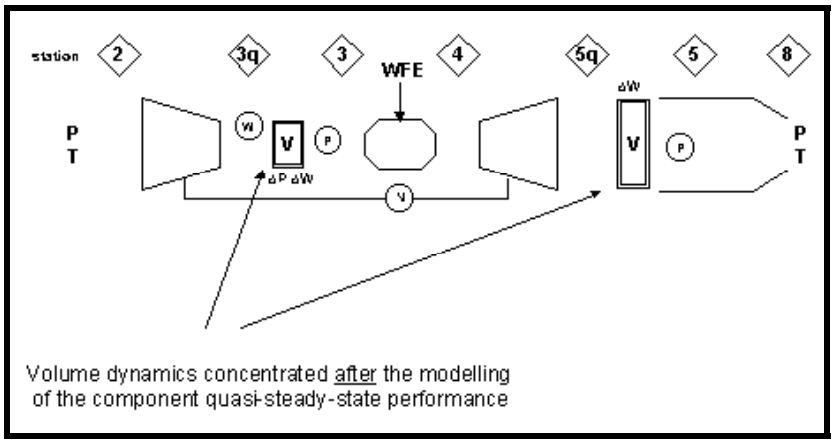

Figure 3.44: Model of Non-Iterative Calculation Process.

State variables: N, P3, W3q, P5 (shaft dynamics, mass and momentum conservation in compressor, mass conservation in turbine – using simplified gas dynamics equations)

At time = t, the state variables are known (predicted from last case)

1) Perform compressor calculations:
   - The compressor must use characteristics which have been manipulated into an alternative form where pressure ratio and efficiency = f(W2√T2/P3, N√T); and
   - W2 = W3q (known) … hence P3q, T3q (and T3), compressor power.
2) Perform combustor calculations:
   - Use W3 = W4last – WFE now to calculate pressure loss … hence P4, T4.
3) Perform turbine calculations:
   - Pressure ratio is already known (P5q = P5) … hence W4, W5q, T5q (and T5).
4) Perform nozzle calculations … hence thrust, etc.
5) Calculate state-derivatives:
   - hence ΔP, ΔW and ΔPW now known; and
   - hence N, P3, W3q and P5 for next case.

Note that some calculations in this method are reliant on using values from the previous timestep (see combustor calculations above). This can force extra limitations on timestep to get sufficient accuracy and stability. Iteration avoids this problem, and is generally more flexible for performance work.

3.2.5.6 Iterative Real-Time Simulation

There are a number of model applications where a model must produce results in real-time. SAE **AIR4548** [3.24] usefully defines a Real-Time Engine Model (RTEM) as a 'transient computer program whose engine outputs are generated at a rate commensurate with the response of the physical system it represents'. Examples of real-time applications are:

- Embedded models for flight systems;
- Engine models within aircraft simulators; and
- Engine system integration testing.

The SAE **AIR4548** [3.24] covers the requirements of these applications in detail, and in terms of 4 criteria*: consistency, bandwidth, versatility* and *execution speed*. *Consistency* is a term used in preference to 'accuracy' and refers to the ability of a model to represent the *reference* source of data – whatever that reference is. *Reference* may change in various stages of the project: from the detailed performance prediction in the early stages, to engine test data later in a program. *Versatility* refers to the ability of the engine model to be refined or reworked in line with the evolving design. The model must be capable of simulating all aspects of engine behavior that that the controller is capable of sensing or controlling – hence the bandwidth criteria. *Execution speed* refers to the timestep at which the simulation must run in order to produce accurate [consistent], and numerically stable results. Of course, bandwidth and timestep are linked. The advantage of cycle-match models is that if a low bandwidth is required, then the model may be stable at the large integration timesteps commensurate with the dynamics of interest, e.g. an aircraft simulator may only require outputs at 50 ms.

The prime issue at stake here, is the use of iteration in a model on which is placed strict constraints on execution time. Clearly, no specific guarantees can be made on the number of iterations to match the cycle and so a limitation has to be imposed in order to give a model that has predictable execution times. It has been shown that a model limited to as few as 2 passes is viable. Truncation of iteration in this way may lead to loss of consistency, however this discrepancy is likely to be less than the difference between the iterative model (which is taken as the reference computer definition of the engine cycle) and a separate, non-iterating real-time model.

This being so, there are also potential run-time advantages to be cashed for some model applications. A model requiring 4 passes every 50 ms uses less computing power than a non-iterative model running every 1 ms (where 1 ms may be required for stable running). The computing effort advantage amounts to a run time factor of around 10. The advantage is not so marked for applications requiring high bandwidth RTEMs. An iterative model would run 2 – 4 passes at 1 ms; a non-iterative model would typically run (1 pass) at 0.5 ms or less. The comparison in this case may not be so spectacular!

Correct handling of gas dynamics in a non-iterative model may need extremely small timesteps, perhaps 0.1 ms or less. Such a small timestep is not desirable for real-time work, a larger timestep is required. The usual way of ensuring numerical stability with a larger timestep is apply factors to selected volumes. Consequently, a larger timestep can be tolerated but at the expense of dynamic fidelity. The run time comparison for *correct* dynamics representation is still therefore in the iterative model's favor. It must be said, however, that with the advance in computing power, run-time advantages become less of an issue; it is the benefits of commonality and versatility that come to the fore.

Why stop at real time? There is perhaps the potential to further exploit Monte-Carlo type methodology to engine and controller design where ultra-fast non-linear models could be used effectively.

3.2.5.7 Other Dynamic Events

There may good reason to include other dynamic terms in an engine model in order to satisfactorily replicate engine behavior, especially on analysis of gross transients such as fuel-spiking to map the compressor stall line. Fuel ignition characteristics (often modeled as pure delays) can significantly affect control stability margins. Metal growth follows on from the heat-soakage modeling described above. Turbomachinery tip clearance has a significant effect on engine performance; this behavior can also be modeled using the techniques outlined above.

3.2.6 Iteration and Numerical Methods

3.2.6.1 Local Iterations

The example hereafter shows the loop nesting required by local iterations when that method is applied to the resolution of the compatibility equation set described in for a free turbine engine turboshaft. The algorithm is given in **Figure 3.45**. It describes four nested loops, one for each compatibility equations (the speed compatibility is directly obtained, because XNH is data) but the equations are solved one after each other.

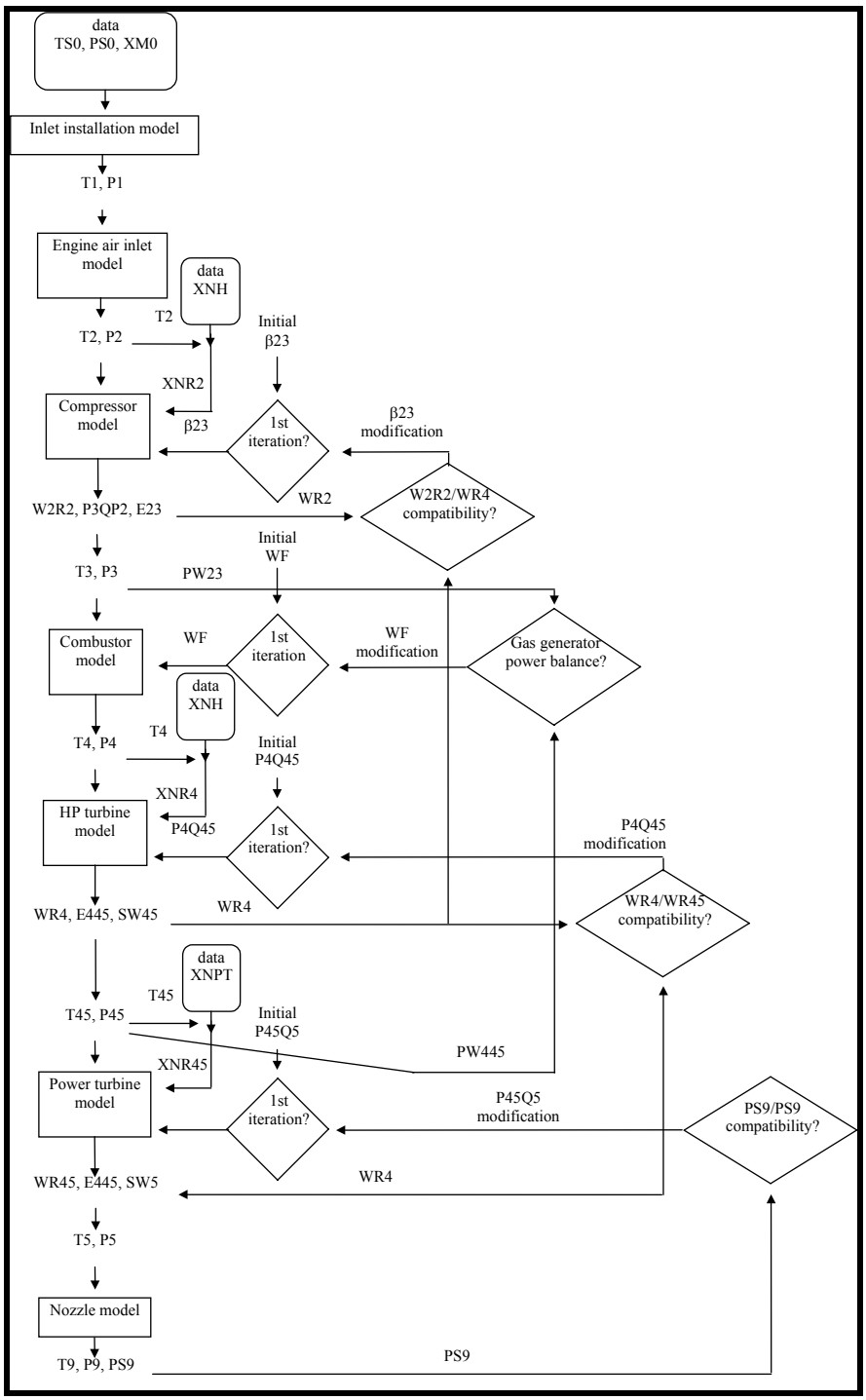

Figure 3.45: 0-D Modeling of a Free Turbine Turboshaft Engine.

In such a model, the calculation at given gas generator speed is privileged. In order to calculate the engine cycle at given output power, or at given HP turbine inlet temperature, etc., it is necessary to add one more loop in which XNH varies until the data parameter reaches its given value.

3.2.6.1.1 Advantages

The local iteration method was, historically, the first one used because it is very close to the manual procedure to calculate an engine cycle. It has the following advantages:

- It is based on a very physical approach because at each step, a part of the compatibility equations are satisfied.
- It exploits all the peculiarities of the engine architecture to reduce the number of loops and to recalculate only the minimum number of components when iterating within a loop. In the turboshaft example, there is a loop iterating on P4Q45 in order to match the compatibility of flows between the HP turbine and the power turbine. Such a loop recalculates the cycle only in the turbine part and not from the air inlet. This allows timesaving, which does not now seem critical but really was at the beginning of off-design simulation.
- Solving the problem by nested loops allows the use of very simple mathematical methods to match convergence, via for example, simple gain correction, dichotomy or the 1-D Newton-Raphson method.
- Using simple methods and reducing the dimension of the problem, it was possible to run the resulting performance code on nearly any computer platforms, even with low computing resources.

3.2.6.1.2 Drawbacks

The local iterations method is, nevertheless, being abandoned by engine manufacturers for many reasons:

- ***Complexity*** – The turbofan example shows that the loop nesting becomes very complex when considering multi-spool, multi-streams engines.
- ***Convergence*** – When numerous loops are nested, it is necessary to have high precision convergence of the internal loops so that the external loops may converge. This may reveal difficulties in the whole operating range, especially in cases where strong cross-coupling appears as in the case of mixed flow or recuperated engines.
- ***Need for Discouplings*** – The local iteration method can, often, be used only because the current component calculation depends only on the flow characteristics at its inlet and a reduced number of operating parameters. But, when accounting for secondary effects, like clearances or ventilation, the couplings between stations increase strongly, and it may become very difficult to find a satisfactory nested loops scheme.
- ***Generality*** – The local iteration method, by nature, uses all of the particularities of the engine architecture and component models. Therefore, the performance program created by this method is strictly limited to one engine type. Even for a given engine, extensive reprogramming may be necessary in case of a component modeling change. For example splitting a single compressor into two separate stages changes the size of the problem, and requires additional loops. Changing a loss model may also require reprogramming of the loops, the convergence criteria and so on. The local iteration method lacks generality and leads the engine manufacturer to have numerous performance programs to identify and maintain. Such a method is quite prohibitive for meeting actual quality requirements and prevents the designer from having a single 0-D performance code that is able to deal with various engine architectures.

Because of all these drawbacks, the local iteration method is less and less used. Global methods are increasingly used, allowing more generality and more modularity, thus avoiding the dispersion of

component models in too many programs. Furthermore, the initial computation time gains, which justified use of this method, are now less because of computer speed increases. A global method may now be run, quite instantaneously, on a portable PC.

3.2.6.2 Global Iterations and Multi-Dimensional Newton-Raphson

Instead of solving separately the equations, the global method is based on an iterative resolution of the whole set of equations.

The previous section, ***3.2.6.1***, described how performance computation consists of identifying the values of characteristic parameters of each component. These parameters may be gathered in a vector of the unknowns, denoted X (dimension n). The set of compatibility equations completed by the power parameters constraints, constitutes a vector denoted F(X) (dimension n) and the performance calculation consists in solving F(X) = 0, with each line of F representing a compatibility error.

The most usual method to solve this set of equation is a multi-dimensional Newton-Raphson method:

- The first step is to initialize the unknowns. This phase may seem simple but it must be sufficiently efficient to define an initial point not too far from the real operating point, within the operating domain. This may be done by assigning constant values at the unknowns, or by using the values of the unknown parameters at the center of the maps for map modeled components, or by using an approximate tabulated working line. The successful convergence and the calculation time are dependent on the quality of this step. Let us denote Xo as the initial unknown vector.
- The second step is to apply the Newton-Raphson method. This consists of linearizing the function F around the point Xo, such that:

  $$\mathbf{F(X) = F(Xo) + A(X - Xo)}, \qquad \textbf{Eq. 3-51}$$

  where A denotes the Jacobian matrix of F (dimension n x n). Each element Aij of A, represents a correlation or influence coefficient of the j-th unknown on the error committed for the i-th equation. These n^2 partial derivatives are obtained by finite difference calculation:

  This matrix contains a lot of zeros, which represent all the local iterations that were exploited in the method local iteration approaches described in ***Section 3.2.6.1***.

  To achieve the goal, which is to have F(X) = 0, we must have:

  $$\mathbf{\Delta X = X - Xo = -A^{-1} F(Xo)} \qquad \textbf{Eq. 3-52}$$

  By inverting the Jacobian matrix A, it is possible to calculate a variation of the unknowns ΔX and thus to determine a new point X1. The linearization process can then be repeated at point X1. This procedure defines a series of values Xn that converges to the solution point X such that F(X) = 0.

The following remarks apply:

- If the Jacobian matrix is singular or ill conditioned, it means that the choice of the unknown parameters and compatibility equations is not appropriate. One of the unknowns may be not representative or an equation may be absurd, or the unknowns are not independent.
- It is often necessary to limit the variation of the unknowns at each iteration because the problem is non-linear and the solution may diverge for big variations of the unknown parameters.

The following algorithm (see **Figure 3.46**) may summarize this method. Other methods are available to solve a non-linear set of equations but Newton-Raphson is very often the most robust.

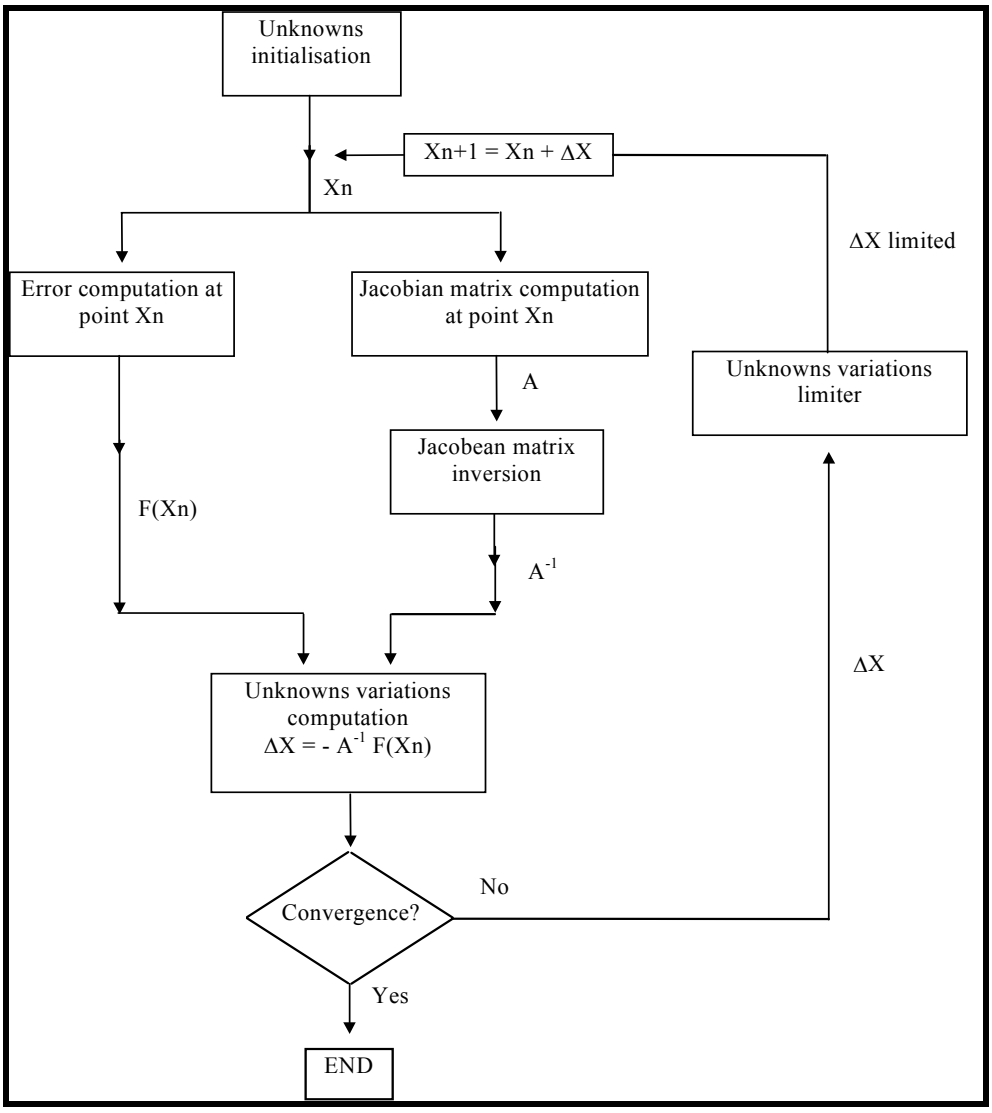

Figure 3.46: Multi-Dimensional Newton-Raphson Iteration.

3.2.6.2.1 0-D Modeling of a Free Turbine Turboshaft Engine

The example hereafter shows an application of the global iterations method when it is applied to the resolution of the compatibility equation set described in for a free turbine engine turboshaft. Let us take the same example as in ***Section 3.2.6.1***. In order to compare both methods, we will analyze the same calculation case, that is to say, taking the gas generator and power turbine real speeds as power setting parameters.

The unknown vector X is:

$$X = \begin{pmatrix} XNR2 \\ b23 \\ WF \\ XNR4 \\ P4Q5 \\ XNR45 \\ P45Q5 \end{pmatrix} \qquad \textbf{Eq. 3-53}$$

The set of equations to be solved is:

Mass flow: HP compressor and HP turbine

$$\frac{WR2(XNR2,b23)P2}{\sqrt{T2}} + WF - \frac{WR4(XNR4,P4Q45)P4}{\sqrt{T4}} = 0 \qquad \textbf{Eq. 3-54}$$

Mass flow: HP turbine and power turbine.

$$\frac{WR4(XNR4,P4Q45)P4}{\sqrt{T4}} - \frac{WR45(XNR45,P45Q5)P45}{\sqrt{T45}} = 0 \qquad \textbf{Eq. 3-55}$$

Speed: HP compressor and HP turbine.

$XNR2\ \sqrt{T2} - XNR4\ \sqrt{T4} = 0$ **Eq. 3-56**

Power equilibrium: gas generator spool.

$PW23 - PW445 = 0$ **Eq. 3-57**

Static pressure: nozzle outlet.

$PS9 - PS0 = 0$ **Eq. 3-58**

Power setting parameter 1: gas generator speed.

$XNR4\ \sqrt{T4} - XNH_{data} = 0$ **Eq. 3-59**

Power setting parameter 2: power turbine speed.

$XNR45\ \sqrt{T45} - XNPT_{data} = 0$ **Eq. 3-60**

Figure 3.47 below shows a typical algorithm that is used to evaluate the errors.

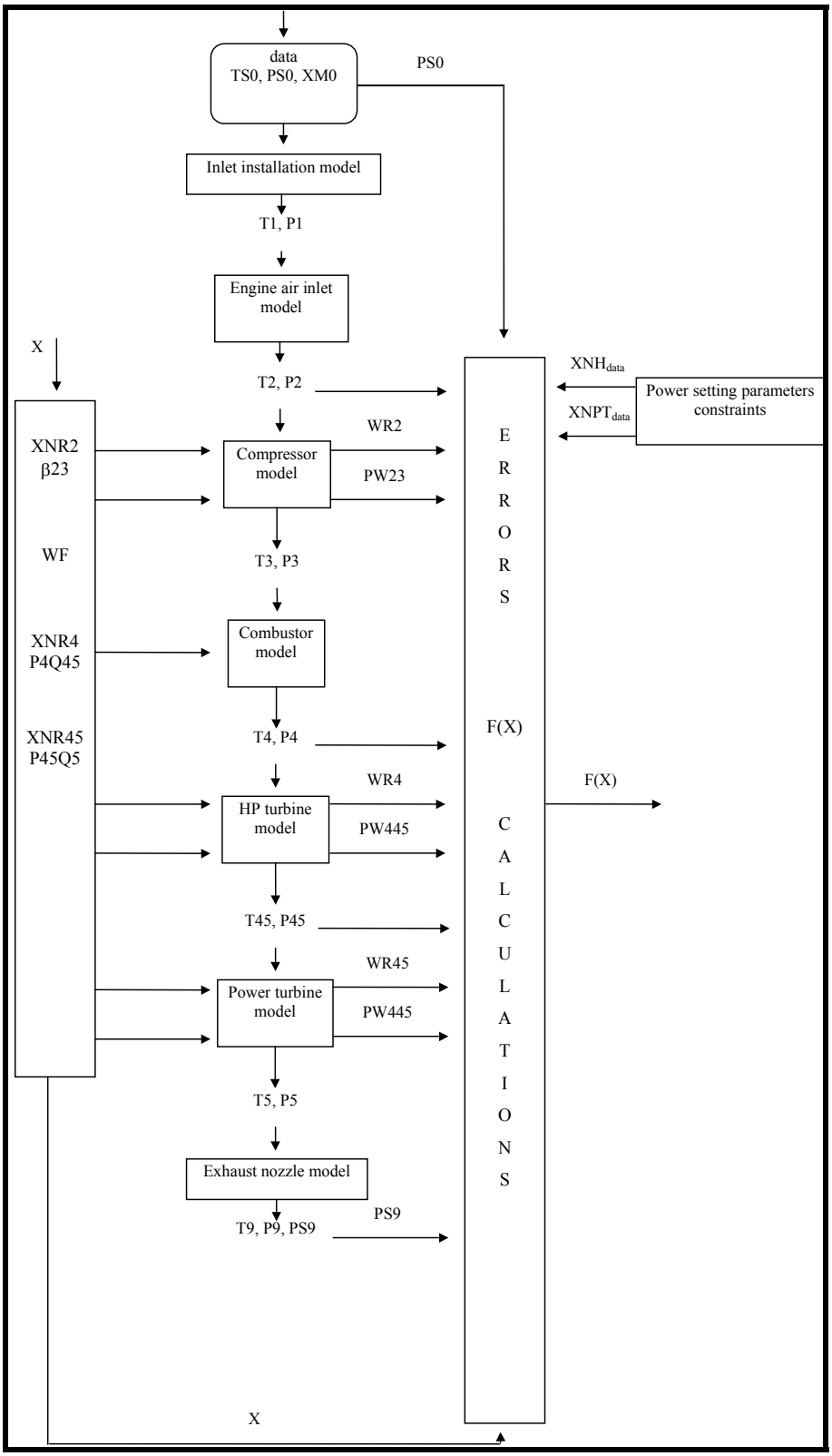

Figure 3.47: 0-D Modeling of a Free Turbine Turboshaft Engine.

At each iteration, this algorithm is used 8 times for the following values of X: β (see **Table 3.3**).

Table 3.3: Values for Iteration

1)	[	XNR2	β23	WF	XNR4	P4Q45	XNR45	P45Q5	]
2)	[	XNR2 + dXNR2	β23	WF	XNR4	P4Q45	XNR45	P45Q5	]
3)	[	XNR2	β23 + dβ23	WF	XNR4	P4Q45	XNR45	P45Q5	]
4)	[	XNR2	β23	WF + dWF	XNR4	P4Q45	XNR45	P45Q5	]
5)	[	XNR2	β23	WF	XNR4 + dXNR4	P4Q45	XNR45	P45Q5	]
6)	[	XNR2	β23	WF	XNR4	P4Q45 + dP4Q45	XNR45	P45Q5	]
7)	[	XNR2	β23	WF	XNR4	P4Q45	XNR45 + dXNR45	P45Q5	]
8)	[	XNR2	β23	WF	XNR4	P4Q45	XNR45	P45Q5 + dP45Q5	]

The first calculation gives the error at current point F(Xn) and, combined to the following seven by finite differences, the Jacobian matrix A. It is then possible to calculate the following point Xn+1 by applying the algorithm from the local iteration description.

3.2.6.2.2 0-D Modeling of a Twin-Spool Mixed Flow Turbofan Engine

3.2.6.2.2.1 Advantages

The advantages of the global method are clear when comparing the algorithms of the two method types used for the two former examples. In the global method, the cycle and components calculation is clearly separated from the mathematical resolution instead of being mixed because of numerous nested loops in the local iteration method.

Thanks to this separation, the resolution algorithm does not depend on the engine architecture under consideration. There are only small differences between the algorithms of the two former examples:

- Size and unknown types of the vector X;
- Size and equation types of the vector F; and
- Component calculation.

Therefore, the global method allows multi-architecture 0-D performance programs to be built easily, which was impossible with the local iterations method.

By separating component calculation and resolution, it is easier to modify the engine modeling and thus to maintain the program because the resolution part remains unchanged. This includes accounting for secondary effects.

The global method allows a simultaneous convergence of all the unknowns instead of accumulating nested loops in which only one unknown converges. This generally results in timesaving as soon as the modeled engine becomes complex or presents cross-couplings.

3.2.6.2.2.2 Drawbacks

The global method does not have really drawbacks but its usage requires more attention.

Being based on non linear equations resolution, the global method uses more sophisticated mathematics. Thus it requires more development work than the local iterations method.

In particular, the development of the initialization step and variation limitation step requires a very careful analysis in order to ensure convergence in the whole range of computation cases (high max variation of the unknowns reduce iteration number but also stability of the method).

3.2.6.3 Relaxation

Relaxation techniques use the same derivatives that are created for either local or global iteration. However, instead of solving the system at each step, the information is used to project a solution without explicitly resolving the errors. A damping factor, to reduce the sensitivity of the change in independent variables to the change in error term, drives the solution to the same result as direct iteration solution but with much less mathematical calculation. A relaxation approach is often more effective in highly non-linear regions of the simulation.

3.2.6.4 Constraint Handling

The iteration schemes described above are used to satisfy continuity and the implicit nature of the simulation. They also assume the dependent and independent variables in the iteration are within the limits of the component and engine simulation. Options for constraining the iteration for these limits are to add additional iteration variables to match data or maintain other limitations.

3.2.7 Non-Component Based Parametric Models

These simple, fast models are used as surrogates of more complex thermodynamic models in a variety of applications that span the full range of gas turbine design, development and operation. Parametric models are employed in applications where speed is valued over accuracy or where uncertainty in the engine component characteristics or engine environmental conditions does not warrant thermodynamic model complexity. Generally, they achieve computational simplicity and speed at the expense of accuracy and resolution relative to the thermodynamic models from which they are derived. However, they typically offer equal or better accuracy than a simplified thermodynamic model of comparable speed. The formulation of parametric model always involves some form of data fitting such as polynomial functions or piece-wise linearization. In addition to speed, these models also provide a means of conveying engine performance characteristics while protecting proprietary component characteristics and modeling methodologies.

3.2.7.1 Applications

Some typical applications of parametric models are discussed below. Model formulations and synthesis procedures are discussed in the following sections.

3.2.7.1.1 Conceptual Design

The first parametric models were simple tabular listings or graphs of dependent versus independent performance variables. These continue in use today and in the foreseeable future in the form of multi-variate computer databases, which are used in conceptual vehicle design. The objective of the conceptual design

process is to effectively converge on an optimum vehicle design including engine system requirements for engine size, performance and operability. Detailed component requirements are defined later.

Parametric models (whatever the formulation) offer several advantages in the conceptual design process:

- Computing resource requirements are reduced for highly repetitive calculations;
- Results can be pre-certified by engine manufacturer;
- Numerical convergence issues are avoided;
- Proprietary or sensitive information can be omitted; and
- Dependent and independent variables can be transposed for inverse design.

A parametric model may be employed as a living engine specification, conveying the anticipated steady and dynamic characteristics of an engine.

3.2.7.1.2 Control Design and Validation

Parametric dynamic models have long been used in the design of control laws where linear control theory required representation of the engine dynamic behavior as a Laplace, state-space, or other linear formulation. Today, sets of these single point dynamic models are assembled with the corresponding steady-state models to provide full range transient models that are employed in the control validation process as well. These models are especially effective in the real-time validation of integrated flight/propulsion controls systems where fast execution is a requirement.

3.2.7.1.3 Module Performance Analysis

Module performance analysis (also called gas path analysis) is a process employed in fleet (on-wing) monitoring and trending to determine the health of gas turbine components and forecast operational impacts and logistics requirements. Today, statistical parameter estimation algorithms are employed to determine component performance indices that can not be computed directly from the small number of on-wing measurements. These estimation algorithms are founded in linear control theory and typically are based on state-space parametric models as described in the control application above. In deriving the estimation algorithm, the normal cause-effect relationships represented in the model are transposed mathematically into effect-cause relationships.

Module performance analysis can be applied to either steady state or transient data and can even be embedded in the real-time control.

3.2.7.2 Model Formulation

A parametric model is a surrogate for a physics-based parent model and must represent the important characteristics of the parent for the intended application. In general, the physics of the parent model are represented implicitly rather than explicitly in the surrogate model. Parametric models map the complex relationships between the dependent and independent variables in the parent model into simple relationships between outputs (fluid pressures, temperatures, flows) and inputs (fuel flow, variable geometry, bleed) and internal dynamic states (rotor speeds, metal temperatures), if the model is dynamic.

The choice of input, output and state parameters is important because it determines the model accuracy and the extensibility to operating conditions beyond those where model was synthesized. The choice of parameters is commonly based on intuitive insight and experience, but can also be based on numerical analysis of parent model characteristics. Conventional gas turbine correction factors are commonly used to account for inlet conditions.

There are a variety of mathematical formulations for parametric models ranging from simple multi-variate tables for steady-state models to state-space formulations for dynamic models. In general, the state space formulation offers the greatest accuracy and flexibility and is well supported by commercially available software toolkits (XMath, MATLAB). Multiple state-space models can be assembled to cover the full engine operating range. Simple transfer function representations are a popular alternative model formulation often employed in preliminary design when engine are not well characterized. This formulation does not even require a parent model, and can be based on expected characteristics.

3.2.7.3 Model Synthesis Procedures

A parametric model synthesis process can be used. In this case, the appropriate steady state and dynamic characteristics are extracted from the parent model. These characteristics may be computed using a variety of techniques such as simple mapping, factorial experiments, and system identification procedures. It is desirable to automate the synthesis procedures to reduce development time and eliminate errors. This is important because model synthesis is normally a recurring process that must be performed whenever there are substantial revisions to the parent model. The overall representation of the parametric model must be validated with the parent model. Typically, validation is performed by simply comparing the parent model with parametric model outputs for a set of input cases. Dynamic validation can be by comparing the frequency response of the parent and parametric models.

3.3 GAS TURBINE ENGINE PERFORMANCE ANALYSIS

During an engine test a force, spool speeds, many pressures and temperatures at various locations along the flow-path and positions of the variable geometry (guide vanes, nozzle area) are measured. However, these values alone are of limited use without special interpretation. The task of the engine test analysis is to find the operating points of the compressors and turbines in their maps, from the measured data.

This section deals mainly with turbofans because tests of this type of engine are especially difficult to analyze. It is difficult to get a precise value for the mass flow that enters the core. This mass flow, however, is required for the calculation of the burner exit temperature, which cannot be measured directly for a variety of reasons. After a thorough test analysis the performance model can be calibrated and – if necessary – improved with newly found correlations.

3.3.1 Performance Instrumentation

For a dedicated engine performance test to check the specific fuel consumption, it is not sufficient to analyze only the thrust and fuel flow. The engine inlet conditions in terms of total pressure and temperature are also needed. A precise value for the mass flow entering the engine is very important. The measured force must also be corrected for testbed specific effects, like cradle drag, to finally obtain the thrust.

Between and downstream of the compressors there must be a sufficient number of total pressure and temperature probes. In the hot part of the engine the total pressure measurements at the inlet and at the exit of the low-pressure turbine are very important. The total temperature rakes at these locations are of limited use for engine performance analysis. There are severe temperature gradients both radially and circumferentially making it extremely difficult to get a representative mean value for the total temperature of the main gas stream.

3.3.2 Model Validation and Calibration

A conventional engine test analysis is quite simple and straightforward. The power required to drive the fan is calculated from the engine mass flow and the total temperature increase. The fan efficiency for the

core and the bypass stream can be found from total pressure and temperature measurements. Similarly the efficiency of the high-pressure compressor is derived.

The power required to drive the core compressor cannot be calculated without knowing the core mass flow. There are many methods to determine this flow, and the associated by-pass ratio. However, two of them are used frequently: the *turbine flow capacity* method and the *heat balance*. The indices in the formulas below refer to the station designation in **Figure 3.48**.

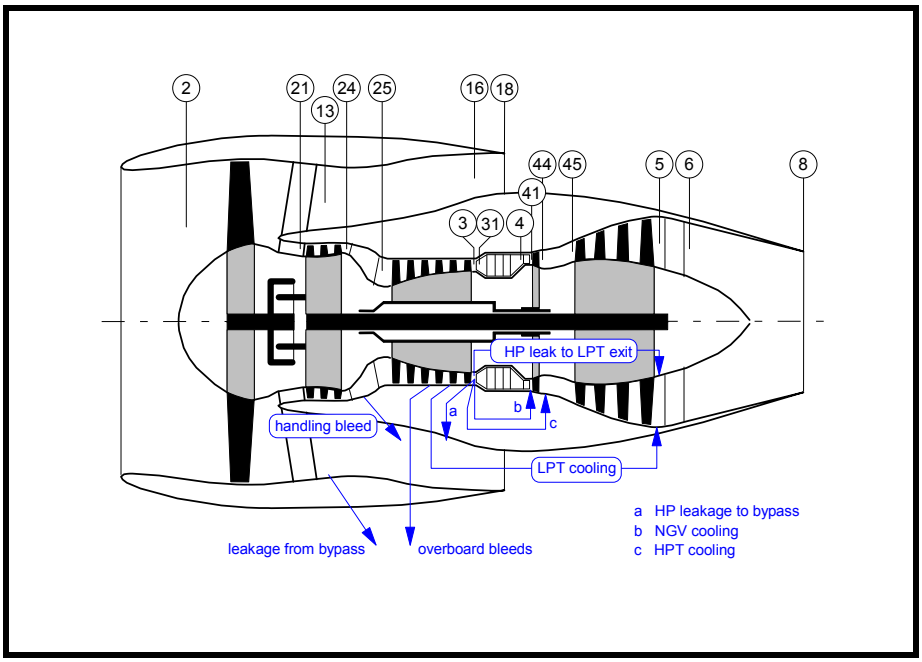

Figure 3.48: Turbofan Station Designation.

3.3.2.1 Turbine Flow Capacity

The basis of the *turbine flow capacity* method is that in the nozzle guide vane of the high pressure turbine, the flow in the throat is usually sonic or very near to sonic. For sonic flow the quantity $W*\sqrt{T}/(A*P)$ is a function of the gas constant and the isentropic exponent only. Since we know the gas properties we only need to measure the turbine throat area to evaluate $W*\sqrt{T}/P$. This term is the *turbine flow capacity* which gives the method its name.

When the fuel is a hydrocarbon with the hydrogen carbon ratio of kerosene the gas constant of the combustion products will be practically the same as that of air. Typically the isentropic exponent of the gas in a turbine is around 1.3 while that of air at room temperature is 1.4. This difference in the isentropic exponent has approximately the opposite effect on $W*\sqrt{T}/(A*P)$ as the difference in temperature has on the throat size due to the thermal expansion of the metal. Therefore the term $W*\sqrt{T}/P$ is practically constant for all engine operating conditions with near sonic flow in the high-pressure turbine throat.

To make use of the known value for $W_{41}*\sqrt{T_{41}}/P_{41}$ we need some further correlations. The total pressure at the turbine throat P_{41} is calculated from the measured compressor exit pressure P_3 and the burner loss characteristic.

From the fuel flow W_F, the fuel heating value FHV and the measured burner inlet temperature T_3, the turbine throat temperature T_{41} can be found:

$$T_{41} = T_3 + f(far, FHV)$$ **Eq. 3-61**

Note that for the fuel-air-ratio, FAR = $W_F/(W_{41}-W_F)$ and for the calculation of the gas mass flow W_{41} one needs to know the secondary air system:

$$W_{41} = W_{25} - W_{\sec} + W_F$$ **Eq. 3-62**

During the first pass through the test analysis computer program the core inlet mass flow W_{25} is a guess and later modified in such a way, that $W_{41}*\sqrt{T_{41}}/P_{41}$ has the prescribed value.

When W_{25} and the inter-stage bleed flows are known then the power to drive the core compressor can be determined. After taking into account gearbox drag, power off-take from the high-pressure spool and the cooling and leakage air mass flow, the work done by the turbine can be calculated. We get the ideal work from P_{41} (as calculated above) and the measured total pressure P_{45}. Turbine efficiency can be evaluated with this information.

Besides the efficiency we get a calculated value for the high-pressure turbine exit temperature T_{45}. The power balance for the low-pressure spool allows calculation of the low-pressure turbine exit temperature T_5. These two temperatures will not be identical to the measured data T_{45m} and T_{5m}. Actually, the measured hot end temperatures are ignored when doing a *turbine capacity* core flow analysis.

3.3.2.2 Heat Balance

The *heat balance* method is based on a measured hot end temperature and ignores the eventually known turbine capacity. This method makes sense when T_{45} or T_5 is measured with many rakes. On rare occasions a rotating rake is used downstream of the low-pressure turbine which allows calibration of the standard instrumentation with only a few rakes for T_5.

Similarly to the turbine capacity method, the core-flow analysis starts with an estimated value for W_{25}. The high-pressure turbine inlet temperature T_{41} is found with the same assumptions as described above. The energy balances for the high and the low-pressure spool will yield T_{45} and T_5. The estimated value for W_{25} is modified, in such a way that after convergence the calculated value for either T_{45} or T_5 equals the measured value.

3.3.2.3 ISA Corrections

During a normal engine test at a standard sea level testbed, for example, both the inlet pressure and the inlet temperature will deviate from ISA sea level standard conditions (T = 288.15 K, P = 101.325 kPa). The test results must be corrected to these engine inlet conditions to make the data comparable. This is often done on the basis of the Mach number similarity.

The operating conditions of a turbomachine are similar when the Mach numbers are the same everywhere in the flow-field. For a fluid with known properties of isentropic exponent and gas constant, this is the case when the corrected flow $W\sqrt{T}/P$ and the pressure ratio are the same. Also the temperature ratios and the corrected spool speed $N/\sqrt{T}$ will be identical for strictly similar flow-fields. Note that the variable geometry settings (guide vanes, nozzle area, bleed valve positions) must remain unchanged during any data correction on the basis of the Mach number similarity.

It can be easily shown that when the Mach numbers are the same, the terms F_N/P_0 (corrected thrust) and $SFC/\sqrt{T_0}$ (corrected specific fuel consumption) will also be the same.

With the help of these and other simple correction formulas for flow, pressures, temperatures, spool speeds, thrust, power off-take and SFC one can easily derive all engine data for a standard day.

The correction procedure on the basis of the Mach number similarity is not very accurate because the formulas are strictly valid only when: the gas properties do not change, thermal expansion of the engine has no effect on tip clearance, and Reynolds number effects do not exist. The quality of the correction procedure can be improved empirically by slight modifications of the original formulas:

$$\frac{F_N}{P_0} = F_N * P_0^{-1} \Rightarrow F_N * P_0^{-x} \qquad \textbf{Eq. 3-63}$$

The exponent x in this formula is adjusted empirically to give the best fit to measured or calculated data. The same approach can be used with other quantities like SFC. For example:

$$\frac{SFC}{\sqrt{T_0}} = SFC * T^{-0,5} \Rightarrow SFC * T^{-y} . \qquad \textbf{Eq. 3-64}$$

After having corrected all measured data from several engine tests one has a sound basis for the calibration of the engine performance model. Engineering judgment, experience, patience and many trials are necessary to get a good match of the model to the data.

3.3.2.4 Accuracy

Engine tests are performed to evaluate the overall characteristics in terms of thrust and specific fuel consumption. However, especially during the development phase, the main purpose of performance testing is to find the efficiency of the engine components and to prove that the design assumptions were valid. For such an analysis one needs to know the total pressure and temperature at all component interfaces as well as the mass flows.

Any measurement (as for example a temperature probe on a rake between two components) has an uncertainty that is affected by both random and systematic measurement errors. When it is repeated several times, the instrument readings will not agree exactly but will show some scatter.

In gas turbine engine tests random effects in the measurement chain are caused by this scatter, and also by small changes in engine geometry and operating conditions. An engine is never running in absolute stability because of small changes such as inlet flow conditions, variable geometry settings, and thermal expansion of casings and disks.

In a carefully controlled engine performance test the random errors mentioned above are not negligible, but smaller than the systematic errors caused, for example, by non-ideal positioning of the probes. There is seldom space in an engine to put enough pressure and temperature pickups at the component interface plane. Besides that, instrumentation intrusion effects must be minimized.

Every effort is made to correct the measurements for all known effects. However, an uncertainty remains.

The difference between the measurement (after applying all known corrections) and the true mean value is called a bias. There are no exact data available to calculate the magnitude of a bias and therefore it is usually estimated from experience with component rigs, for example.

3.3.2.5 Example: Low Pressure Turbine Efficiency Analysis

The efficiency of a low-pressure turbine (LPT) is:

$$\eta = \frac{\Delta H_{actual}}{\Delta H_{ideal}} \approx \frac{1 - \frac{T_5}{T_{45}}}{1 - \left(\frac{P_5}{P_{45}}\right)^{\frac{\gamma}{\gamma - 1}}} \qquad \textbf{Eq. 3-65}$$

where γ is the mean isentropic exponent of the gas.

The total pressures P_{45} and P_5 must be measured with several rakes and many leading-edge probes. These measurements must be looked at in much detail. Rakes, for example, will modify the flow-field in such a way, that they increase the local pressure slightly. This must be corrected by rake position correction factors.

Further corrections to the measured values are necessary, when it is known that the rakes do not pick up a representative mean value for the relevant thermodynamic station. For example, rakes positioned in an interduct will not see the wall losses caused by the struts and thus may indicate the total pressure upstream of the interduct even when the pickups are positioned towards the end of the duct.

Also the total temperatures around the low-pressure turbine are not easy to measure. One of the total temperatures (either T_{45} or T_5) is a direct result of the core flow analysis, which yields W_{45}. Since the total temperature measurements in the hot part of the engine are due to the severe circumferential and radial profiles, and not very accurate it is better, to derive the specific work-done from elsewhere. The work-done, ΔH_{LPT} is proportional to the total temperature difference T_{45}-T_5 from measurements in the cold part of the engine. The energy balance yields

$$\Delta H_{LPT} = \frac{W_2}{W_{45}} \Delta H_{Fan} + \frac{W_{21}}{W_{45}} \Delta H_{Booster} \,. \qquad \textbf{Eq. 3-66}$$

Any error in the analysis result for the engine inlet mass flow W_2 will have an impact on the LPT efficiency result.

Getting a precise value for the specific fan work ΔH_{Fan} is very difficult for high bypass engines. It must be derived from the total temperature measurements upstream and downstream of the fan. **Figure 3.49** shows in the left part the typical temperature rise in the fan as a function of bypass ratio. In the right part one can see that a measurement error of 1 °C will cause an error in specific fan work of 1% for engines with bypass ratio of 4 and nearly 3% for very high bypass engines.

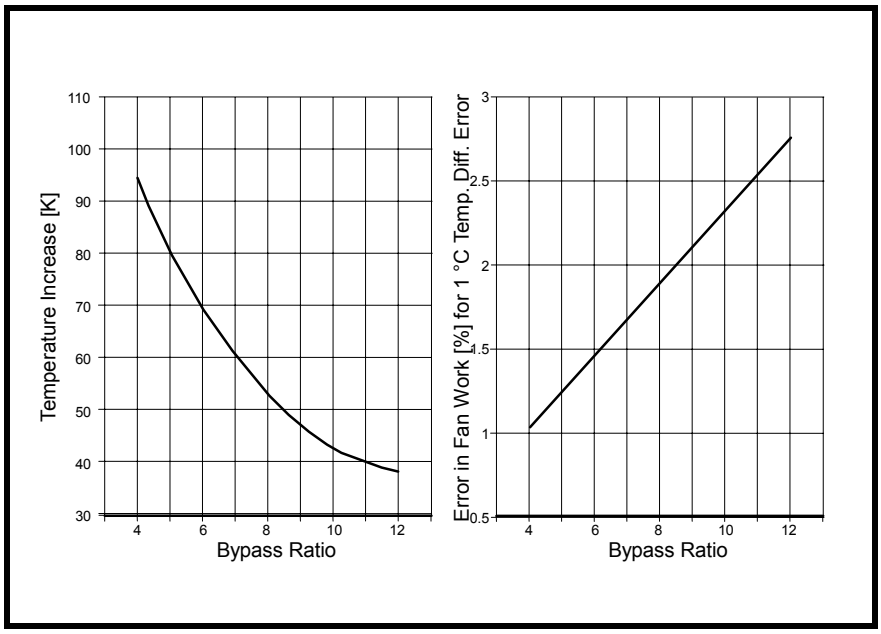

Figure 3.49: Effect of Fan Temperature Measurement Accuracy.

An analysis error of 1% in fan work is totally unacceptable. Therefore the temperature difference must be measured with a tolerance much lower than 1 °C and everything must be done to get the best values for the temperature increase over the fan.

The desired accuracy of the analysis dictates the number of rakes and immersions needed. A thorough static calibration of the thermocouples is required. Total temperature measurements require a recovery correction, which must be applied to the measured values as a function of the flow Mach number and density. Before using the individual pickup measurements for calculating a mean value they should be checked by coarse and fine filters. Erroneous measurements should be neglected or substituted by reasonable data, which can be derived from averaging good values.

Due to thick struts downstream of the fan, it is possible that the temperature increase may vary circumferentially. It might be necessary to apply position correction factors to the reading of the rakes, which can be found from detailed CFD calculations that provide information about wall and boundary layer effects.

In summary we need very good values for the pressures P_{45} and P_5, a precise engine inlet and core flow analysis (which sets the temperature level of the LPT) and an accurate measurement of the temperatures upstream and downstream of the fan, which yields the temperature difference T_{45}-T_5.

Even with the best effort it remains extremely difficult to find the low-pressure turbine efficiency of a high bypass engine from the measurements around the low-pressure spool components alone. However, when looking at all engine components simultaneously and comparing the results with all available information one can get a better test analysis quality.

3.3.2.6 Analysis by Synthesis

The conventional test analysis as described in the chapters above makes no use of information, which is available from component rig tests, for example. It will give no information about the reason why a component behaves badly. A low efficiency for the fan may be the result of either operating the fan at an

aerodynamic over-speed or a poor blade design. To improve the analysis quality in this respect is the aim of *Analysis by Synthesis* (ANSYN).

3.3.2.6.1 Principle

When doing analysis by synthesis a model of the engine is automatically matched to the test data. This is done with scaling factors to the component models, which close the gap between the measured efficiency and the model. For example, efficiency scaling factors greater than one indicate that the component performs better than predicted.

Let us explain the procedure for the example of a compressor. The model of the compressor is a calculated or measured map, which contains pressure ratio over corrected flow for many values of corrected spool speed $N/\sqrt{T}$.

During the test analysis, we obtain from the measurements, the pressure ratio, the corrected mass flow, the efficiency and the corrected spool speed. Normally we will find that the point in the map defined by the measured pressure ratio and the measured corrected flow (marked in the figure by the open circle) will not be on the line for $N/\sqrt{T}$ in the original map.

We can shift the line marked $N/\sqrt{T_{map}}$ in such a way, that it passes through the open circle. This is done along a scaling line that connects the open with the solid circle. The mass flow and the pressure ratio scaling factors describe the distance between the two circles. The efficiency scaling factor compares the analyzed efficiency with the value read from the map at the solid point.

The shifting direction along the scaling line is somewhat arbitrary. There is no strict rule for defining the local gradient of the scaling line. However, it is obvious that neither strict horizontal nor strict vertical shifting would work under all circumstances.

One can try to give the scaling line some physical meaning. For example, it is possible to define the scaling line as constant corrected flow at the exit of a compressor or alternatively as a line with constant specific work over speed squared.

More important than the gradient of scaling lines is a high fidelity model of the compressor. A map is strictly valid only for the inlet temperature and inlet pressure for which it was calculated or measured. When the inlet temperature is different from the reference the isentropic exponent of the fluid will change and cause small changes in the flow-field around the blades. Since the Reynolds number of the flow in the compressor depends on both inlet pressure and temperature, there will be additional differences when the compressor is not operated at the reference inlet conditions.

Temperature and pressure differences can also result in small geometrical changes like tip clearance and blade untwist, which have an effect on the performance of the compressor.

All known effects that have an impact on the performance of any component should be modeled carefully. The better the model the smaller the distance between the two lines for $N/\sqrt{T}$ in **Figure 3.50** will be and the gradient of the scaling line becomes an academic question.

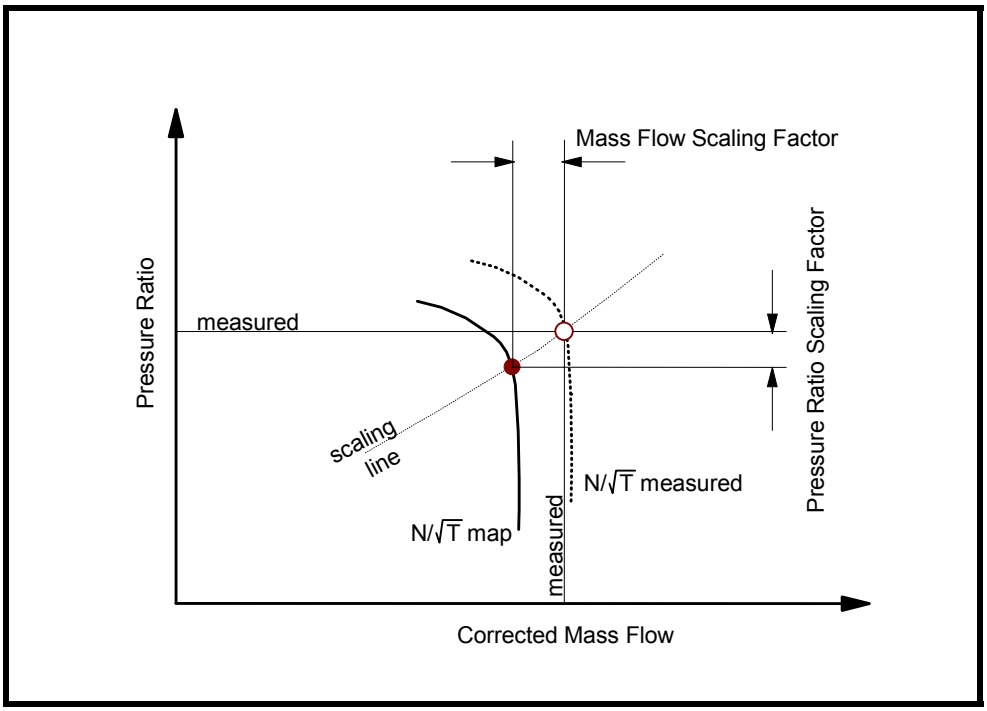

Figure 3.50: Matching the Measured Data to a Map.

3.3.2.6.2 Mathematical Procedure

A numerical model of a turbofan requires the iterative solution of a system of equations with about six variables. Some of the measured quantities that must be consistent with the model value (like all measured pressures and temperatures) will require additional variables. With a sophisticated test analysis model one can end up with 20 to 30 variables in the numerical problem to be solved.

This is not a real problem as long as all measured values are reasonable and the model of the engine is good. However, when a measurement has a significant error, it can happen that the iteration will not converge.

Consider for example the analysis of a scan taken at idle where both static and total pressures are very near to each other. Even when the measurement accuracy is normal, it might happen – when there are not enough static pressure pickups, for example – that the mean static pressure is evaluated to be higher than the total pressure. The model will not allow for that and the consequence is that the iteration will fail to converge.

The same can happen at minimum afterburner rating when the pressure losses due to heat addition become insignificant. The model will never produce negative pressure losses. The measurements, however, might require such a result.

Other reasons for convergence problems can be that the actual hardware is different to the model assumptions.

While on the one side, it is very annoying when iteration does not converge, on the other side a very important hint is given that something is wrong either with the measurement or with the model. The conventional test analysis method does not give this information.

3.3.2.6.3 Best Match

Analysis by synthesis can be formulated as a turbine capacity method or as heat balance method. However, these are not the only methods to find the core flow for a turbofan engine test. In fact, there are quite a lot of options:

- High pressure turbine flow capacity;
- Heat balance;
- Low pressure turbine flow capacity;
- High pressure compressor flow capacity;
- Nozzle flow check;
- Bypass loss characteristic; and
- Any other correlation of P/Ps with corrected flow.

The laws of physics require that all methods for core flow analysis give the same answer. However, the unavoidable problems with measurement biases, random scatter and misinterpretations will cause every core flow analysis method to yield a different result.

Selecting only one core-flow analysis-method, means that some information is ignored. It is very advisable to run several different methods and to compare the results. This will give many hints about the quality of the measurements and the model. The measurements should be consistent with the pre-test uncertainty-analysis.

Another option is, to use several analysis methods simultaneously. We can combine, for example, the turbine capacity method with a heat balance. Remember that the turbine capacity is based on the measured value of the turbine throat area and the heat balance method on a measured value for T_5. From a turbine capacity analysis we will get a difference between the measured and the calculated T_5 and from a heat balance analysis we get a difference between the measured and the calculated turbine throat area A_{41}.

We can set up the analysis in such a way, that we minimize the weighted sum of $[T_5\text{-}T_{5,m}]^2$ and $[A_{41} - A_{41,m}]^2$. The weighting factors will be selected in such a way, that they take care of the confidence that we have in the temperature and turbine throat area measurements.

Obviously we need not restrict ourselves to the turbine capacity and the heat balance methods for core flow analysis. We can use all available measurements simultaneously, and thus we will get a compromise between all conflicting indications of the true core flow. The resulting set of ANSYN scaling factors describes the best match of the model to the test data.

3.3.2.6.4 Simultaneous Analysis of Several Data Sets

Up to now we have discussed only the analysis of a single scan, at a single steady state operation point. For each scan, we will get a set of scaling factors for all component models. When we have to analyze a full performance curve we will get many sets of scaling factors.

When we plot the scaling factors over corrected fan speed, for example, we will normally observe that they are not equal to 1.0 (which would indicate perfect agreement between the model and the test results) and in addition to that there is a trend in the data.

There are two ways to deal with these deviations between the model and the measurements. The first is, we attempt to find the reason for the deviation. When we have found it then we can improve the model by

introducing revised or even new correlations. It might also happen, that we have to modify the way we interpret the measured data.

The second option for closing the gap between test data and model is to use representative curves for the scaling factors and thus calibrate the model.

3.3.2.6.4.1 Developing Model Improvements

When we are looking for the reason why the model deviates from the test data then a straightforward core flow analysis like the turbine capacity method should be used. A *best match* core flow analysis as described in the previous chapter would make trends in the data less visible because it will, to some extent, distribute the deviations between measurements and model over all components of the engine.

How can we find the source of the discrepancies between the test results and the engine model? We must check the scaling factors against parameters that might be the reason. Compressor scaling factors should be checked against compressor parameters, and turbine scaling factors against turbine parameters. All model improvements must be based on the component inlet flow conditions (Reynolds number, temperature, pressure, etc.), the component geometry (i.e. variable vane settings, tip clearance, mechanical deformation by pressure loads, thermal expansion of rotors, blades and casings, etc.) and the operating point in the component map. Also a variable amount of bleed or cooling air which is not modeled correctly will show up in a trend of the ANSYN scaling factors.

When looking for model improvements the basis should always be the original source of the component model. For example, when a compressor map from a rig test is available, this should be the basis for all test analyses with the aim of model improvement. It would be the wrong approach to use a compressor map, which was modified during an earlier model calibration exercise. When doing that one would lose the connection to the original compressor rig data. Without realizing it, one could deviate from the precise rig test result more than is justifiable by rig to engine differences.

It must also be taken into account, that there are many interrelations between the components. An erroneous assessment of the fan work will show up in a trend of the low-pressure turbine, for example. However, it would obviously not be correct to introduce a new correlation into the model of the LPT to eliminate such an efficiency scaling-factor trend. The correction must be applied to the fan model or to the fan exit rake measurement interpretation.

A quite common problem is the efficiency split between fan and high-pressure compressor or between high and low pressure turbine. Within a certain tolerance the efficiency levels can be shifted from the high-pressure spool to the low-pressure spool or vice versa without affecting the overall compression respectively expansion efficiency.

3.3.2.6.4.2 Calibrating a Model

When no further improvement of the physics within the model seems appropriate or feasible then we can introduce empirical calibration curves into the model.

The ANSYN scaling factors (i.e. the factors that make the model line up with the measurements) are a good basis for that. One can either manually draw lines through the set of scaling factors or employ a mathematical procedure. The manual approach has the advantage that spurious data will be ignored by proper engineering judgment.

The mathematical approach is a numerical optimization task. The ANSYN scaling factors are represented by some mathematical functions and the coefficients of these functions are optimally matched to the test data.

The basis of the model calibration can be one or several performance curves taken from a single engine. It might also be data from several engines. The method can be equally applied to data from a sea level testbed and to data from an altitude test facility.

Calibration does not really improve the quality of a model. It adjusts it in such a way that it reproduces the measured data of a single engine or an engine family in the best way in a mathematical sense. A model with empirical adjustment factors of significant magnitude is not very well suited for engine development work. The calibration factors represent the not understood behavior of the engine. They should be kept separate from the physically based models. One should not tweak a compressor map and thus make the calibration an integral part of the compressor model, for example. The calibration factors should always be clearly visible and easy to remove, at least for the engine model creator. The engine test analysis by synthesis should always start from a model with the not understood calibration factors removed. Otherwise it gets very difficult to find the true reason for differences between the model and measurements.

3.3.2.6.5 ISA Correction

The correction of the measured values to ISA standard day conditions is very easy when the ANSYN approach is used. The scaling factors found from the analysis of the scan are applied to the model and then the model is run at the same corrected spool speed $N_L/\sqrt{T_2}$ and the ISA engine inlet conditions.

The operating conditions of the engine will not be exactly the same for both the test and the calculation of the ISA corrected performance. This can be seen from the calculated value for $N_H/\sqrt{T_{25}}$ which will be only very near to (but not exactly the same as) the measured value. The reason for that is the many small effects which do not allow strict Mach number similarity between the tested and the ISA corrected cases like:

- Gearbox drag;
- Fuel, oil and hydraulic pump power;
- Changes in gas properties;
- Reynolds number effects; and
- Thermal expansion of rotors, blades and casings.

We have discussed how the results from a single scan can be corrected to ISA conditions. However, the rated performance also has to be derived from engine performance tests. With the conventional test analysis this requires a set of scans which include the power range of interest. Then a curve fit is applied to the ISA corrected data and the resulting curve is read at the exact value of the rating parameter. This might be a rated temperature, a spool speed or an engine pressure ratio.

With the ANSYN approach one can easily evaluate the rated performance by just running the calibrated model (which is either based on single or on multiple scans) at rated power. During this evaluation one can even simulate an engine without rakes by setting the rake pressure losses to zero in the model.

3.3.2.7 Summary of Analysis by Synthesis

The calibration of an engine performance model with test data is a time consuming task. Traditionally, special test analysis programs are employed for deriving ISA corrected performance data that are then compared with the results of a cycle program. In a second step the model is manually adjusted in such a way, that the simulation results match the test data.

The *Analysis by Synthesis* approach integrates the simulation task with the test analysis. It gives a better insight into the differences between rig and engine test results and allows automation of the process of matching the model to the test data.

3.3.3 Calculation of Installed Performance

The modeling of the installation boundary conditions can be handled either directly by the engine model or by an external application using an engine model. When included as part of the engine model, standard requirements are defined in the SAE **AS681** [3.10].

3.3.3.1 Inlet Recovery

Inlet recovery is an indication of the pressure drop in the air before it enters the engine. For supersonic aircraft this includes the losses associated with the shock and airflow capture process that may be internal or external to the physical inlet. Basic models for both sub-sonic and supersonic operation are generally correlations with a flight condition for a particular aircraft inlet system**. MIL-E-5007D(3)** [3.25] contains default super-sonic recovery curves for a standard inlet and is used for studies and comparison purposes. More detailed inlet models will calculate the pressure loss at a more detailed level and may include the dynamic response of the inlet to changes in the engine. An example of this at a 1-D level is the NASA LAPIN code**,** [3.26], which allows modeling of the high frequency inlet response to both external environment and engine inlet changes. This type of detailed model is particularly useful for examining the start/unstart process in a mixed compression inlet or in evaluating the stall and surge initiation and recovery process in conjunction with a dynamic engine model. More detailed 2-D and 3-D models allow calculation of the pressure and temperature variations that are usually collapsed into distortion indices in simpler models.

3.3.3.2 Distortion

The SAE **ARP 142**0 [3.27] provides definitions and guidelines for addressing inlet pressure distortion in engine simulations. Some of the typical approaches are described below.

3.3.3.2.1 Margins

The simplest and most common method is to consider the stall margin impact on the compression components only, by lumping the impact on component performance into the margin calculations. These are typically quoted as the difference in operating pressure ratio and the stall pressure ratio on either a constant speed or a constant flow basis. Choice of whether constant speed or flow stall margins are more meaningful depends on both the application issue and the control strategy for the engine.

3.3.3.2.2 Impact on Component Performance

When the impact on component performance and stall margin is included, it will generally also include the distortion transfer effect of the components as described in ARP 1420. This includes the creation of temperature distortion that may not have been present at the inlet. This can affect other components not normally affected by pressure distortion such as the combustor pattern factor. Stall line movement with distortion is still modeled but is relative to more representative component reference conditions. This is particularly true in low to medium bypass turbofans where radial pressure distortion can have a significant impact on engine performance.

3.3.3.2.3 Detail Models

Detail description of the distorted flow-field is required for 2-D and 3-D physics based models. Detailed models of inlet distortion of similar complexity to the 2-D and 3-D turbo-machinery models are often required in dynamic simulations where the engine inlet interaction becomes important.

3.3.3.3 Installed Thrust

Installed thrust modeling beyond the adjustments for basic ram drag is included where the nozzle or thrust generation mechanisms cannot be adequately modeled outside the context of the aircraft installation.

The best possible estimate is desired given the uncertainty of both the measured inputs and the assumed environmental and possibly deteriorated engine condition. Often a Kalman filter or other numerical technique is used in conjunction with test data and a full aero-thermo simulation to create a simple in-flight thrust algorithm.

3.3.4 Deterioration and Manufacturing Tolerance

Manufacturing tolerance effects on component performance are rarely measured for production engines. However, the uncertainty in blade and seal clearances, and coating and surface finish contribute to significant variation, even in a brand new engine. During operation, the severity and duration of use affect these characteristics. Some performance changes can be related directly to operating condition (over-speed, over-temperature, maneuver, water wash, and sand-dust-saltwater environment) while others simply follow a general long-term trend. Deterioration is typically based on some combination of continuous and cyclic operation measurement. Cyclic use measurements include throttle movement (TACs in US military engines), take-off and landing, speed excursions, augmentor light-ups). Continuous measurement can include the number of operating hours or hours of operation in a particular condition (hot time, IRP time).

3.3.4.1 Uncertainty of Component Performance

Uncertainty in measured component performance generally depends on the level of instrumentation, instrumentation accuracy, repeatability of the test conditions and the level of correction required to go from the measured conditions to the conditions at which the component performance will be compared and quoted.

Uncertainty in component performance prediction prior to test is generally based on accuracy of design and analysis tools and historical information. For derivative turbo-machinery component designs with some previous calibrated agreement, it may be possible to quantify uncertainty. Predicting turbo-machinery aero performance and operability is one of the most difficult problems in CFD, a subject of on-going research. For new concept aero designs, the accuracy improvement over the historical spread has not been established.

3.3.4.2 Change of Component Performance

As the engine passes through its usage life, component performance changes in typical, if not predictable, ways. Engine deterioration level is easily observed. Determining the underlying component performance change is difficult, and usually impossible, without special instrumentation or analysis. In general, opening of clearances, increased leakage, surface roughness, etc. combine to reduce component performance. Although temporary improvement measures (such as a water wash to remove residue from compressor airfoils and recover performance) are possible, most component deterioration occurs gradually over the engine life. It is modeled via hours of use, or other factors such as time at high temperature, time at high power, and number of throttle movement cycles.

3.3.4.3 Deterioration and Uncertainty in Engine Performance Level

Although engine deterioration will be consistent with the implied effect of component deterioration, the engine user does not typically have the required data to separate out these component performance changes. Data is generally only available for system characteristics such as fuel burn, EGT, rotor speeds, trim settings, thrust, etc. With appropriate data and analysis, this data may be used to estimate component performance changes using simulations or other numerical analysis. However, engine level parameters are most often used directly for condition and health monitoring.

The engine level characteristics vary between engines based on the measured data and the engine control modes. Deterioration is typically based on data where there are limited effects from the standard engine

control modes. For engines controlled to measured pressure ratio, the change in rotor speeds and temperature will be monitored. For engines with exhaust temperature controls, engine speeds or variable control geometry limits may be used. Variation in these performance or monitoring parameters is generally consistent with the difference between the overhaul acceptance level and the engine removal level. This indicates a change in performance such that the aircraft performance requirements are no longer met or the reduced efficiency or potential further deterioration justifies the engine removal.

3.3.5 Emissions

This is a key area of detailed combustor component models. The modeling is usually done at engine level using correlations based on overall performance.

With the increasing attention to gas turbine exhaust gas pollution, exhaust gas emission levels must be predicted at varying operating conditions. On the manufacturers' side, the processes in the combustor are modeled in detail, with CFD, in order to develop new technologies to reduce emissions, such as LPP and RQL combustion. On the operational side, there is interest in how to minimize emissions by optimizing operating conditions such as engine condition, aircraft flight procedures, and fuel type and water and steam injection. The latter two variables mainly relate to ground based gas turbines, using LNG, LH_2 or fuel obtained from gasification of coal or bio-mass. However, it must be noted that LNG and LH_2 fuels for aircraft are already being considered.

ICAO tests are done for all commercial engines prior to certification. They include data for 4 points roughly corresponding to take-off, ground-idle, descent idle and max climb. The test conditions are defined in terms of a fixed percentage of certified engine thrust and may not correspond to the actual engine operation at these power settings on the aircraft.

These are done at sea level static but are used to generate the total emissions for a typical landing and take-off cycle. The ICAO points have been generalized to be applicable across all engines and may not correspond to the actual engine power settings in use. For example, the ICAO setting at 7% of rated power may not correspond to the actual descent or ground idle power setting. Furthermore, the ICAO points do not represent high altitude cruise conditions at which emissions exist for most of the time. To determine cruise condition emission levels, research is directed at both in-flight measurement methods and advanced emission models.

For more general estimates, emission coefficients can be defined as a function of engine conditions. The simplest of these make CO and HC estimates as a function of T3 and NO_x as a function of T3, P3 and ambient humidity. These models usually represent deviation of the emissions from a reference level along with P3 or T3 and are often referred to as *Ratio of P3T3* models. Results can be improved by using these values along with fuel flow and airflow. These improved correlations are usually based on a combustor loading parameter that corresponds to an average residence time. These parameters are typically calculated from T3, P3 as well as combustor airflow and fuel flow. Accuracy of these models generally is limited and only valid for new engines that maintain the design relationships between P3, T3, fuel flow and emissions. Deterioration and other off-design effects are not covered and for these the combustion process has to be modeled in more detail such as with CFD codes. Engine manufacturers use CFD codes to develop low emission combustors.

Emissions models are often incorporated into gas turbine performance models. A lot of work on modeling the processes in the combustor in order to predict emissions has been done. This ranges from simple relationships between engine performance parameters and emission levels to 0-D parametric models like the P3/T3 or ratio models mentioned above, to complex CFD computations. The more simple, often empirical, models usually require some sort of calibration to a reference condition before they can be used for sensitivity analysis, so they can be referred to as 'off-design' or 'ratio' models. For accurate direct

prediction of emissions without any reference data, CFD calculations will be required. It should be noted that best results with combustion CFD modeling may still differ from test from by 10 – 30% on new configurations.

P3T3 and ratio models can easily be implemented in an engine performance model in order to provide a tool to directly relate operating condition to emission level, via combustor operating condition. However, the potential of the single equation ratio models to analyze a large variety of effects is very limited.

In order to obtain better insight into the effects of using other fuels, varying air properties, and deterioration, a more detailed model is required. However, the integration of CFD computations into a whole engine simulation is still very difficult and often not considered feasible due to computing power limitations.

A compromise between the CFD models and the simple empirical models is the use of multi-reactor models, which apply a limited degree of spatial differentiation inside the combustor. Multi-reactor models usually include separate flow and chemical models and offer a means of calculating a number of intermediate temperatures along the combustion process such as primary and dilution zone temperatures.

The simplest *combustor flow models* employ 'well-stirred' reactors that assume immediate mixing of separate user defined reactant flows. Explicit modeling of the distribution of cooling flows and the mixing processes involves a significant increase in complexity, such as multi-dimensional models.

Simple *chemical models* assume complete combustion in each reactor with no dissociation. Higher fidelity is obtained when calculating chemical equilibrium and best 1-D detail is obtained when calculating chemical kinetics. Many publications suggest multi-reactor models are valuable for the prediction of NO_x emissions. These models include detailed fuel and gas composition data and NO_x formation kinetics. An approach to integrate generic multi-reactor models in whole engine simulation models is presented by Visser, [3.28]. More detail on these topics is included in the combustion section in ***Chapter 5***.

3.3.6 Bleed and Power Off-Takes

Most component-based engine models include the direct effect of bleed between components as a standard feature. For empirical models, the greater the flexibility in bleed level and location, the more tables or correlations are required to achieve the desired effects. Internal bleed must consider the impact on component performance and the method of determining the conditions of the bleed air. In trying to match bleed supply conditions to user requests, a single bleed location may not be adequate. Bleeds from multiple locations may be selected or mixed to create the required bleed with minimal impact on the overall engine performance.

External load models are generally fixed or simple relationships, and are treated by simply including them as one of the power-outputs from the rotating shaft. For some applications, these models become more complicated and are included as part of the basic engine simulation. This is particularly true where control systems are part of the model and customer load affects the ability to maintain the required conditions.

3.4 CONTROL SYSTEM MODELS

Early engines featured extremely simple fuel systems, often with limiting by pilot observance of cockpit gauges. Accordingly, the engine internal margins (compressor working lines) had to be large, thereby wasting performance. As engine complexity increased, the control-systems became more refined to ensure accuracy and safety as margins were cashed for greater performance. In recent years there has been a progressive shift away from hydro-mechanical systems to electronic systems, which have greater flexibility.

Modern engines have many control inputs, most of which can be categorized into two main groups:

- *Fuel Flow* – to main and reheat combustors. (Fuel may be distributed into different zones within each combustor to satisfy local combustion constraints.)
- *Geometry* – final nozzle area, both convergent and divergent, compressor inlet guide vanes, bleed valves, blocker doors, variable mixer, bypass injector, and turbine throat areas.

Other control inputs may include water or methanol injection.

The fundamental requirement for any control-system is to deliver the required (rated) level of thrust (or shaft power) at a particular flight point (e.g. Mach no, altitude combination). This is achieved by controlling certain engine parameters to prescribed levels that are related to pilot input (pilot-lever angle – PLA). Direct prescription (open-loop control) of some control inputs is clearly inappropriate, for example, relating fuel flow to pilot demand. So, closed-loop control is employed for most control inputs.

Open-loop control of some variable geometry such as convergent nozzle area, or more correctly nozzle control ring position, is common. However, it relies on the actuator position accuracy to achieve the required engine condition. Because the optimum geometry setting is unlikely to remain constant over life, open-loop schedules must be periodically trimmed, if optimum operation is to be maintained. In addition, engine deterioration and scatter, airframe off-takes (bleed and shaft power) and intake distortions, all of which are random (within acknowledged limits) conspire to make open-loop control undesirable. This said, a mix of closed and open-loops is often found; judgment on the *mix* for a specific application is made on the basis of requirement, complexity (and therefore cost) and feasibility. Multiple closed-loops can interact, and although there are standard multi-variable control techniques for compensating for this interaction, certain combinations may not be practical.

3.4.1 Main Engine Control

Consider a two-spool, non-afterburning, mixed turbofan: The power level is fundamentally dictated by the fuel flow. However, if thrust setting is of interest, closed-loop control of a measured parameter that is closely related to thrust is required. Common thrust-rating parameters are LP shaft speed and engine pressure ratio (EPR). Off-line prediction tools can be used to generate schedules of the chosen rating parameter against flight condition, and the fuel flow controlled to achieve the scheduled value. Other parameters may be controlled in part-dry or idle conditions as appropriate. Idle condition is commonly defined using a schedule of HP shaft speed. The suitability of some rating parameters may differ between applications. Civil engines are prime users of EPR as a main control loop. However, this is not so appropriate in the military field due to the stringent EPR measurement accuracy required in *all* parts of the flight envelope. Because this is usually much more extensive than that of a civil aircraft, a higher sensor turndown ratio is required. Also the response of the EPR measurement is likely to be slower than LP shaft speed, a consideration which may sway a decision for a fast-handling military engine.

Some engines may not use thrust-related rating parameters. Turbine exit temperature has been a common rating parameter in the past. This has the disadvantage of thrust decaying over life as the engine gets progressively hotter at a thrust. Thrust rating has the advantage of ensuring a common rated thrust across a mixed-life fleet, and can extend engine life because the engine runs cooler at the start of its life.

Limiting values of other measured parameters such as compressor delivery pressure and temperature, turbine blade temperature, and derived parameters such as aerodynamic speeds, override the rated level.

Transition between power levels is controlled to give repeatable handling times and to ensure safe compressor (HP) running line excursions. It is common to see HP shaft acceleration limiting as this is closely related to HP working line excursion, and gives repeatable handling characteristics. Other, more

aerodynamic-based transient control methods could be employed. As the rate-of-change of thrust is of prime interest from the pilot's view, LP shaft acceleration may be a more relevant control parameter, with a HP compressor exit flow-function limitation for surge protection.

Open-loop control of fuel flow is still commonly relied upon for engine starting, where fuel flow is scheduled against HP shaft speed, and for providing surge protection. Maximum fuelling limits during acceleration are expressed in terms of fuel-flow/P3, which has the property of quickly reducing fuel flow in the event of surge (P3 reduces sharply). Closed-loop control of both events is being sought, as retaining provision for open-loop fuel meter prevents simplification of the fuel system down to the ideal *Pump* and *Tap* architecture. Further simplification may be attainable, using rapidly variable capacity pumps to eliminate the *tap* element.

Compressor variable inlet guide vanes (VIGVs) are provided to ensure correct compressor operation throughout the running range. Whereas they may exhibit the property of modulating inlet flow at a given speed, their prime use is local *care* of the compressor. Vane angle is often scheduled against aerodynamic speed, according to a relationship derived on compressor rig tests. As with all control inputs, there are two issues:

- Where is the optimum position?
- Where is the safety limit?

All the disadvantages of open-loop control as discussed above apply in this case and thus impact on the safety limit. Closed-loop control may better attain the optimum, but would require a measured parameter that indicated compressor *distress* if safety were to be assured. Closed-loop control of variable geometry *within open-loop limits* is an option that may be beneficial – but at what cost to complexity? There may be some engine handling benefit in using the flow modulating properties of VIGVs especially if an engine has variable fan geometry, because fast thrust response may be achieved at constant shaft speed.

Staged combustion is emerging as a solution to stringent emissions requirements. The total fuel flow required for a demanded power level has to be distributed in the combustor to maintain flame stability and minimize emissions. There will inevitably be some interaction between differing fuel distribution (at a constant total fuel flow) and overall engine operating point. Perhaps arising from the different profile presented to the HP turbine. This is a complication that must be addressed to ensure that the staging is effectively *transparent* to the pilot. Direct, closed-loop control of measured emissions might be most desirable – but difficult! Indirect control of emissions using local fuel-air-ratio or flame temperature control is considered simpler. Open-loop distribution of fuel based upon an initial understanding of the combustion process is another option.

Control of the final nozzle area (A8) is not an issue for dry operation unless a variable nozzle has been provided for afterburning. In a dry (not reheated) engine, a variable nozzle provides a means to appropriately set the fan working-line for all flight cases. Closed-loop control of the nozzle to achieve a specified level of EPR is common (in conjunction with closed loop control of the fuel flow via the LP shaft speed – say). Open loop scheduling of the nozzle area may also be a viable approach.

For a convergent-divergent nozzle, the divergent area (A9) may be mechanically linked to the convergent part thus leading to some compromised operation at some conditions. Independent (2-parameter nozzle) control of divergent area may be justifiable. In these cases, A9 could be scheduled against nozzle pressure ratio and A8, or controlled in such a way to maximize whole vehicle performance in conjunction with the aircraft autothrottle (again, the *operation within open-loop safe limits* issue arises).

3.4.2 Afterburner Control

The primary purpose of reheat is to provide a thrust boost with a low mass penalty. The main premise is to increase the jet velocity by burning the remaining oxygen in the jetpipe, while ensuring stable engine operation, particularly with respect to the fan working line. In order to maintain the dry engine operating point: as jet velocity is progressively increased by modulation of reheat fuel flow, so must the nozzle area increase to compensate. Thus two extra, interrelated control loops are introduced for reheated operation. As with the main engine control-system, it is desirable to eliminate reliance on open-loop fuel metering. Closed-loop reheat control-systems could be based on EPR control of the nozzle and some means of controlling fuel flow. Direct scheduling off the actual nozzle area is common, or a closed-loop control might be employed, based on some indication of jetpipe gas velocity, e.g. total-to-static pressure, or – though difficult to measure – jet pipe gas temperature. Reheat staging to achieve optimum combustion and emissions require control of fuel distribution. As with main combustion, the distribution of the fuel may affect the overall engine operating point.

The speed at which reheat is allowed to modulate depends on how well the fuel and nozzle area modulation can be coordinated. Out-of phase modulation can upset the fan!

Reheat light-up is also potentially fan-unfriendly. Open-loop limits on fuelling may be employed to safeguard the fan operating point. Automatic sensing and compensation for dangerous reheat instabilities (buzz and screech) may also be required.

3.4.3 Variable Cycle Engines

So-called variable cycle engines (VCEs) could more correctly be called variable bypass-ratio engines. They employ variable geometry devices to progressively change the engine from a low bypass ratio engine (high specific thrust) to a higher bypass ratio engine (low specific thrust). This is to meet performance criteria at widely differing flight conditions. Bypass blocker doors and variable bypass exit mixers are primary features of such engines. The doors may be of the 2-position type – in which case the control task is: *when to switch* and *ensure safety in the transition* (when doors close – others might be opening and vice versa). Alternatively, doors may be of the continuously variable type, in which case the task becomes more involved. The variable mixer is positioned to ensure correct HP to LP matching for the two types of engine at either end of the operating range.

3.4.4 Performance-Seeking Control (Performance Optimization)

Judicious selection of control-loops and derivation of suitable schedules is seen as the basic *optimizer* of engine performance; however 'smarter' approaches have been demonstrated which employ searching techniques to find the minima or maxima of a particular *cost function*. The cost functions are typically: lowest temperature at a thrust, minimum fuel burn, best thrust, etc. Such techniques are reliant on the use of embedded engine models in the control system. Models included in this way are therefore also available for on-board diagnostics and fault detection. The use of smart control techniques may reap most benefit when combined with the flight control-system (which often includes any variable intake geometry) to optimize the whole vehicle.

3.4.5 Modeling Control System Components

Although it is often classed as an engine accessory the control-system has a fundamental role in defining what the engine does, that is, it dictates functionality. The individual components of the control-system have differing levels of influence on the functionality. However, the engine is subordinate to the control-system.

Whole-engine models (engine + control-system) are used for various purposes:

- Operability investigation, e.g. surge-margin stack-up;
- Refinement of control-system software;
- Analysis and referral of test data;
- Planning of engine testing;
- Diagnosis following of engine test *events*;
- Hardware development and validation;
- Evaluation and selection of control-system concept; and
- Pilot-in-the-loop simulation (flight simulator).

The level of model detail required for different activities may vary. For instance, actuator and sensor dynamics can often be simplified when the effects of long-range engine transients are being studied. Greater dynamic fidelity may be required in other cases such as selection of control gains to meet specific stability margins. Similarly, the requirements placed on the engine model vary for each application. Engine model requirements are covered in detail in ***Chapter 2***.

The applications listed above are focused on different parts of the whole system. In some cases the reaction of the engine in response to the controller is of interest, whereas for other studies the converse applies. Accordingly, the computing environment and analysis facilities may vary. Control-system models and engine models invariably emerge from specialist departments, sometimes using different tools and programming languages. Interfacing models and systems can be an issue, although the use of CORBA-compliant tools will facilitate the co-execution of differing systems. This is discussed further in ***Annex B***.

Any dynamic system model requires initialization. Initialization can be achieved by iteration or trimming, although this can be problematic. As initialization is concerned with the initial values in numerical integrators, the initialization task can be simplified by reducing the number of integrators present, by reducing the level of dynamic modeling. Such a trade-off may be acceptable for some applications – usually those that require a whole-engine model. Detailed dynamic models, with fewer shortcuts, may then be needed for detailed design and optimization of the fuel system. Such models are usually run in isolation. Fuel-systems have fast dynamic terms, which are usually insignificant in terms of overall engine response. However, where the combustion process is modeled in detail – such as for an advanced combustor type – the fuel-system dynamics may significantly interact with combustor dynamics and hence affect engine response.

3.4.6 Description of a Typical Control System

Figure 3.51 below shows typical control-system architecture for a combat engine.

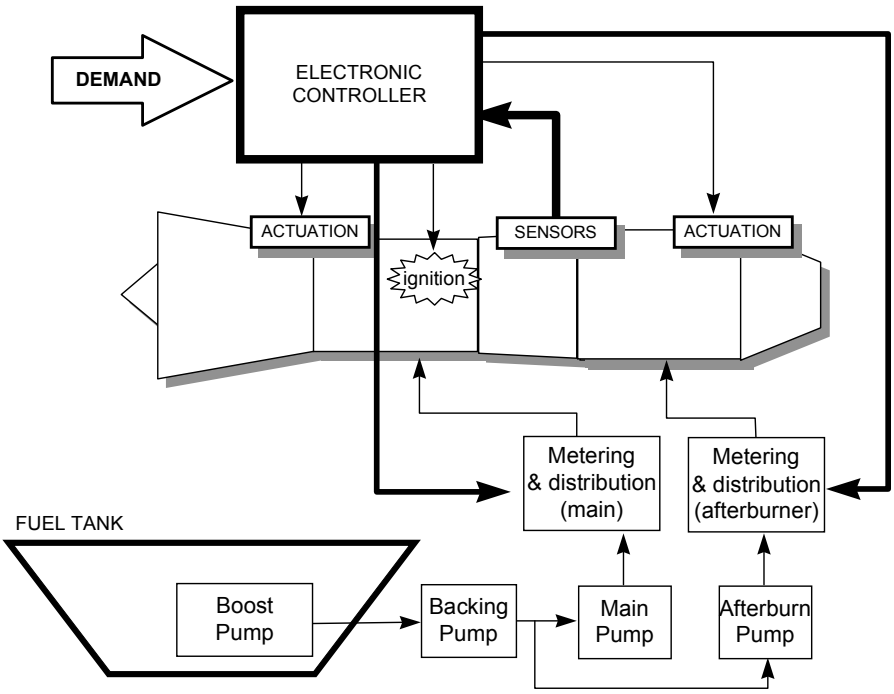

Figure 3.51: Typical Control System Architecture.

The main system element is the electronic control system. The control laws are now usually implemented digitally, with a degree of redundancy to meet reliability constraints. Within the electronic controller, checks are made on electrical inputs and outputs. Depending on the status of various inputs, outputs and internal flags, control model changes that may cause a significant change in engine operation may be performed. ***Annex B, Section 8*** discusses the selection and rationale of typical engine control-loops that are implemented electronically.

3.4.6.1 Sensors

An engine will carry several sensor systems, to provide feedback about the engine state to the electronic controller. A sensor is itself a sub-system containing 3 elements:

- Transducer – converting physical parameter into electrical signals;
- Interconnect; and
- Signal conditioning interface – e.g. filtering, linearization, plausibility checking.

Sensor systems may be required for any of the following:

- Shaft speed;
- Gas temperature;
- Gas pressure (total and static);
- Metal temperatures (static and rotating);
- Acoustic resonance;
- Flame detection;

- Fuel flow-rate; and
- Position.

Accuracy, reliability, cost and response constraints will dictate the sensing method used for each parameter.

3.4.6.2 Variable Geometry Actuation

Actuators can move variable guide vanes, final nozzle area, bleed valves and other variable geometry features on an engine. The common types are:

- Hydraulic;
- Pneumatic; and
- Electrical.

3.4.6.3 Pumping

Fuel is injected into the engine under high pressure. Pumping systems are required to overcome the back-pressure on, and the losses within the system, and to generate the required spray pattern. High-pressure fuel can also be used for servo power within the fuel system and for actuation (*fueldraulics*).

There are normally 3 pumping stages:

- Boost pump – usually electrically driven and part of the aircraft system, it ensures a constant supply of fuel to the engine fuel system at all aircraft attitudes;
- Backing pump – to provide suitable inlet conditions for the HP pump; and
- Main (high-pressure) pump – provides the main pumping effort.

Centrifugal and positive-displacement pumps are generally used for aero-engine applications, although other types such as air-jet extractor types are used for low pressure duties, e.g. accessory cooling by fuel circulation. Pumps may be driven mechanically (shaft power via gearbox), by air-turbine (using bleed or ram air) or electrically. Electrically driven pumps offer greater control of fuel flow by varying the motor speed.

3.4.6.4 Metering

The rate of fuel flow to the engine is the prime component of the definition of engine power output. Stable and fast responding metering is required – especially for afterburners and staged combustion systems which involve the fast selection and de-selection of burners. The most common metering system is based on a variable orifice with a regulated pressure drop – the orifice being varied by hydro-mechanical or hydro-electrical means. Valve position feedback is required for the determination of fuel flow or for closed-loop control of the valve position. In order to reduce the overall system mass, there is an effort to remove the provision for fuel metering and to provide a system based on a relatively simple *tap* that operates in a relative sense (more fuel or less fuel) rather than metering fuel in an absolute sense.

3.5 REFERENCES

[3.1] Halliwel., I., “Preliminary Design of Gas Turbine Engines – An Overview”, A Tutorial for ASME Turbo Expo 2001.

[3.2] Sandu, C. and Brasoveanu, D., “Exceeding 2000 °K at Turbine Inlet: Relative Cooling with Liquid for Gas Turbines Integrated Systems”, ASME GT 2003-38031, June 2003.

[3.3] Wilcock, R.C., Young, J.B. and Horlock, J.H., "Gas Properties as a Limit to Gas Turbine Performance", ASME Paper # GT-2002-30517, June 2002.

[3.4] Gordon, S. and McBride, B.J., "Computer Program for Calculation of Complex Chemical Equilibrium Compositions and Applications – I. Analysis", NASA Reference Publication 1311, October 1994.

[3.5] McBride, B.J. and Gordon, S., "Computer Program for Calculation of Complex Chemical Equilibrium Compositions and Applications – II. Users Manual and Program Description", NASA Reference Publication 1311, June 1996.

[3.6] Kurzke, J., "Gas Turbine Performance Simulation with GasTurb™", www.gasturb.de/.

[3.7] Horlock, J.H., Watson, D.T. and Jones, T.V., "Limitations on Gas Turbine Performance imposed by Large Turbine Cooling Flows", ASME Paper # 2000-GT-635, June 2000.

[3.8] Rolls-Royce plc., Aero Data, TS 1491, February 1998.

[3.9] SAE Standard, AS755: Aircraft Propulsion System Performance Station Designation and Nomenclature, August 2004.

[3.10] SAE Standard, AS681: Gas Turbine Engine Steady-State and Transient Performance Presentation for Digital Computer Programs, March 1999.

[3.11] SAE Standard, ARP1210: Gas Turbine Engine Interface Test Data Reduction Computer Programs, December 2002.

[3.12] SAE Standard, ARP1211: Gas Turbine Engine Status Performance Presentation for Digital Computer Programs (Cancelled July 2002).

[3.13] SAE Standard, ARP1257: Gas Turbine Engine Transient Performance Presentation for Digital Computer Programs (Cancelled July 2002).

[3.14] SAE Standard, ARP4148: Gas Turbine Engine Real Time Performance Model Presentation for Digital Computers, July 2003.

[3.15] SAE Standard, ARP4868: Application Programming Interface Requirements for the Presentation of Gas Turbine Engine Performance on Digital Computers, October 2001.

[3.16] SAE Standard, ARP4191: Gas Turbine Engine Performance Presentation for Digital Computer Programs Using Fortran 77.

[3.17] ISO 2533; Standard Atmosphere, Addendum 2, 1997.

[3.18] U.S. Standard Atmosphere, 1976, U.S. Government Printing Office, Washington, D.C., 1976.

[3.19] U.S. Standard Atmosphere Supplements, 1966, U.S. Government Printing Office, Washington, D.C., 1966.

[3.20] Global Climatic Data for Developing Military Products (MIL-STD-210C), 9 January 1987, Department of Defense, Washington, D.C.

[3.21] Gordon, S., "Thermodynamic and Transport Combustion Properties of Hydrocarbons with Air. I – Properties in SI Units", NASA TP-1906, 1982.

[3.22] Mathioudakis, K. and Tsalavoutas, A., "Uncertainty Reduction in Gas Turbine Performance Diagnostics by Accounting for Humidity Effects", Paper ASME Journal of Engineering for Gas Turbines and Power, October 2002, Vol. 124, pp. 801-808.

[3.23] Mathioudakis, K., "Evaluation of Steam and Water Injection Effects on Gas Turbine Operation using Explicit Analytical Relations", Proceedings of the Institution of Mechanical Engineers, PART A, Journal of Power and Energy, Vol. 216, No. A6, December 2002, pp. 419-431.

[3.24] SAE Standard, AIR4548: Real-Time Modeling Methods for Gas Turbine Engine Performance.

[3.25] MIL-E-5007D(3): Military Specification: Engines, Aircraft, Turbojet and Turbofan, General Specification for, Rev. D, Amendment 3, December 1995.

[3.26] Varner, M.O., Martindale, W.R., Phares, W.J., Kneile, K.R. and Adams, Jr., J.C., "Large Perturbation Flow Field Analysis and Simulation for Supersonic Inlets", NASA CR 174676, September 1984.

[3.27] SAE Standard, ARP1420: Gas Turbine Engine Inlet Flow Distortion Guidelines, March 2002.

[3.28] Visser, W.P.J. and Broomhead, M.J., "GSP, A Generic Object-Oriented Gas Turbine Simulation Environment", ASME Paper # 2000-GT-0002, ASME Conference Munich, June 2000.